INFORMATION TO USERS

This manuscript has been reproduced from the microfilm master. UMI films the text directly from the original or copy submitted. Thus, some thesis and dissertation copies are in typewriter face, while others may be from any type of computer printer.

The quality of this reproduction is dependent upon the quality of the copy submitted. Broken or indistinct print, colored or poor quality illustrations and photographs, print bleedthrough, substandard margins, and improper alignment can adversely affect reproduction.

In the unlikely event that the author did not send UMI a complete manuscript and there are missing pages, these will be noted. Also, if unauthorized copyright material had to be removed, a note will indicate the deletion.

Oversize materials (e.g., maps, drawings, charts) are reproduced by sectioning the original, beginning at the upper left-hand corner and continuing from left to right in equal sections with small overlaps.

ProQuest Information and Learning
300 North Zeeb Road, Ann Arbor, MI 48106-1346 USA
800-521-0600

Study of Hand Transmitted Vibration from a Hand-Held Rotary Power Tool

Ahmed Youssef Elkaied

A Thesis
in
The Department
of
Mechanical and Industrial Engineering

Presented in Partial Fulfillment of the Requirements
for
The Degree of Master of Applied Science
at
Concordia University
Montreal, Quebec, Canada

March 2003

Abstract

Study of Hand Transmitted Vibration from a Hand-Held Rotary Power Tool

Ahmed Youssef Elkaied

Operators of hand-held power tools are exposed to high magnitudes of hand-transmitted vibration. Prolonged occupational exposure to such vibration has been associated with many disorders in the vascular, neural and musculoskeletal systems of the hand and arm. This dissertation research addresses a study of vibration transmitted to the operators' hand while operating a hand-held angle grinder and mechanisms to control the magnitude of hand-transmitted vibration. An experimental setup is designed to study the vibration response of a grinder under different values of mass unbalance that represent the residual unbalance of the grinding wheel and non-uniform distribution of cutting forces. A series of experiments are conducted to study the influence of mass unbalance, feed force and the presence of an autobalancer. The measured data are analyzed to derive the eight-hour energy equivalent vibration and the number of years of exposure that may cause vascular symptoms in 10% of the worker's population. The results suggest that exposure to hand-transmitted vibration under 510 gm-mm mass unbalance at a speed of 7500 rpm could cause vibration-induced white finger among 10% of the exposed population in approximately 2.8 years. The addition of autobalancer, however, could reduce the eight-hour energy equivalent value to nearly 20%. A preliminary attempt is made to derive a simplified model of coupled hand-grinder system. The model assumes rigid shaft-disc assembly, rigid tool body, linear bearing properties and the handles being attached rigidly to the tool body. A single-degree-of-freedom model of the hand and arm

is also integrated along the y and z-axis of the basicentric axis system used in the study. The model results under varying degrees of mass-unbalance suggest that the magnitude of hand-transmitted vibration increases considerably with increasing mass-unbalance and angular speed. The results of the parametric study suggest that bearing damping does not influence the magnitude of transmitted vibration due to considerably higher natural frequency of the shaft-disc assembly. Increasing the damping properties of the hand-handle interface by introducing anti-vibration gloves or handle grips, however, could reduce the magnitude of transmitted vibration. From the results obtained from the analytical and experimental studies, it is concluded that the use of an automatic-balancer is vital to reduce the magnitudes of hand-transmitted vibration.

Acknowledgements

Since I started writing this thesis almost two and a half years ago, I have benefited from the kindness and talent of many people who have helped, encouraged, and, at times, provoked me. I began this project with two prominent scientists Dr. Rama Bhat and Dr. Subhash Rakheja.

My deepest gratitude is due to Dr. Rama Bhat, who for his sage counsel, enthusiastic guidance and continuous support. His knowledge goes beyond his field of study into so many other fields. The author is sincerely grateful to Dr. Subhash Rakheja whose rigorous scrutiny of the all aspects of this research work, and whose erudition and wisdom taught me so much. His dedication to work and his meticulousness that are examples, I will strive to follow.

I would like to express my thanks to Mr. Dainius Juras for facilitating all the means to make this work turn to a reality, Mr. José Esteves for making all the equipments ready in the laboratory, and Weimin Pu for his computer assistance throughout the time I spent doing this research. The author is very grateful to Msł Arlene Zimmerman for her creative assistance and continuous support during the research period.

Also I would like to thank my colleagues and friends for their help and useful discussions during the period I spent with them. The financial support by the Mechanical and Industrial Engineering Department at Concordia University was of great help to me to do the experiments and complete the work. I would like to thank my parents for their patience and moral support to me throughout the research period.

Contents

2. Modeling of Rotor for Gyroscopic Effects

3. Experimental Investigations

4. Development of the Hand-Grinder Model

List of Figures

List of Tables

List of Abbreviations and Symbols

ω Angular Velocity (rad/s)

a Eccentricity of the disc (m)

θ Slope of Bending in YZ plane (rad)

ϕ Slope of Bending in XZ plane (rad)

i Imaginary unit ($i=\sqrt{-1}$)

I_p Polar moment of inertia of the rotor (kg.m^2)

I_d Transversal rotor moment of inertia (kg.m^2)

γ Precessional frequency (rad)

m_d Mass of rotor (kg)

m_b Mass of the machine (kg)

m_T Total mass of the rotor (kg)

m_u Mass of the unbalance (kg)

m_h Mass of human hand (kg)

α Rotation of the model around Z-axis (rad)

β Rotation of the model around Y-axis (rad)

d Distance between the two bearings (m)

l Distance between the rotor and the first bearing (m)

c_{b1} Damping coefficient for bearing no# 1 (Ns/m)

c_{b2} Damping coefficient on for bearing no# 2 (Ns/m)

c_{h1} Damping coefficient on left hand side for human hand (Ns/m)

c_{h2} Damping coefficient on right hand side for human hand (Ns/m)

k_{b1} Stiffness coefficient for bearing no# 1 (N/m)

k_{b2} Stiffness coefficient for bearing no# 2 (N/m)

k_{h1} Stiffness coefficient on left hand side for human hand (N/m)

k_{h2} Stiffness coefficient on right hand side for human hand (N/m)

Chapter 1

Introduction, Literature Review and Thesis Objectives

1.1 General

Operators of hand-held power tools are often subjected to high levels of vibration. Such vibration occurs over a wide frequency range from 10-2000 Hz and arises from the dynamic interactions between the tool and the work piece. Invariably, the hands and the arms of the operators absorb these high levels of vibrations. Many occupational health disorders, such as tingling, numbness and blanching of the fingers, in the long run, may appear on the hand-arm of the operators. Many epidemiological studies have established that there is a strong relationship on the effects of hand-transmitted vibration (HTV) on the white finger attacks (Griffin, 1982). White finger attacks are often referred to as "Vibration Induced White Finger (VWF)" or hand-arm vibration syndrome (HAVS), or the "Traumatic Vasospastic Disease (TVD)". The hand-arm vibration syndrome is related to many occupational, neural and muscular disorders, which develop gradually over many years of vibration exposure. Vibration White Finger (VWF) is considered as the most severe symptom that happens due to prolonged exposure to vibration. The feeling of intermittent tingling and numbness of the fingers is usually experienced by the operators (Cherian, 1994).

The intermittent tingling is followed by an attack of finger blanching confined to the tips of one or more fingers with continued exposure to hand-transmitted vibration. Further exposure to vibration causes the finger blanching to propagate to the base of the hand. The attack may last from 15-60 minutes and in advanced cases it can continue up to

2 hours. Continued exposure to vibration in the advanced stages causes nutritional changes in the finger pulps, which leads to the formation of coarse areas of the skin (Griffin, 1996).

The risk of occurrence of VWF disease is related to the dose and magnitude of vibration and the years of exposure. A dose-response relation has been developed to study the health risks associated with the hand-arm vibration exposure (ISO-5349-1, 2001). Considerable efforts have been made to study the hand-arm vibration syndrome etiology, such as dose response standards and biodynamic response characteristics of the human hand arm (Griffin, 1996). Owing to the potentially severe health effects of exposure to hand-transmitted vibration, considerable efforts have been made to reduce the magnitudes of vibration in hand-held machines. A number of anti-vibration gloves have been commercially developed to mitigate the transmission of vibration to the human hand. A series of studies performed on assessment of gloves have concluded that the gloves provide either negligible or limited isolation from vibration (Rens, 1987; Gurram et al., 1994; Hewitt, 1998). Alternatively, only limited efforts have been made to integrate vibration isolators within the tool due to the compact nature of their designs (Cherian, 1994). Such means have been used in chain saws (Suggs, 1968). The development of vibration isolators necessitates a thorough dynamic analysis of tools to enhance the knowledge of sources of vibration and its transmissions. Only a few studies have attempted to study the dynamic behavior of power tools and dynamic interactions among the components (Rakheja et al., 2002). Alternatively, automatic balancers have been developed to reduce the magnitudes of tool vibration caused by unbalance forces in the

rotary tools (Lindell, 1996; Rajalingham et al., 1998). However, the potential performance benefits of the balancer have not been fully explored.

In this study, the hand-transmitted vibration response of a hand-held rotary tool (grinder) is investigated through analytical and experimental means. Laboratory experiments are performed to study the impact of unbalance and the balancer on the hand-transmitted vibration. An analytical model of a grinder coupled with the human hand is formulated to study the influence of unbalance and the nature of hand-transmitted vibration.

1.2 Review of Literature

A study of vibration behavior of a coupled hand-tool system involves systematic analysis of the tool dynamics and vibration, biodynamic modeling of the human hand and arm, analysis of the coupled hand-tool model, and analysis of important design and operating factors on the nature of hand-transmitted vibration. The published studies relevant to various components are reviewed to formulate the scope of the dissertation research. The highlights of the relevant studies are briefly summarized in the following sections.

1.2.1 Epidemiological Studies

Numerous epidemiological studies have been carried out in several countries to identify the population of workers affected by occupational exposure to vibration and to assess the impact of the workplace vibration environment. An extensive study in the U.S. estimated that of the 8 million workers exposed to vibration, approximately 7 million are

exposed to whole body vibration and 1 million are exposed to hand-arm vibration (Wasserman, 1974). In Canada an estimate made by the National Research Council of Canada indicated that approximately 200,000 workers are exposed to hand arm vibration (Brammer, 1984). Recent Studies conducted in Great Britain also supported the findings of North America, and identified the population of workers exposed to occupational hand-arm vibration (Bendal, 1987). The results of the study, presented in Figure 1.1, reveal that approximately 700,000 workers are exposed to occupational hand-arm vibration in different industries in Great Britain. Traditionally cross-sectional and longitudinal epidemiological studies have concentrated on three classes of power tools: (a) pneumatic tools (chippers, grinders, jackhammers, riveters, and drills); (b) electrically operated tools (sanders, pedestal grinders, impact hammers); and (c) chain saws. Many investigators have performed numerous field measurements to characterize the nature of vibration generated by different hand-held power tools, while in operation. The studies revealed that the magnitude of vibration encountered on different tools varies significantly, from 10 m/s^2 weighted to 2014 m/s^2 unweighted, depending upon the tool, application, speed, feed, location of point of measurements, etc. (Gurram, 1993; Radwin et al., 1998; Lundström, 1989). The dominant frequencies of vibration, however, appear to be clustered in the 25-320 Hz range, irrespective of the tool and operating conditions.

While the measured acceleration levels differ considerably for different tools, the magnitude of acceleration is evidently very high irrespective of the type of tool or the operating conditions. All the epidemiological studies reported the prevalence of HAV syndrome among the population of workers exposed to hand-arm vibration, independent

of the level and nature of vibration exposure. The prevalence of VWF symptoms among the operators using different tools is illustrated in Table 1.1.

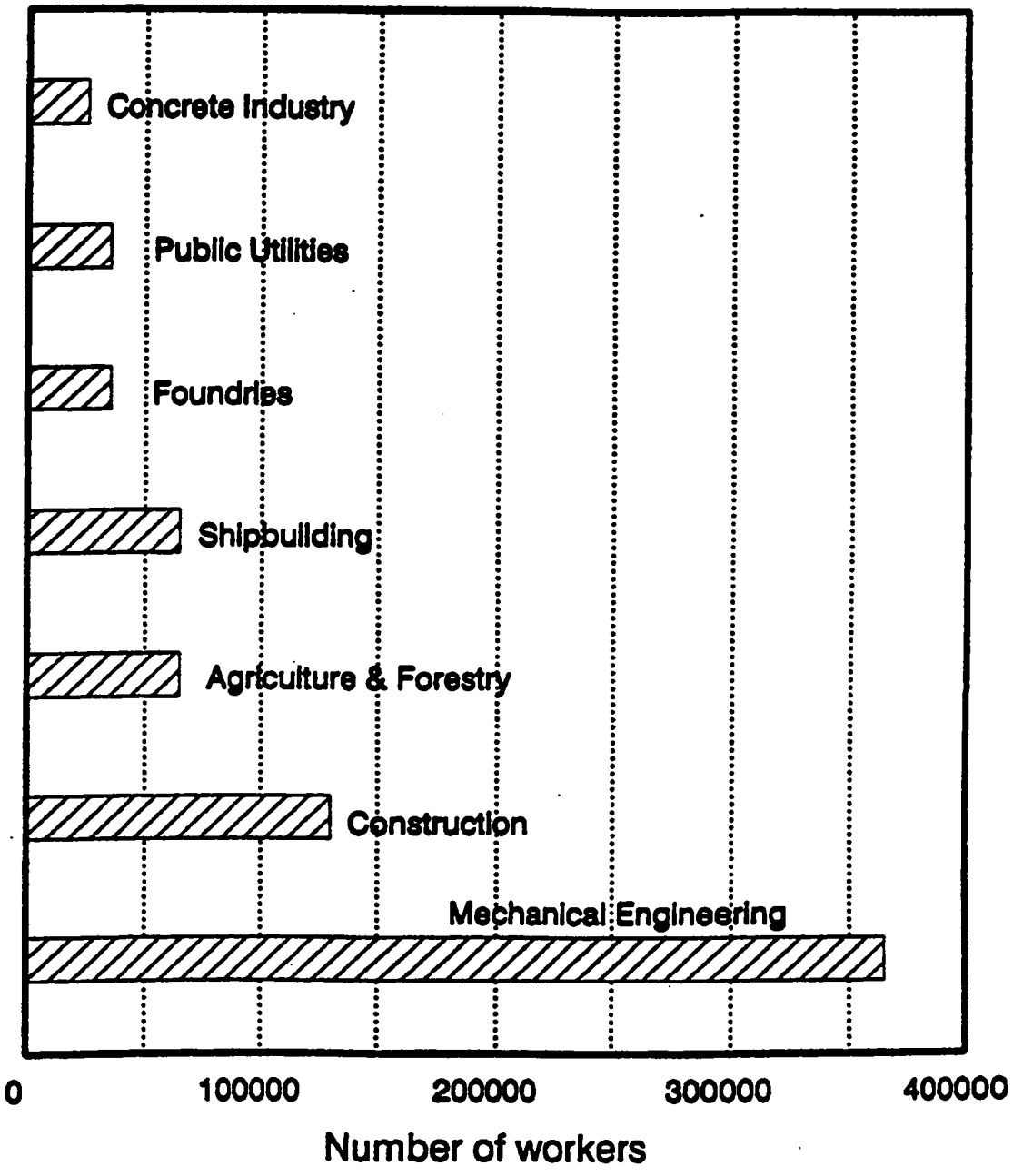

Figure 1.1: Manual workers exposed to hand-arm vibration in Great Britain (Bendal, 1987).

Table 1.1: Acceleration levels measured on different tools and associated VWF rates reported in different studies.

Tool Type (Reference)	Reported acceleration Level (m/s^2)*	Prevalence of VWF Symptoms (%)
Chipping hammer (Taylor et al., 1984)	2014	80
Riveter (Oliver et al., 1979)	1183	75
Chipping hammer (Taylor et al., 1981)	424	45
Pedestal grinder (Agate et al., 1949)	382	86
Chipping hammer (Matsumoto, 1981)	378	64
Jack-leg drill (Chattergee et al., 1978)	362	50
Jack-leg drill (Robert et al., 1977)	339	70
Jack-leg drill (Matsumoto et al., 1979)	335	80
Chipping hammer (Behrens et al., 1984)	251	47
Grinder (Bovenzi et al., 1980)	205	31
Pavement breaker (Walker et al., 1985)	195	10
Pedestal grinder (Pelmear et al., 1975)	125	96
Pedestal grinder (Starck et al., 1983)	122	100
Jack-leg drill (Iwata, 1968)	121	72
Chain saw (Matsumoto et al., 1979)	75	38
Jack-leg drill (Brubaker et 8l., 1986)	20#	45
Hand grinder (Pelmear et al., 1975)	20	35
Riveter (Engstrom et al., 1986)	10#	25

* Unweighted Acceleration except as mentioned
# Weighted acceleration as per ISO- 4 hour value

Table 1.2: Types of disorders associated with hand-transmitted vibration exposure (Griffin, 1982).

Type	Disorder
A	Vascular disorders
B	Bone and joint alterations
C	Peripheral neurological disorders
D	Muscle disorders
E	Other disorders (e.g. of the whole-body and central nervous system)

The National Institute of Occupational Safety and Health (NIOSH), in the U.S. has established a linear relationship between measured acceleration levels and the prevalence of vascular symptoms (NIOSH, 1989). While the epidemiological studies do not provide a relationship between the vibration levels and the occurrence of HAV syndrome among the power tool operators, these studies provide ample evidence that the use of vibration producing tools is associated with the development of HAV syndrome.

1.2.2 Effects of HTV

Prolonged occupational exposure to hand-transmitted vibration, arising from operation of hand-held power tools, has been associated with an array of health disorders in the vascular, sensoneural and musculoskeletal structures. Such disorders have been collectively defined as the hand-arm vibration syndrome (HAVS) (Taylor, 1973; NIOSH, 1989). The vascular effects, which appear as episodes of finger blanching together with tingling and numbness in the exposed hand, have been evaluated and documented far more than the other components, such as musculoskeletal and sensoneural. All the components of the HAVS, however, appear to be coupled in view of their known mechanisms, and occur in a certain sequence depending upon the nature of vibration exposure and individual factors (Griffin, 1996).

The vascular component of the syndrome has also been termed as Raynaud's disease of occupational origin, traumatic vasospastic disease (TVD) and the white finger (VWF) (Wasserman, 1987). Many studies have concluded that exposure to vibration together with cold and poor ergonomic factors are responsible for the symptoms of VWF (Brammer, 1984; Wasserman, 1987; Pelmear and Wasserman, 1998). Many other studies

have also suggested the symptoms of bone alterations; joint deformations and soft tissue damage that restrict the blood flow to the infected areas among the hand-arm vibration exposed workers (Nerem, 1977; Gurram, 1993). The wide range of health effects and disorders associated with exposure to hand-transmitted vibration has been grouped into five types. Each type of disorder may represent a complex combination of several disorders. It would be possible that disorders of one type arise as a consequence of a disorder of another type (Griffin, 1996). These classes of disorders are summarized in Table 1.2.

It has been reported that operators of chain saws, rock drills, chipping hammers, pedestal grinders and many other power tools are subject to same risks for developing HAVS. The specific symptoms may range from tingling, numbness, to partial or total blanching of their fingers over long term exposures. Episodes of white fingers, dead fingers, or dead hand were first reported between 1911 and 1920, in studies cited by (Loriga, 1911), cited in (Brammer, 1984; Wasserman, 1987; Wasserman and Pelmear, 1998). The spasm of the arteries in the fingers was commonly attributed to vibration of the rotary-percussive air-driven drills used by stonecutters and rock miners at that time. Tingling and numbness are the first symptoms of VWF that occur immediately after vibration exposure. The tingling of the fingers can also be caused by other factors, such as exposure to cold (Griffin, 1996). Few studies have attempted to distinguish between the tingling experienced by individuals immediately after even short periods of vibration exposure and the tingling that is not associated with vibration exposure.

Blanching of the fingers is considered as the first visible sign of VWF. Blanching mostly appears on the fingertips on the lateral side of the hand that imparts majority of

the contact force on the vibrating handle (Brammer NRC, 1984; Gurram et al., 1995). Under continued exposure, the blanching may progress along the finger and to other fingers. It has also been suggested that the workers affected with VWF have an impaired local circulation, which may further reduce under exposure to cold (Nerem, 1977). The cessation of blood supply to the exposed hand and fingers may lead to loss of finger colour. Attacks of finger blanching may last for 15 minute to 1 hour, and sometimes even longer, depending upon the severity of the symptoms (Griffin, 1996). The phase of an attack may be marked by a strong red flush on the affected parts, accompanied by pain. Such symptoms are similar to those experienced by the non-exposed individuals when the hands are warmed followed by exposure to cold.

The fingers suffering from an attack of blanching do not normally experience any pain and their sensitivity to heat, cold, vibration, touch and pain may be reduced. Reduction in sensitivity is due to reduced skin temperature during the attack. Loss of sensitivity and reduced finger temperature during an attack poses some difficulties in performing fine tasks and manual dexterity (Griffin, 1996). Working with hot or abrasive materials can be dangerous when there is a lack of feel and it is advised to avoid such tasks during the attacks of blanching. The extent of interference with activities is largely related to temperature. In the winter, time may be spent warming the body to terminate an attack before commencing work if either the workplace is cold or the body has become cold on the way to work.

Neurological effects, such as disturbances in the sense of touch, increased sensitivity to cold, as well as ulnar paresis and paralysis, acroparesthesia accompanied by cramp pains at the body edges and fatigue have been observed in the operators exposed to

vibration (Cherian, 1993). The decrease in the temperature of the fingers suffering from vibration-induced White finger (VWF) is partly responsible for the numbness. When the finger temperature falls below 20 °C, the sensitivity and other neural functions efficiency decreases. Some workers place the fingers in boiling water until the skin comes off without adverse feeling (Cottingham, 1918).

It has been reported that prolonged exposure to hand-transmitted vibration, which is transmitted directly to the hand-arm, impairs the tactile sensation (i.e. touch, pain, vibration and temperature) of the end organs or their neural links to the central nervous system. Muscular and neurological disorders are interdependent, and so it is somehow difficult to distinguish between them. Hand gripping is an uncommon complaint from operators who use vibratory hand-held tools (Griffin, 1996). Studies reported by Färkkilä and Starck (1984) showed that vibration exposed persons with the greatest handgrip force had the greater probability of developing symptoms of VWF. Radiographic studies of the wrist, elbow, shoulder and the cervical vertebrae of workers with weakened grip revealed abnormal findings in the elbows (Cherian, 1994).

Dupuytren's contracture is a disease of the tissue on the palm of the hand (named after the French surgeon guillaume Dupuytren (1777-1835) and has been thought to be more common in users of hand-held vibrating tools. In this disease the tough fibrous tissue under the skin of the palm of the hand thickens and shrinks. Another disease is tendonitis, where the fibrous tissue of a tendon are torn and inflamed-Tenosynovitis, affects some tendons, including those, which move the fingers and thumbs. This occurs when the subject uses fingers in high repetitive movements. The evidence of nervous disorders indicating involvement of central nervous system among the operators of

vibrating tools has aroused the interest of many researchers. Griffin (1996) reported that hand-arm vibration could impair the central nervous system (CNS) function through damage to the autonomic centers in the brain, and then the whole body is affected. There have been several applications of the electroencephalogram (EEG) to the study of the effects of vibration on the CNS. Studies show vibration can affect operator's central nervous system in different ways such as causing anxiety, depression, insomnia, headache, palm sweating, irritability and emotional instability.

1.2.3 Factors that Influence Hand-Arm Vibration Severity

Many operating factors such as vibration magnitude, direction of vibration, and frequency range of vibration, working posture, nature of task, and hand forces can strongly affect the severity of the hand-transmitted vibration. The factors affecting the severity of HTV exposure have been grouped in three categories: physical factors related to nature, duration and patterns of vibration exposure; biodynamic factors related to coupled hand-tool system, such as hand forces, and postural effects and hand-arm response to vibration; and individual factors that relate to health and condition of the tool and operator. Table 1.3 summarizes the factors affecting the severity of HTV (Brammer, 1974). Among these factors, the physical factors related to direction, magnitude and frequency of HTV are considered to be the most important for engineering design and analysis of the tools and risk assessment. These factors are thus further discussed below to enhance an understanding of the nature of hand-transmitted vibration.

Table 1.3: Summary of factors affecting hand-transmitted vibration (Brammer, 1974).

Category	Factors
Physical	• Dominant vibration amplitudes entering hand. • Dominant vibration frequencies entering hand. • Years of employment involving vibration exposure. • Total duration of exposure each workday. • Temporal pattern of exposure each workday. • Dominant vibration direction relative to the hand. • Non-occupational exposure to hand.
Biodynamic	• Handgrip forces. • Surface area, location and mass of parts of the hand in contact with source of vibration. • Posture. • Other factors influencing the coupling of vibration into the hand (e.g. texture of handle etc.)
Individual	• Factors influencing source intensity and exposure duration (e.g. state of tool maintenance, operator control, machine work rate, skill and productivity). • Biological susceptibility to vibration. • Vasoconstrictive agents affecting the peripheral circulation (e.g. smoking, drugs, etc.) • Predisposing disease or prior injury to the fingers, hands. • Hand size and weight.

1.2.4 Magnitudes, Frequencies and Directions of Vibration

The studies on vibration severity of tools and hand-arm responses to vibration mostly consider the response in terms of acceleration, which is associated with the force or stress, and is believed to have a strong positive correlation with the damages caused by the hand-transmitted vibration. Moreover, the responses are conveniently measured in terms of acceleration. The hand-arm vibration response is thus mostly characterized by the acceleration of the source or the transmitted vibration (ANSI, 1986; NIOSH, 1989;

ACGIH, 1998; ISO-5349-1, 2001). The human hand-arm is a complex dynamic system with complex viscoelastic and inertial properties. It exhibits motions along the three-translational and three-rotational axes. Two coordinate systems, anatomical and basicentric have been defined for characterizing the translational motions of the human hand-arm, as shown in Figure 1.2 (ISO-8727, 1997).

The nature of hand-transmitted vibration from a tool is invariably measured at the tool handles in the vicinity of the operator's hand. The guidelines for measurements have been documented in the international as well as American standards (ANSI, 1986; ISO-5349, 1986; ISO-5349, 2001). This is based upon the findings of the epidemiological studies that describe the risk of HAV syndrome as a function of the magnitude of tool handle vibration in the vicinity of the hand. Such epidemiological studies have resulted in a dose-response relationship (ISO 5349, 1986; ISO 5349-1, 2001). The internal standard, (ISO-5349-1, 2001), outlines a frequency weighting filter and a dose response relation to asses the risk of VWF on the basis of frequency-weighted rms acceleration of the tool handle (ISO 5349-1, 2001). The vibration due to the hand-held power tools may occur along all the three translational axes. The international standard, ISO-8727 (1997), recommends that measurements be performed using the basicentric coordinate system, as shown in Figure 1.2. In basicentric coordinate system, the origin is located on the hand surface underneath the head of the third metacarpal bone of the hand. It is important to define the location of the origin on the tool, since the rotational motions of the tool may yield considerably different magnitudes of translation at different points on the handle. Reasonable location of the basicentric coordinate systems depends on the point of

maximum pressure between the hand and the source of vibration, or the estimated location of the center of the hand or finger pressure (Griffin, 1996).

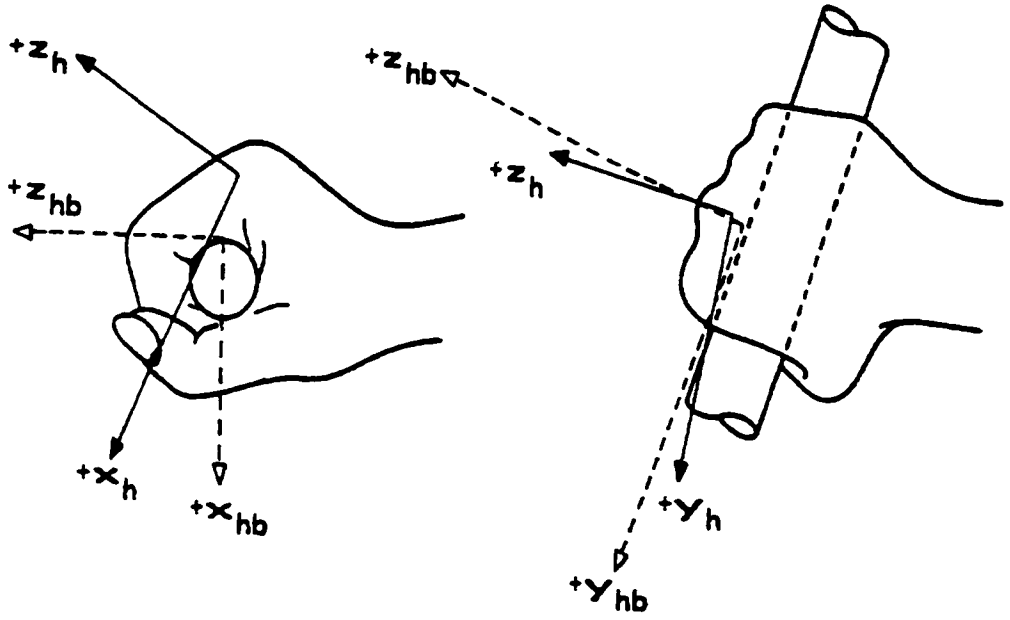

Figure 1.2: Reference coordinate system proposed in (ISO-8727, 1997).

The international standard ISO-5349 (1986), prior to its recent revision in 2001, recommended the assessment of hand-transmitted vibration (HTV) along the axis of the dominant vibration. The direction of the predominant vibration and the corresponding magnitudes of hand-held power tools, however, may vary considerably due to significant variations in the working posture and the task. Many investigators have recommended measurements along all the three axes and assessment on the basis of the vector sum of the three components (Ikeda, 1998; Bitsch, 1986). The revised standard, ISO-5349 (2001) also recommends the use of vector sum or the root-sum-of-square of the acceleration components. It is thus believed that the HTV along all the three directions is equally

important. The standard, however, provides identical frequency weighting for all three axes. Figure 1.3 illustrates the recommended frequency-weighting curve.

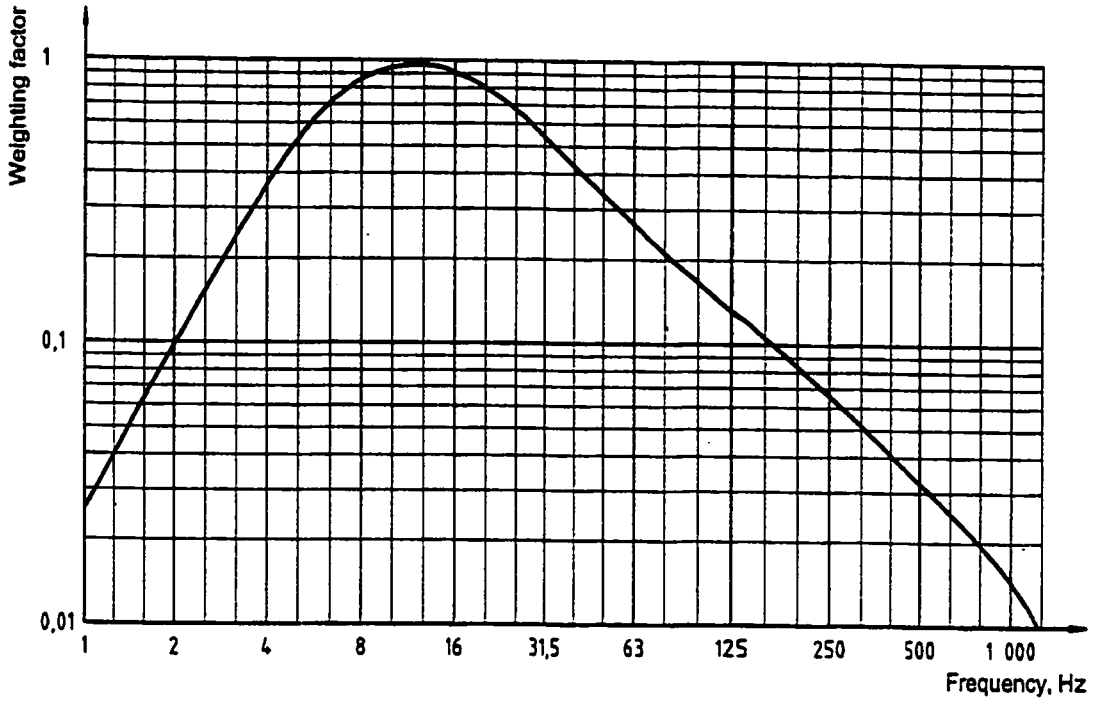

Figure 1.3: Frequency weighting function proposed in ISO-5349-1, (2001).

The magnitudes of HTV arising from different tools vary extensively depending upon the power and size of the tool, type of tool, task, speed, feed force, measurement location, etc. The measured acceleration data is frequently expressed in terms of its root mean square (rms) value, computed from:

$$a_{rms} = \sqrt{\frac{1}{T}\int_0^T a^2(t)\,dt} \qquad (1.1)$$

where a_{rms} is the rms acceleration, $a(t)$ is the instantaneous acceleration and T is the duration of the measured sample considered. The vibration levels of the tools are mostly measured using miniature accelerometers. Non-contact laser-based measurement systems

have also been used to measure the HTV (Nelson, 1997; Rossi, 1994). On the basis of the reported data, the magnitudes of vibration generated by various tools could be as high as $2*10^3$ m/s^2. The reported studies also suggest that vibration due to various tools dominate in the 25-320 Hz-frequency range (Gurram, 1993; Radwin, 1998; Lundström, 1998). Majority of the tools, specifically the percussive tools, are known to yield vibration at considerably higher frequencies attributed to the contact or cutting actions (Griffin, 1982; Pelmear and Wasserman, 1998). Table 1.4 summarizes the dominant frequencies, magnitudes and direction of vibration measured on different tools. The dose response relationship presented in ISO-5349-1 (2001) considers frequency-weighted rms acceleration due to vibration. The weighting function presented in Figure 1.3 suggests that the greatest risk of the hand-arm disease is associated with exposure to tool vibration below 20 Hz.

1.2.5 Vibration Duration

Exposure duration of the hand-transmitted level can be described either on a daily average basis or on the lifetime basis. The exposure duration plays an important role on how it affects the human hand-arm in the long term. It is necessary to recognize the exposure duration as a non-continuous operation. There may be a recovery for the hand-arm between exposures or after the final exposure. Different types of injuries need different 'time constants' to achieve recovery. Small injuries need only a short time while adverse injures need longer periods to achieve recovery.

Table 1.4: Frequency range and directions of dominant vibrations generated by different power tools (ISO 5349, 1986).

Type of Tool (Reference)	Dominant Frequency (Hz)	Dominant Direction of Vibration*
Heavy duty sander *(Radwin,* 1986)	70-150	X_h Y_h Z_h
Orbital sander *(Radwin,* 1986)	60-100	X_h Y_h Z_h
Vertical polisher *(Radwin,* 1986)	70-125	X_h Y_h Z_h
Bush cleaner *(Daikoku et al.,* 1989)	100-150	X_h
Garden tool *(Daikoku et al.,* 1989)	63-80	X_h
Chain saw *(Reynolds et al.,* 1982)	100-150	X_h Y_h Z_h
Chain saw *(Futatsuka et al.,* 1985)	100-125	X_h Y_h Z_h
Chain saw *(Pelmear et al.,* 1982)	63-125	X_h Y_h Z_h
Chain saw *(Hempstock et al.,* 1975)	80-125	N/A
Pneumatic *hammer (Hempstock et al.,* 1975)	40	N/A
Pneumatic hammer *(Farkkila et al.,* 1978)	80	Z_h
Chipping hammer *(Reynolds et al.,* 1982)	25-125	X_h Y_h Z_h
Pedestal grinder *(Hempstock et al.,* 1975)	250	N/A
Horizontal grinder *(Reynolds et al.,* 1982)	63	X_h Y_h Z_h
Vertical grinder *(Reynolds et al.,* 1982)	40	X_h Y_h Z_h
Motorcycle handle *(Harrison et al.,* 1982)	320	X_h
Motorcycle handle *(Harrison et al.,* 1982)	125	Y_h Z_h

A daily dose of vibration can be defined for specific type of assessment. A daily dose measure is expressed in terms of constant magnitude of vibration, which will result in the same dose over fixed time duration. This measure is of great importance in giving a numerical meaning on severity of a complex exposure. The determination of vibration dosage and exposure requires measurement of vibration amplitudes and frequencies entering the hand from all directions as a function of time for handgrip forces in well defined postures (Cherian, 1994). The risk of VWF due to HTV is strongly dependent upon the years of occupational exposure and average daily exposure. The dose-response relationship presented in the standard considers the frequency-weighted value of HTV.

ISO 5349-2,2001 outlines a procedure to account for the duration of vibration exposure. When the power tool is operated continuously for long periods and the hand is always in contact with the power tool or hand-held work-piece, then the exposure time is the time for which the power tool is used. Another classification where the hand is always in contact with the power tool or hand-held work-piece during use, but the power tool is not operated continuously, for the exposure time will be the time for which the power tool is used during working day. In both cases it is necessary to recognize that exposure durations are non-continuous. A daily dose measure is expressed in terms of duration (e.g. 8 hours). Such measure is valuable in giving a simple numerical indication of the severity of a complex intermittent exposure. The period of daily tool use can be difficult to estimate due to highly varied and intermittent operations involved with some processes. This becomes more complicated when several different tools are used or other aspects involving frequent job changes are encountered. The calculation of the daily equivalent vibration magnitude from short sample measurements of rms weighted acceleration and simple estimates of exposure time may differ greatly from measurements obtained over longer periods or through out the entire day (Griffin, 1990). The minimum acceptable duration of measurements depends on the signal, instrumentation and operating characteristics. The total measurement time should be at least 1-minute. A number of shorter duration samples should be taken in preference to a single long duration measurement. It is advisable to take more than three samples to ensure a total sample time greater than 1-minute (ISO-5349-2, 1999).

1.2.6 HAV Standards

A number of standards have been established to assess the vibration dosage and the severity of hand-transmitted vibration. These efforts however, have achieved only moderate success due to lack of understanding of the etiology of VWF. While the relationship between the vibration dosages associated with vibration intensity, frequency and cumulative exposure duration, and the symptoms are not exactly known, certain norms on measurements, evaluations and reporting procedures have been established.

All standards suggest that vibration exposure be expressed in terms of rms acceleration in m/s^2 in the 1/3 octave band with center frequencies ranging from 6.3 Hz to 1250 Hz. These include the International Standard (ISO-5349, 1986), British Standards (BSI, 1987), American National Standard (ANSI, 1986) and American Conference of Governmental Industrial Hygienist (ACGIH, 1990). Different standards recommend the threshold values for the hand-arm vibration. It is considered that acceleration levels that fall below the recommended curves for a specified duration of exposure are considered to be acceptable. Figure 1.4 illustrates a comparison of the threshold limits of rms acceleration outlined in different standards (Taylor, 1973).

1.2.7 HAV Models

The severe health and safety risks posed by prolonged exposure to hand-held power tool vibration have prompted many studies to enhance an understanding of the vibration response characteristics of the hand-arm system. The epidemiological studies have identified the high prevalence rates of the vibration syndrome among the operators of power tools (Taylor, 1973; Suggs, 1982). Although many subjective and objective

clinical studies have identified various HAV symptoms, the primary injury mechanisms are not yet well known. The engineering studies have mostly concentrated on the design of effective protective devices and tools (Miwa, 1982; Suggs, 1982). All the studies however, have emphasized the need to enhance thorough understanding of the biodynamic response behavior of the hand-arm system.

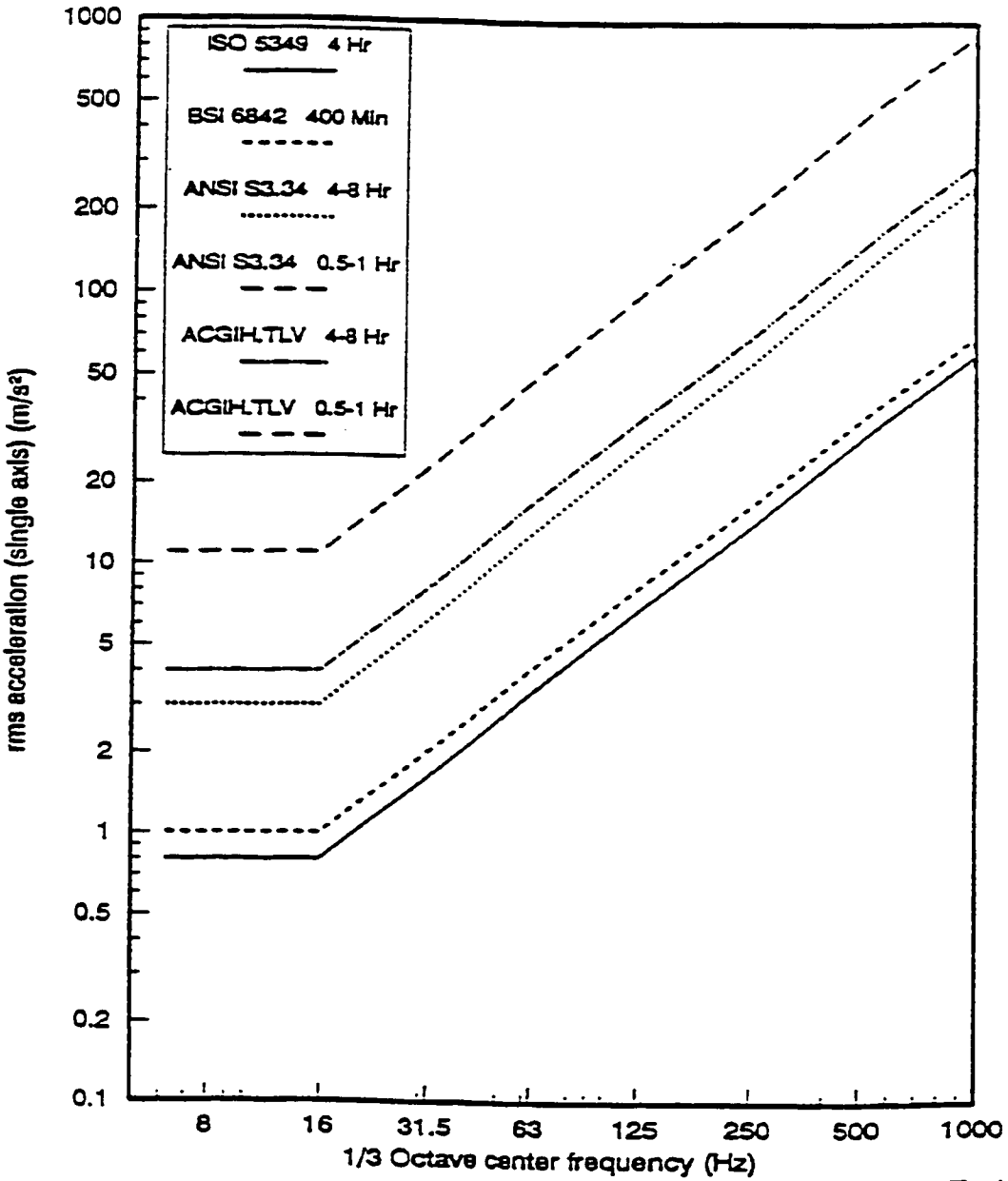

Figure 1.4: Hand-Arm Vibration standards proposed by different organizations (Taylor, 1973).

Owing to the complexity of the human hand-arm system, the hand-arm responses to vibration are mostly evaluated at the driving-point, the hand-handle interface, while treating the biological system as a "black box". Its response to vibration has been mostly described by the force-motion relationship at the driving point. Many studies have reported the biodynamic responses in terms of different measures that describe the force-motion relationship at the driving-point. This include: the dynamic stiffness, the complex ratio of force to displacement at the driving-point; the driving-point mechanical impedance (DPMI), the ratio of force to driving point velocity; the apparent mass (APMS), the ratio of force to driving-point acceleration; and the energy absorbed by the hand (ISO-10068, 1998; Reynolds, 1984; Burström, 1987, 1990; Mishoe, 1977; Hess, 1989).

Apart from the force-motion response, the biodynamic responses of the human hand-arm have also been characterized in terms of vibration transmissibility of the hand-arm system (Abrams, 1969; Abrams, 1968; Reynolds, 1977; Cherian, 1994; Pyykkö, 1976; Aatola, 1989; Rodriguez, 1989). These studies describe the vibration transmissibility of different segments of the hand-arm system, such as the metacarpal bones, wrist, elbow and shoulder. Majority of the studies involving measurements along the radius bone revealed presence of resonances near 125 Hz and 500 Hz.

The primary objective of the studies in biodynamic response of the human hand and arm have been two fold: (i) to enhance an understanding of the vibration transmission characteristics of the human hand and arm; and (ii) to develop simple models of the hand-arm system for applications in the performance analyses of the tool and vibration attenuation devices. The reported studies have, however, employed considerably different

vibration conditions and measurements methods. The reported biodynamic responses thus exhibit considerable differences among them, which have been partly attributed to variations in intrinsic and extrinsic variables, test conditions and methodologies (Gurram, 1995). On the basis of a synthesis of the reported data under somewhat comparable conditions, the International Standards Organization (ISO-10068, 1998) has proposed the range of idealized values of driving –point mechanical impedance of the human hand and arm exposed to vibration along the X_h, Y_h, and Z_h axes (ISO-10068, 1998).

A number of biodynamic models have also been developed on the basis of the measured data to characterize both the force-motion response in terms of DPMI and the vibration transmission behavior. These include the lumped-parameter (Mishoe, 1977; Reynolds, 1977; Miwa, 1979; Meltzer, 1979; Daikoku, 1990; Gurram, 1993; Reynolds and Soedel, 1997) and distributed-parameter models (Wood and Suggs, 1978), although majority of the models are of the lumped-parameter type. The lumped parameter models include the linear single-DOF (Abrams, 1969; Reynolds and Soedel, 1972), linear two-DOF (Mishoe, 1977; Miwa, 1979), and linear and non-linear three- and four-DOF models (Mishoe, 1977; Reynolds, 1977; Meltzer, 1979; Daikoku, 1990; Gurram, 1993).

These models do not represent biomechanical properties of the human hand and arm. While the impedance models provide considerable insight into the influence of various design and operating factors, such as grip force, handle size, direction and magnitude of vibration, and push-pull force, these models fail to characterize the vibration transmitted to the hand and the arm. The direct relationship between the severity of HAV syndrome and the characteristics of the hand-transmitted vibration have prompted a strong desire (i) to enhance an understanding of the vibration transmission

characteristics of the hand-arm system; and (ii) to improve the vibration attenuation on performance of protective devices. Although many studies have been carried out to assess the vibration isolation performance of protective devices, only a few efforts have been mounted to investigate the vibration transmission characteristics of the hand-arm system (ISO-5349, 2001; Reynolds, 1977; Pyykkö, 1976; Aatola, 1989; Hartung, 1992). Sub-miniature accelerometers and laser-based sensors have been employed to measure the vibration transmitted to the hand, forearm and upper-arm (Reynolds, 1977; ISO-5349, 2001). The vibration transmitted to various locations of the hand-arm system have been measured on a cadaver arm by Abrams (Abrams, 1968; Abrams, 1969)

The reported biodynamic models of the human hand and arm have been compared in a recent study (Rakheja et al., 2002). The study involved relative analyses of various lumped-parameter models in terms of three criteria: (i) ability of the models to characterize driving-point mechanical impedance modulus and phase responses of the human hand and arm within the range of idealized values (ISO-10068, 1998); models deflections under applications of a static feed force; and (ii) the natural vibration behavior of the hand and arm in terms of natural frequencies and damping ratios. The study concluded that the vast majority of the reported models couldn't be applied for development of mechanical hand-arm simulator or for the assessment of dynamic behavior of the coupled hand-tool system. While the higher order models provide impedance values within the range of idealized values, they exhibit excessive static deflections. Up to 0.5 m under a 50 N push force. Moreover, these models involve very light masses, in the 1.2-4.8 grams range, and exhibit first and/or second modes of vibration at frequencies below 10 Hz.

1.2.8 Control of Hand-arm Vibrations

High levels of hand-held power tool vibration, high prevalence rates of the VWF symptoms among the exposed workers and severe health effects, have all prompted a strong desire to reduce the magnitudes of hand-transmitted vibration. The control of hand-transmitted vibration in general, is achieved through reduction of the source vibration and the use of vibration isolators. The reduction in vibration at the source can be realized by operating the tool at suitable speed, proper maintenance of the tool and the drive and through improved designs of the drives (Politschuk, 1977).

Attenuation of hand-transmitted vibration is primarily attained using two methods. In the first method, the tool is isolated from the vibrating source, while the hand is isolated from the vibrating handle in the second method (Suggs, 1982; Abrams, 1969; Suggs, 1983; Cherian, 1994; Dong, 2001). Tool handle isolators, successfully integrated within certain tools, have proven to be effective in attenuating the handle vibration (Abrams, 1969). Alternatively, handle grips and anti-vibration gloves have been proposed to isolate the hand from the vibrating handle. The vibration attenuation properties of different types of visco-elastic glove materials have been investigated in many studies (Suggs, 1982; Miwa, 979; Macfarlane, 1979; Rakheja et al., 2002; Gurram et al., 1993).

Isolators, comprising rubber or metal springs, are currently being used within the chain saws to reduce the magnitude of HTV (Suggs, 1968). It has been established that these isolators effectively attenuate the high frequency vibrations. The low frequency vibration is transmitted to the handle with only little attenuation or amplification in certain cases. A study on vibration transmissibility characteristics of industrial gloves concluded that these gloves do not attenuate vibration to protect the hand from hazardous

levels of HAV encountered in the industry (Macfarlane, 1980; Dong et al., 2001; Rakheja et al., 2002). Numerous anti-vibration gloves comprising natural rubber, neoprene, sorbothane, plastic foam, air-filled alveolar, etc., have been commercially developed to isolate the hand from the vibrating handle (Suggs, 1982; INRS, 1983; Clarke, 1985). Rens (1987) reported that some of the gloves tend to amplify the hand vibration below 400-500Hz, and the attenuation approaches only 5 dB at certain frequencies. These gloves, however, attenuate vibration at higher frequencies with 15-20 dB attenuation at 1000 Hz, and these conclusions have been further confirmed by (Gurram et al. 1994). The uses of anti-vibration gloves, in general, are considered to be ineffective for attenuating the hand-transmitted vibration. The vibration attenuation performance of the gloves can be improved only at the expense of the dexterity loss (Rakheja et al., 2002).

1.3 Scope and Objectives of the Dissertation Research

Many epidemiological studies have identified several vibration-induced diseases among the hand-held power tool operators. The workers are affected by vibration white finger (VWF) disease at the fingertips and hands, loss of grip and muscle strength, injuries to bones and joints. Such severe effects of vibration on the operators have prompted several clinical studies to identify the primary injury mechanisms, and engineering studies to design protective devices and vibration isolators. Although the epidemiological studies have provided the vibration syndrome prevalence rates among the operators of typical offending tools, they do not provide an insight into the injury mechanism. Moreover these studies do not provide guidance on safe levels of vibration

exposure, as the syndrome was prevalent in all industries irrespective of the levels of vibration generated by the tools used in that industry.

Despite the lack of knowledge of the injury mechanisms, it is generally agreed that reducing the magnitude of vibration can reduce the health and safety risks associated with exposure to hand-transmitted vibration. Ergonomic design considerations would further help in reducing the risk. The reduction of vibration, however, has been mostly sought through anti-vibration gloves or resilient materials. Vast number of studies performed on the performance of gloves has invariably concluded that the gloves do not provide noteworthy vibration isolation. Moreover, the gloves may even amplify the vibration for certain tools. The reduction of vibration at the source and the hand, through appropriate design of the tools has drawn only limited number of studies.

The efforts made for chain saws have been quite successful in reducing the magnitude of HTV (Abrams, 1969). Apart from this study, only minimal effort has been made to study the vibration behavior of the tools. A first step in exploring low vibration emission tools would be to enhance an understanding of the behavior of tool vibration and contributing design factors. The vibration behavior of a percussive tool was investigated in a recent study that considered the impacts among various components of the tool and the effects of component properties on the transmitted vibration (Rakheja et al., 2002). The rotary tools, such as grinders, are known to yield vibration due to unbalance of the disk caused by the cutting action and non-uniform wear. The vibration analysis of a hand-held grinder, however, has not been reported in the literature. Furthermore, the fundamental response behavior of an automatic balancer has been reported only in a few studies (Nilsagard and Richmond, 1993; Rajalingham et al., 1998).

The scope of this study is thus to study the vibration behavior of a hand-held angle grinder due to mass unbalance. The dissertation research involves experimental and analytical studies of the HTV due to a hand-held grinder. The influence of automatic balancer on the magnitude of HTV is also investigated experimentally.

1.3.1 Objectives of the Dissertation Research

The primary objective of this dissertation research is to investigate the vibration behavior of a hand-held grinder due to mass unbalance. The dissertation research focuses on the measurement of the hand-transmitted vibration from an angle-grinder and the influence of the mass unbalance and the automatic balancer on the magnitudes of vibration. The nature of HTV is assessed in relation to the duration of vibration and the associated risk of developing VWF. A simple analytical model of the grinder coupled with the human hand-arm is also developed to study the effects of mass unbalance.

The specific objectives of this thesis are:

a. Develop a method for measuring the vibration levels of an angle-grinder transmitted to the hand-arm system.

b. Investigate the influence of various operating conditions on the nature of vibration transmitted to the hand-arm system, specifically the mass unbalance, feed force and speed.

c. Analyze and assess the severity of the measured vibration magnitudes with reference to (ISO-5349-1, 2001).

d. Study the influence of an automatic balancer on the magnitudes of transmitted vibration.

e. Develop a simple model of the coupled hand-grinder system and perform analyses.

1.3.2 Thesis organization

The thesis is divided into five chapters. The relevant literature is briefly discussed in each chapter to highlight the research contributions. Chapter 2 discusses the fundamental theoretical aspects of a rotor supported on a cantilever beam, subject to gyroscopic forces and moments, in order to build the necessary background for the formulation of the grinder model. Chapter 3 describes the laboratory experiments undertaken to characterize the nature of HTV, as a function of the mass unbalance and feed force. The basicentric coordinate system is used in this dissertation to define a 2-DOF human hand-arm model. This chapter further presents the measured data and the analyses for the assessment of HTV. The results are discussed in terms of frequency-weighted and time rms accelerations, 8-hour energy equivalent values and the limiting number of exposure years that could cause VWF symptoms in the 10% of the population. A simple analytical model is formed in chapter 4 to study the impact of mass unbalance on the handle vibration response. A simple two-DOF human hand-arm model is integrated with the shaft-rotor model to study the response behavior of the coupled hand-tool system. The major highlights and conclusions of the study are discussed in chapter 5. Moreover, Chapter 5 attempts to obtain the conclusion from the whole dissertation and suggestions for future investigations.

Chapter 2

Modeling of Rotor for Gyroscopic Effects

2.1 Introduction

Hand held grinding tools are widely used in the shipyard and foundry sectors. These may include vertical or horizontal grinders, which are mostly operated using pneumatic drives with air pressure ranging from 620.5-to 758.4 kpa (90 to 110 psi). It has been reported that the foundry workers use hand-held grinders for 2.5 hours to 4.5 hours on a daily basis (Wasserman et al., 1994). The vibration measurements performed on horizontal grinders revealed rms accelerations ranging from a low of 0.64 g while operating on cast iron to as high as 79 g while operating on gray iron. The vibration levels for vertical grinders were observed to be as high as 50 g rms. Owing to such high levels of hand-transmitted vibration and relatively longer exposure duration, a number of studies have identified high prevalence of vibration syndrome among grinding workers (Kihlberg, 1995; Wasserman et al., 1994; Kihlberg and Hagberg, 1997).

A horizontal grinder comprises a shaft rotor system supported on two closely spaced bearings. The vibration transmitted to the handle arises from the dynamic interaction of the rotor with the work surface and mass unbalance inherent in the rotor. An analysis of the grinder vibration under the forces and moments arising from the grinding action is highly complex due to difficulties associated with characterization of the excitation forces and moments. The measurements performed on hand-held grinders have shown the presence of predominant components in the vicinity of the rotating speed (Wasserman et al., 1994). This may be attributed to rotating mass unbalance inherent

within the rotor and that induced by the non-uniform cutting action. The dynamic analysis of hand-held grinders, in the first stage, may thus be carried out with consideration of the mass unbalance alone. A simple analytical model of the shaft-rotor system is thus formulated in this chapter that could be applied to study the mass unbalance induced grinder vibration.

2.2 Modeling Considerations

A horizontal angle grinder, shown in Figure 2.1, is considered to study its vibration behavior. The grinder consists of a spindle where a grinding wheel is attached. The angle grinder considered in this study has two handles; one along the grinder body and the second is adjustable with a range of ± 45°. The grinding wheel and the spindle is driven by a turbine pneumatic motor. The motor operates at a speed of 12,000 rpm and drives the wheel through a pair of bevel gears. The spindle is supported within the tool body through two ball bearing units. A balancing unit may also be attached to the spindle and the wheel to achieve automatic compensation for the mass unbalance induced forces and moments and thus the vibration.

The shaft rotor system may be considered as a cantilever rotor supported on two closely spaced bearings in the vicinity of the drive. Although a vast number of studies on the shaft-rotor systems have extensively investigated the dynamic response of the cantilever rotors (Bhat, 2001), no efforts have yet been made to apply these formulations in the study of grinders. The theoretical formulations associated with the shaft-rotor system are therefore systematically reviewed in this chapter in order to build background knowledge for formulating a simple model of the grinder, which is presented in chapter 4. These relevant theoretical formulations are presented in the following section

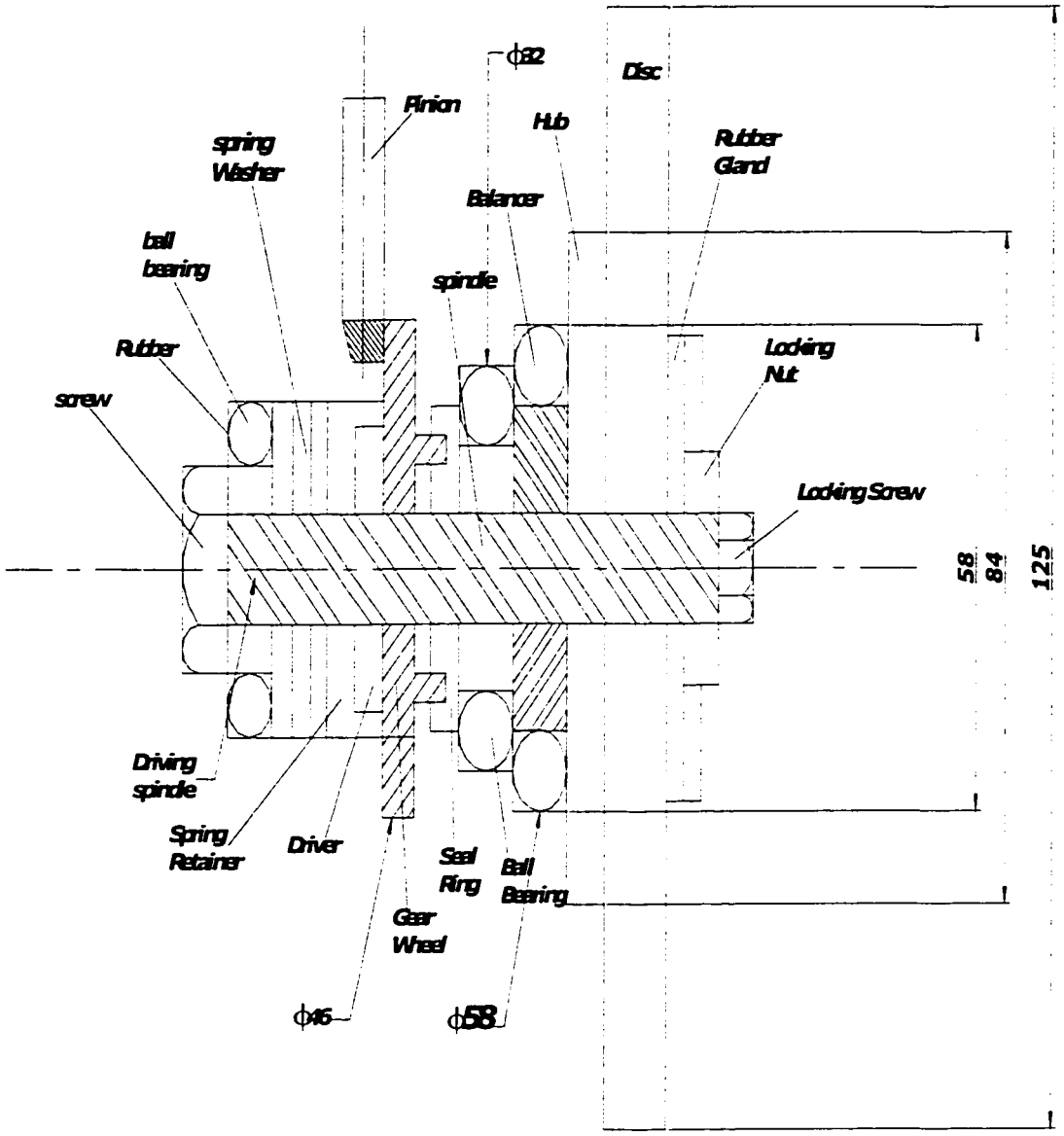

Figure 2.1: A cross-section of an angle grinder considered in the study.

2.3 Analysis of a Cantilever Rotor on a Flexible Shaft

In some grinding machines, the shaft rotor assembly characterizes a cantilevered rotor supported on a flexible shaft. The deflection of the shaft tends to result in a significant change in slope of the shaft, as shown in Figure 2.2. This may be the case when the rotor is not mounted at the center of a symmetrically supported shaft, or when the rotor is overhung. In that case the rotor will tend to whirl in an elliptical path (Goodwin, 1989), while the centrifugal forces may try to straighten the shaft, making it behave as if the forces constrain the shaft slope. This deflection of the shaft will increase its strength and accordingly its stiffness will also increase. As a result the natural frequency of the system will also increase. In Figure 2.2, the disk spins with an angular velocity ω about the rotational axis OZ. At the instant in time the rotor is also precessing with angular velocity $\dot{\phi}$ about the vertical axis, OY. The basicentric coordinate axes are shown in Figure 2.3. It shows the angular momentum vectors drawn parallel to the axis of rotation to which they refer to, the direction of rotation being counter-clockwise when viewed from the face of the rotor. Figure 2.4 shows the system angular momentum at any time t and at a small interval of time later. It can be inferred that the change in angular momentum over the time interval considered is $I_p \omega \phi$, where I_p is the polar moment of inertia of the rotor (Goodwin, 1989). The gyroscopic moment, which must be applied to produce this change, is equal to the rate of change of angular momentum, $I_p \omega \dot{\phi}$. The angular coordinates θ and ϕ represent the slopes of bending in the YZ and XZ planes, respectively.

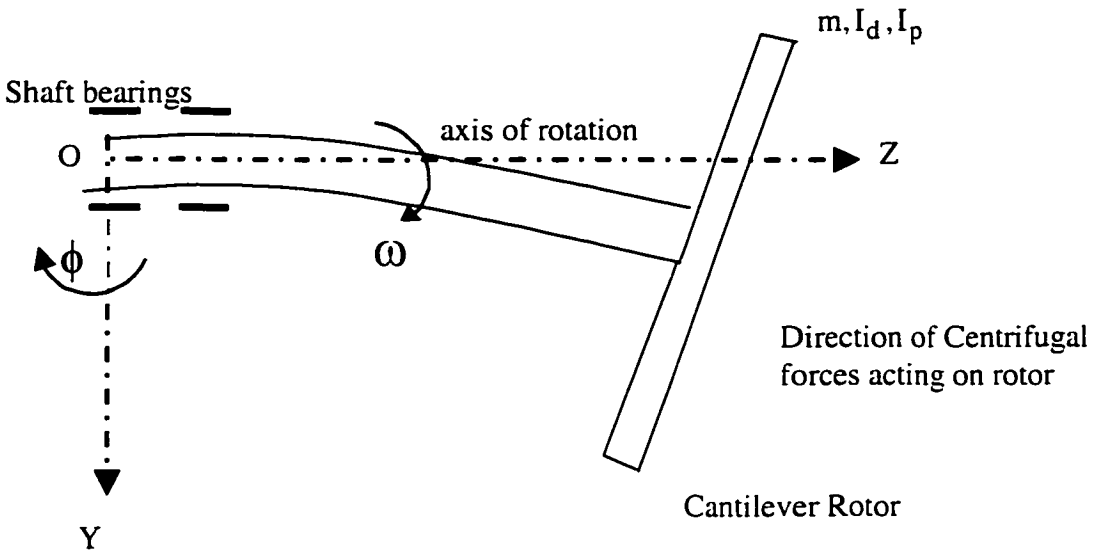

Figure 2.2:Cantilever rotor on a flexible shaft.

Figure 2.3 illustrates that the gyroscopic couple applied to the rotor, M_g, must act about the axis OX, since this axis corresponds with the orientation of the vector $I_p \omega \phi$ shown in Figure 2.4. The angular sense of this couple is clockwise about OX when viewed from O. The net moment about the axis OX is equal to the product of the rotor moment of inertia about the OX axis and the angular acceleration about the OX axis (Goodwin, 1989), such that:

$$M_x - M_g = I_d \ddot{\theta} \qquad (2.1)$$

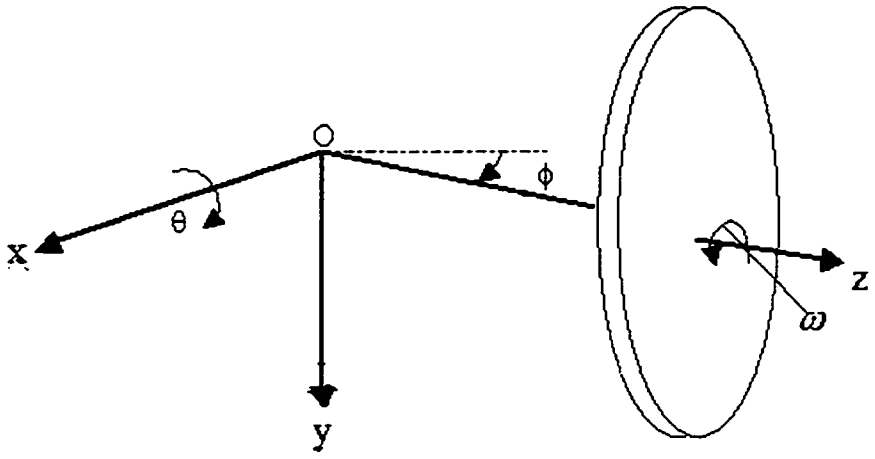

Figure 2.3: Coordinates representing the rotor motion.

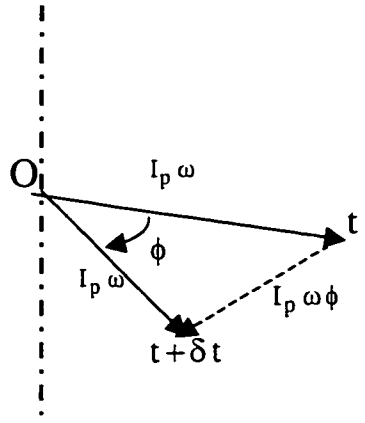

Figure 2.4: Vector diagram of the angular momentum.

where M_x is the moment applied to the rotor by the shaft, and I_d is the rotor moment of inertia about the diameter along the X axis. $\ddot{\theta}$ is the angular acceleration about the X axis. Equation 2.1 can be rewritten in the form:

$$M_x = I_p \omega \dot{\phi} + I_d \ddot{\theta} \tag{2.2}$$

The rotor motion in the XZ plane can also be described in a similar manner, such that:

$$M_y = -I_p \omega \dot{\theta} + I_d \ddot{\phi} \tag{2.3}$$

where M_y is the moment applied to the rotor by the shaft in the XZ plane and $\ddot{\phi}$ is the angular acceleration about the Y axis, and I_p is the polar mass moment of inertia of the rotor. The angular displacement of the rotor will be periodic and will take the form:

$$\phi = \phi_2 \cos \omega t + \phi_1 \sin \omega t \qquad \theta = \theta_1 \cos \omega t + \theta_2 \sin \omega t \tag{2.4}$$

where $\phi_1, \phi_2, \theta_1, \theta_2$ are the amplitudes of oscillatory motions in the XZ, and YZ planes. For an isotropic system, where the rotor support characteristics are identical in both transverse directions, the amplitude of motion θ and ϕ, will be equal. The equation (2.4) may thus be rewritten in the form:

$$\theta = \psi cos\, \omega t, \qquad \phi = \psi\, sin\, \omega t \tag{2.5}$$

where the motion in one direction lags behind that in the perpendicular direction by one quarter of a cycle. Differentiating Equations (2.5) and substituting into equations (2.2) and (2.3) yields the magnitude of the net moment applied to the shaft, which is equal and opposite to that applied by the shaft to the rotor:

$$M = -\left(I_p - I_d\right)\omega^2 \psi \tag{2.6}$$

where M is the magnitude of the net moment applied to the shaft, and the negative sign appears because the net moment acting on the shaft is opposite in direction of the moment applied by the shaft, and ψ is the slope of the shaft. From strength of materials the system deflection, z and slope of the shaft, ψ will take the form:

$$z = C_1 F + C_2 M, \qquad \psi = C_3 F + C_4 M \tag{2.7}$$

where C_1 and C_2 are the coefficients relating force and moment applied to the shaft at the location of the rotor to the shaft deformation, and F and M are the applied force and moment at the end of a cantilever rotor. For anisotropic systems, a similar set of equations may be written for the shaft deformation in the normal direction. In the case of an overhung cantilever rotor mounted on rigid bearings, equation (2.7) becomes (Bhat, 2001):

$$z = \frac{\ell^3 F}{3EI} + \frac{\ell^2 M}{2EI}, \qquad \psi = \frac{\ell^2 F}{2EI} + \frac{\ell M}{EI} \tag{2.8}$$

The force F is equal to $m\omega^2 z$ where m is the rotor mass, while the applied moment M is given by the equation (2.6), E is the Young's modulus for the shaft material, ℓ is the length of the shaft, and I is the shaft second moment of area. The term $\frac{\ell}{EI}$ is considered as the influence function of deflection and slope due to unit force or unit moment acting on the tip of the shaft. When substitutions are made for F, and M in equation (2.8), it becomes:

$$z=\frac{\ell^3 m\omega^2}{3EI}z-\frac{\omega^2\ell^2}{2EI}(I_p-I_d)\omega^2\psi$$

$$\psi=\frac{\ell^2 m\omega^2}{2EI}z-\frac{\ell}{EI}(I_p-I_d)\omega^2\psi \tag{2.9}$$

Rearranging the terms of equation (2.9)

$$\left(1-\frac{m\omega^2\ell^3}{3EI}\right)z+\left(\frac{I_d\omega^2\ell^2}{2EI}\right)(\beta-1)\psi=0$$

$$-\left(\frac{m\omega^2\ell^2}{2EI}\right)z+\left(1+\frac{I_d\omega^2\ell}{EI}\right)(\beta-1)\psi=0 \tag{2.10}$$

Where $\beta=\frac{I_p}{I_d}$,

The above homogenous set of equations would be satisfied for all values of z and ψ, only when the determinant vanishes, which gives the characteristics equation:

$$\left(1-\frac{m\omega^2\ell^3}{3EI}\right)\left(1+\frac{I_d\omega^2\ell}{EI}(\beta-1)\right)+\left(\frac{m\omega^2\ell^2}{2EI}\right)\left(\frac{I_d\omega^2\ell^2}{2EI}(\beta-1)\right)=0 \tag{2.11}$$

$$1+\frac{I_d\ell}{EI}\omega^2(\beta-1)-\frac{m\ell^3}{3EI}\omega^2-\frac{mI_d\ell^4}{3(EI)^2}\omega^4(\beta-1)+\frac{mI_d\ell^4}{4(EI)^2}\omega^4(\beta-1)=0$$

$$\left(\frac{mI_d\ell^4}{4(EI)^2}(\beta-1)-\frac{mI_d\ell^4}{3(EI)^2}(\beta-1)\right)\omega^4+\left(\frac{I_d\ell}{EI}(\beta-1)-\frac{m\ell^3}{3EI}\right)\omega^2+1=0$$

$$\omega^4+\frac{12(EI)^2}{mI_d\ell^4(\beta-1)}\left(\frac{3I_d(\beta-1)-m\ell^3}{3EI}\right)\omega^2-\frac{12(EI)^2}{I_d m\ell^4(\beta-1)}=0$$

$$\omega^4 + \left(\frac{4EI}{I_d \ell(\beta - 1)} - \frac{12EI}{m\ell^3} \right) \omega^2 - \frac{2(EI)^2}{I_d \ell^4 (\beta - 1)} = 0 \qquad (2.12)$$

The natural frequency of a shaft-rotor system assuming the rotor as a point mass is known to be $\omega_p = \sqrt{\frac{3EI}{m\ell^3}}$ (Goodwin, 1989). Substituting for $\omega_p = \sqrt{\frac{3EI}{m\ell^3}}$ and $\alpha = \frac{3I_d}{m\ell^2}$, where α is a coupling term from disc effect, equation (2.12) becomes

$$\omega^4 + 4\omega_p^2 \left(\frac{1}{\alpha(\beta - 1)} - 1 \right) \omega^2 - \frac{4\omega_p^4}{\alpha(\beta - 1)} = 0 \qquad (2.13)$$

Figure 2.5 illustrates a graphical representation of equation (2.13) as a function of α and a dimensionless natural frequency ω_p, for the case of $I_p = 2I_d$ which makes $\beta = 2$.

It is shown in the figure that for rotors with large α parameter values, the system natural frequency is almost double than that for the point-mass rotor system (Goodwin, 1989). α is equal to zero for a disc with a concentrated mass, while when I_d tends to be infinity, no finite angle ψ is possible, since it would need an infinite torque, which the shaft cannot support (Hartog, 1956). Gyroscopic effect tends to be particularly significant in situations where there is either an overhung rotor, with any force causing a slope of the shaft at the rotor, or when the rotor runs at very high speeds. In the case where the rotor itself forms most of the shaft, as opposed to the case where the rotor is disc-like, mounted on a relatively light shaft, gyroscopic effects are less significant, which is similar to the case of the pneumatic tool that will be discussed in chapter 4.

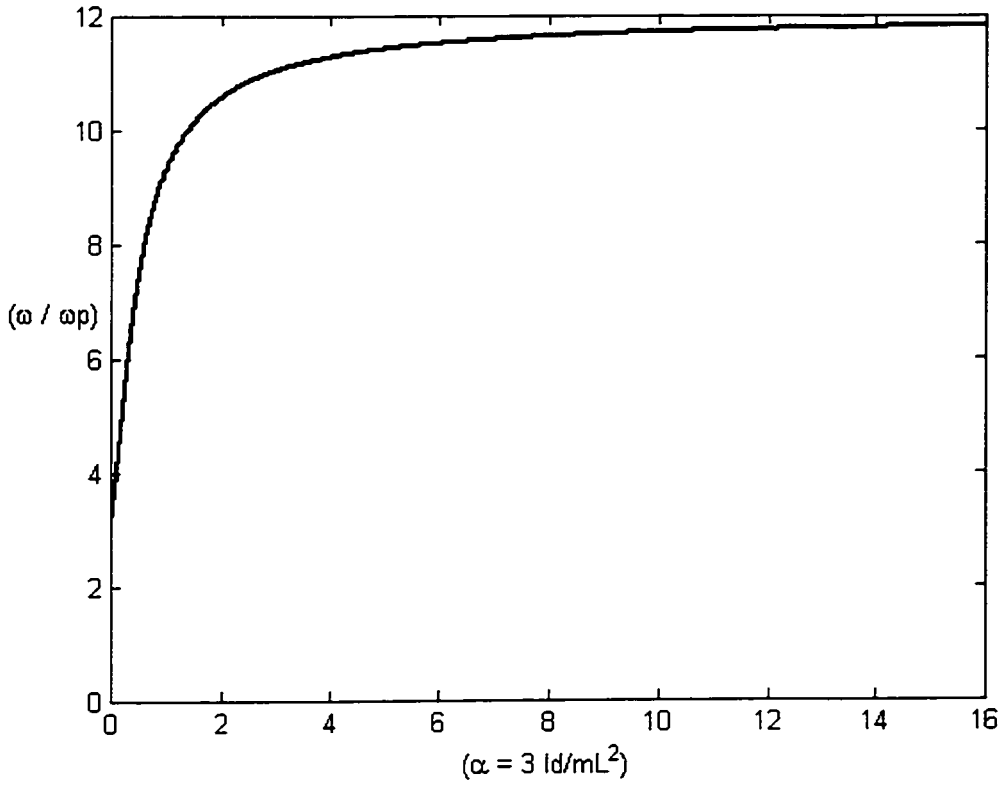

Figure 2.5: Effect of gyroscopic couple on the resonant frequency on a cantilever rotor.

Chapter 3

Experimental Investigations

3.1 Introduction

The severe health risks posed by prolonged exposure to hand-held power tool vibration, supported by the findings of the epidemiological studies, have prompted a strong need for a thorough understanding of the vibration responses of different tools and their assessments in relation to the risk of developing hand-arm vibration syndrome. While subjective measures provide considerable information related to minimum threshold and equal sensation, the inter-subject variations and poor repeatability of the subjective data pose difficulties in characterizing the effects of the tool vibration transmitted to the hand-arm system. Operation of hand-held power tools may expose workers to hand-transmitted mechanical vibration, which is known to interfere with comfort, working efficiency and, in some circumstances, the health and safety (Griffin, 1998). Depending on the nature of the tool and the work, the vibration may enter one arm only, or both arms simultaneously, and may be transmitted through the hand and arm to the shoulder. The vibration of the body parts and the perceived vibration are frequently a source of discomfort and possibly the reduced proficiency (Rajalingham et al., 2001). Continued occupational use of many vibrating power tools, has been found to be connected with various forms of disease affecting the blood vessels, nerves, bones, joints, muscles or the tissues of the hand and forearm.

The vibration exposures required to cause these disorders are not known precisely, neither with respect to vibration magnitude and frequency spectrum, nor with

respect to daily and cumulative exposure duration. The first step towards assessment of vibration exposure and perhaps for seeking design of safer tools, would be to characterize the nature of the hand transmitted vibration. In this study, the vibration levels of a hand-held angle grinder are measured in the laboratory under selected conditions. The measured data is analyzed to study the effects of mass unbalance, a balancer and the push force. The data gathered in this chapter may also assist in the development of improved designs of hand-operated power tools to reduce the risk of vibration-related health effects.

3.2 Description of the Candidate Tool

A hand-held angle grinder, manufactured by Atlas Copco, is considered in this study for performing laboratory measurements of the hand-transmitted vibration. An automatic balancer, considered to compensate for the rotating mass unbalance, is also included in the study. Majority of the hand-held power tools are known to transmit vibration along the three orthogonal directions, which are characterized by the basicentric axis system, defined in chapter 1 (ISO-8727, 1997). The measurement of vibration behavior of a power tool is quite complex as it is coupled with operator's hand and arm. The grinder selected in this study is shown in Figure 3.1. The tool is designed with two handles, and it consists of a pneumatic drive. The grinding wheel is mounted on a spindle that is supported between two closely spaced bearings. The free speed of the grinding wheel and spindle is 12,000 rpm, while it consumes 10 ℓ/s (21 cfm) of air in the 600-700 kpa (87-101 psi) pressure range under no load conditions, The rotating speed may decrease during cutting operation, while the air flow rate increases to 30 ℓ/s (64 cfm) at

the maximum power of 2.0 kW. The specifications of the grinder are summarized in Table 3.1

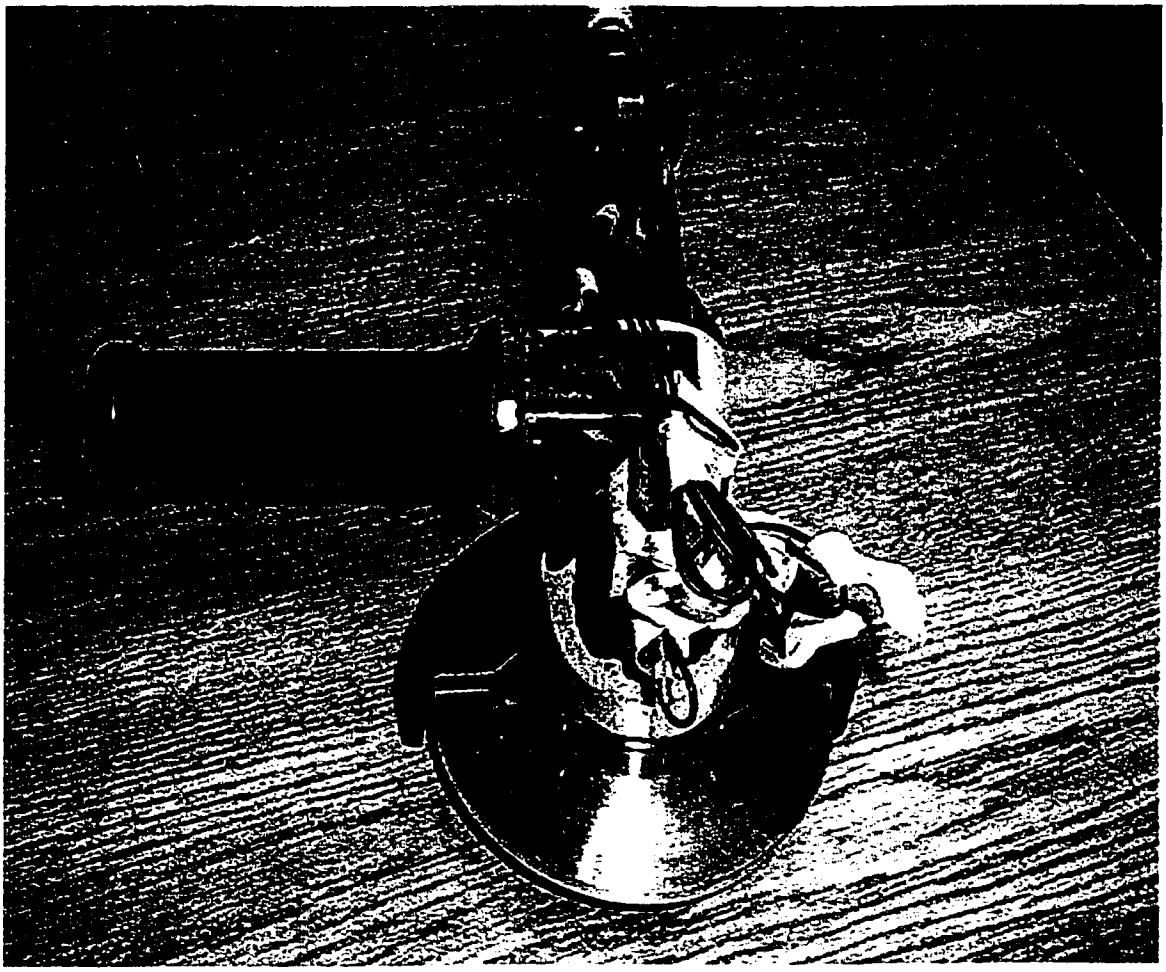

Figure 3.1: Pneumatic grinder with a rotor and handles.

Most of the lightweight hand-held rotating power tools operate at speeds ranging from 3000-5000 rpm. The air quality for such a machine in order to have a good performance and maximum machine life is recommended with dew point between +2 °C and +10 °C. An air dryer is required to increase the lifetime of the grinder. The tool uses lubricating oil of viscosity 32 Poise at 40 °C for the gearbox. A 7 mℓ tube is used to refill the tool with lubricating oil. A wheel guard is attached to the grinder and it covers half of

the rotor in order to ensure safety during operation. An automatic balancing unit (AUB) comprising of rolling balls within a groove, may also be attached to the grinding wheel in order to compensate for mass unbalance.

Table 3.1: Specifications of the grinder.

Description	Specification
Grinder Model	GTG 20 F120-13 angle grinder
Free Speed	12,000 rpm
Mass	1.8 kg
Air consumption at free speed	10 ℓ/s
Sound level	74 dB
Height over spindle	68 mm
Maximum wheel diameter D*T*H	125*7*22 mm
Length	273 mm
Air consumption at maximum power	30 ℓ/s
Air pressure	600-700 kpa

3.3 Test Methodology

The vibration of a majority of hand-held power tools is spread over a broad frequency range from 10 to 2000 Hz (ISO 5349, 1986). The vibration generated by hand-held power tool is a complex result of many factors, such as cutting forces and moments, contact vibration, internal impacts between the components within the tool (specifically the percussive tools), pneumatic or electric drive and associated air flows (Rakheja et al., 2002). A rotary tool, such as a grinder, experiences vibration mostly due to grinding wheel-workpiece interactions and the mass unbalance. The characterization of cutting forces, however, is quite complex due to significant variations in the tasks and processes,

working posture, feed forces, condition of the wheel, etc. The grinding wheels also exhibit considerable mass unbalance due to dirt build up, non-uniform wear, uneven weight distribution, etc. Such unbalance not only causes considerable vibration but also yields poor quality of the workpiece or manufactured product. Owing to extreme complexities associated with characterization of cutting forces, the role of rotating mass unbalance on the nature of the HTV alone is investigated in this study.

Many studies have reported that the nature of HTV from a power tool may be affected by the magnitude of a feed force imparted by the operator (Lindell, 1996). The measurements are thus performed for different magnitudes of feed force held constant in each trial. A weighing scale and cord and pulley arrangement as shown in Figure 3.2 was used to estimate the feed force. The grinder was attached to a load suspended on a cord and passing through a pulley in order to control the feed force. The body weight of each subject operating the grinder was initially recorded. Each subject was advised to stand on the weighing scale while holding the grinder attached to the cord and the counter weights. The subject was advised to hold the tool with each hand placed on each of the two handles, and push the tool downwards until the desired feed force was attained. The feed force was estimated from the difference between the total body weight and the body weight measured while pushing on the handle. The subject maintained the dominant right arm holding the grinder horizontal with 0° elbow angle and the left arm with near 90°-elbow angle. The subject monitored the weigh scale reading and maintained the desired reading within ±2 kg while operating the tool. The feed force applied on the machine was held constant at different values in the 0 to 100 N range in order to study the effect of the feed force. The posture of the operator should be as in Figure 3.2, where the left hand

makes a 90° and the right hand makes an angle near 0°, while the operator assumes an upright posture.

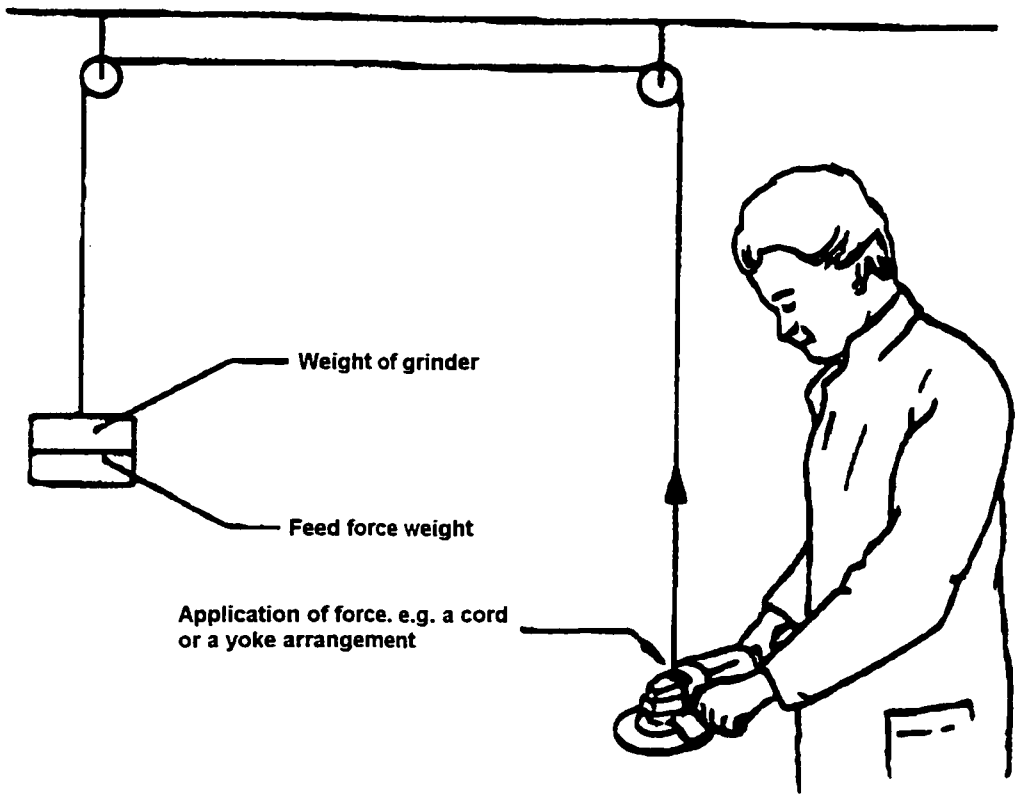

Figure 3.2: A schematic representation of the test setup.

The vibration transmitted from a hand-held power tool is conveniently measured through accelerometers. Since the tools may cause considerable vibration along all the three axes, a three-axis accelerometer was used to measure the vibration levels as recommended in (ISO-5349-1, 2001) and (ISO-8662-4, 1994). The measurements were performed on a new and adequately lubricated tool as outlined in the standard, (ISO-

8662-4, 1994). Three single-axis accelerometers (Brüel and Kjaer 4382) were used to capture the tool vibration signals from the grinder body. This location is considered to represent the vibration measured at the tool handles, since the handles are rigidly mounted to the tool body. Three accelerometers were attached to a square block that was fastened to the tool body near the handles. Instrumentation adhesive was used to attach the accelerometers block to the body. All the three accelerometers were rated for 2000 g peak acceleration with resonant frequency around 30 KHz. Each accelerometer was calibrated prior to the installation. The accelerometer signal was conditioned and amplified using charge amplifiers, which were acquired and analyzed using a two-channel signal analyzer (Brüel and Kjaer 2635). A tachometer was further used to measure the rotating speed of the grinding wheel corresponding to the selected operating pressure of 517 kpa (75psi). A reflective marker was placed on the rotating disc to provide the reflective pulse signal to the photocell tachometer. The international standard (ISO-2866-4) recommends that the measurements be made on both handles along the z-direction. The ISO-8662-4, 1994 recommends that the axes system for straight grinders along z-direction is normal to the axis of rotation, and for vertical and angle grinders the z-direction is parallel to the axis of rotation. The schematics of different types of hand-held grinders are shown in Figure 3.3 together with the transducers and the basicentric coordinate system. The installations of three-axis accelerometers in the present study on the tool body represents a location close to both handles. The basicentric coordinate axis system was used in this dissertation where the y-axis is along the handles of the grinder and z-axis is along the human hand-arm system and the x-axis is along the axis of rotation.

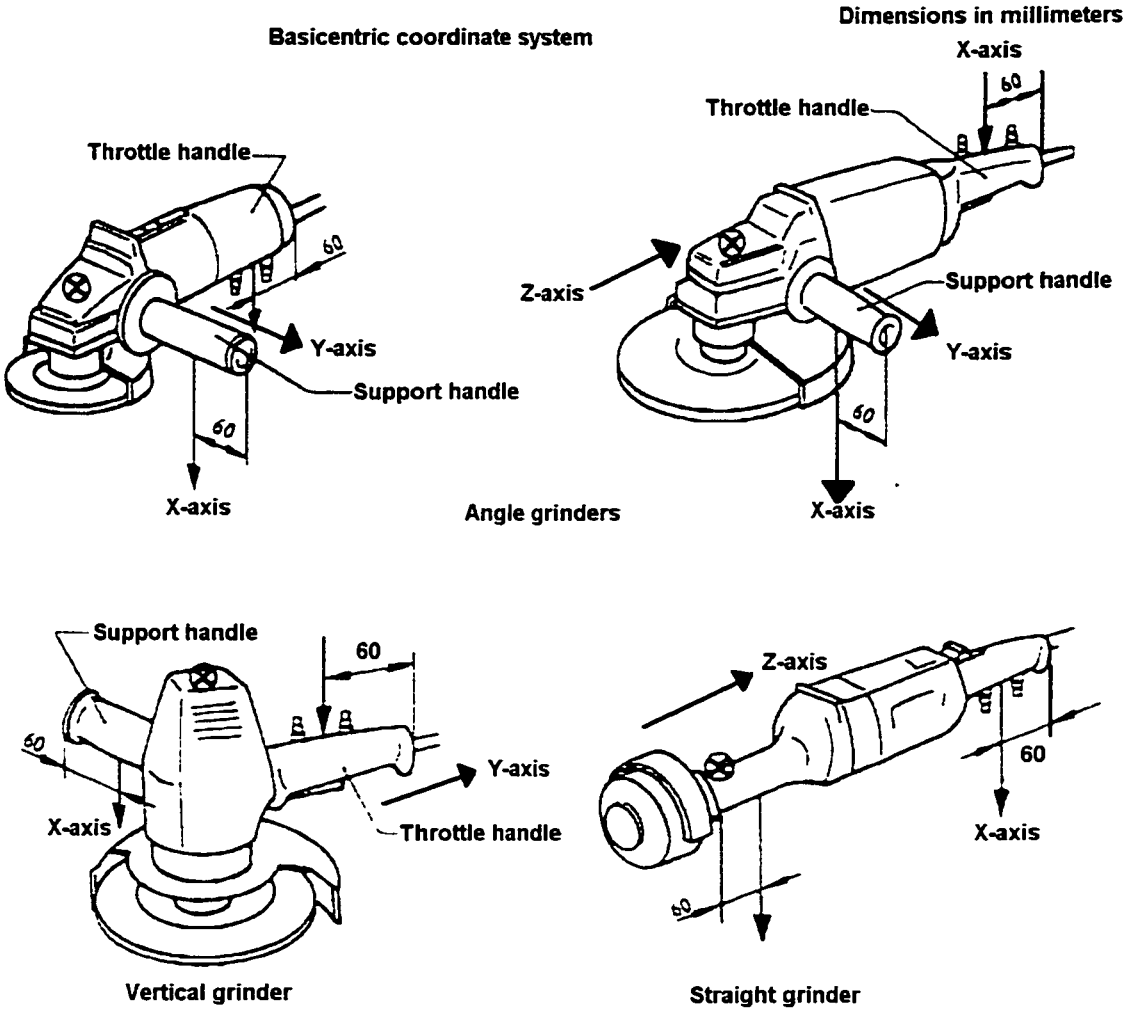

Figure 3.3: Different types of hand-held grinders.

◄——►| Examples of positioning transducers.

⊗ Point of attachment of accelerometers.

——► Direction of measurements.

In order to study the influence of rotating mass unbalance of the disc, a balanced aluminum disc replaced the grinding wheel. Two aluminum discs with outer diameter of 125 mm, thickness of 7 mm, and inner diameter of 22 mm were used in the experiments.

Each wheel was mounted concentrically on the grinder spindle. After mounting they were examined to ensure the absence of clearance or play. A concentric adaptor bushing was used for this purpose. One of the test discs was designed with three 13.4 mm diameter holes to create different controlled values of mass unbalance by attaching different masses to each of the hole. The design illustrated in Figure 3.4 shows the three holes and the automatic balancing unit (AUB). The unbalance due to the three holes was estimated as 76 gm-mm. Attaching a bolt and a washer to one of the three holes obtained additional values of mass unbalance. The mass unbalance values resulting from the bolt attached to the three holes were estimated as 295, 402, and 510 gm-mm, in the respective order from the hole closer to the center of the disc. Both discs were further designed to adapt to an automatic balancing unit (AUB) produced by SKF, which consists of 7 lubricated freely moving balls in a sealed circular shield, as shown in Figure 3.4. The three holes were drilled such that two of them remained outside the periphery of the AUB. The bolt and the washer were attached to one of the three holes during different experiments. The mass of the bolt and the washer together was 10 grams, while that of the balanced and unbalanced discs were measured to be 300 grams and 275 grams, respectively. A pictorial view of an idealized test disc with attached unbalance mass in the form of a bolt is presented in Figure 3.5.

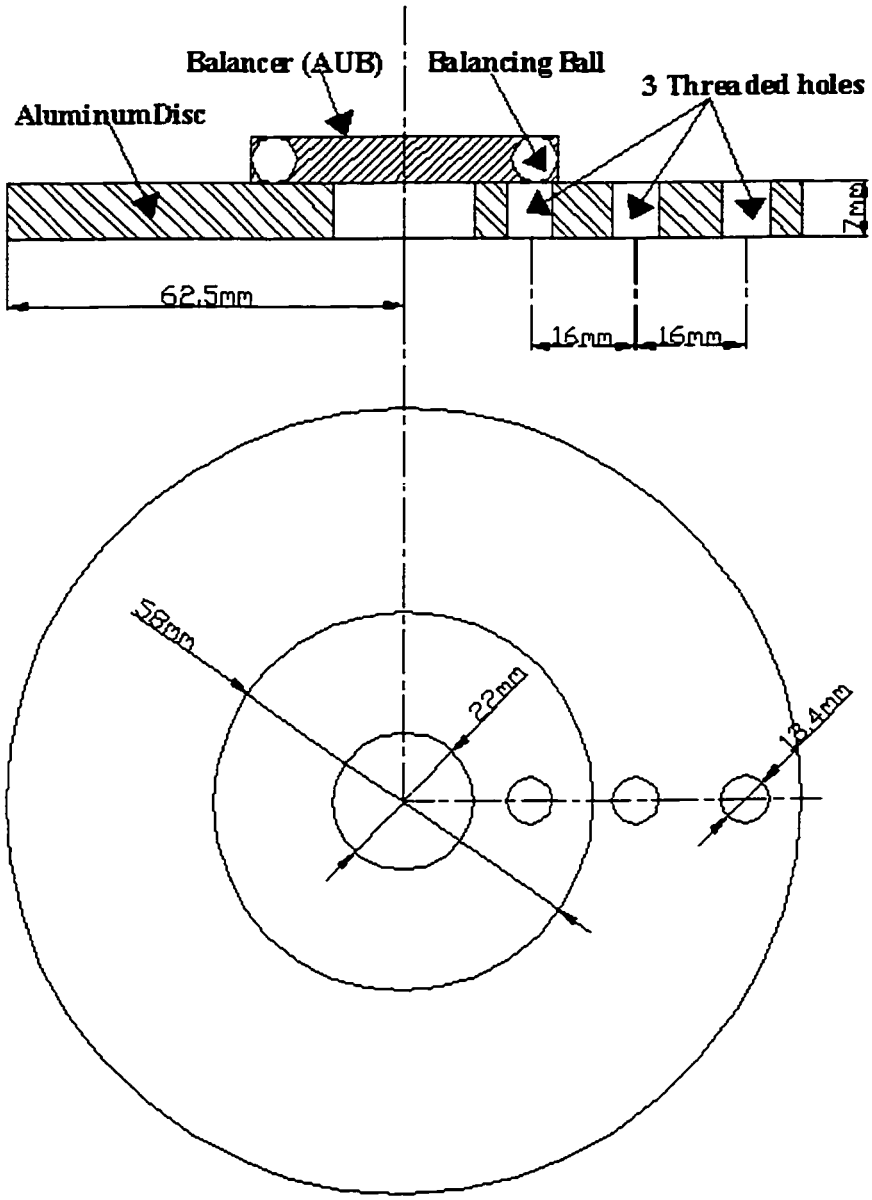

Figure 3.4: The design of the test disc with three holes to realize different values of mass unbalance.

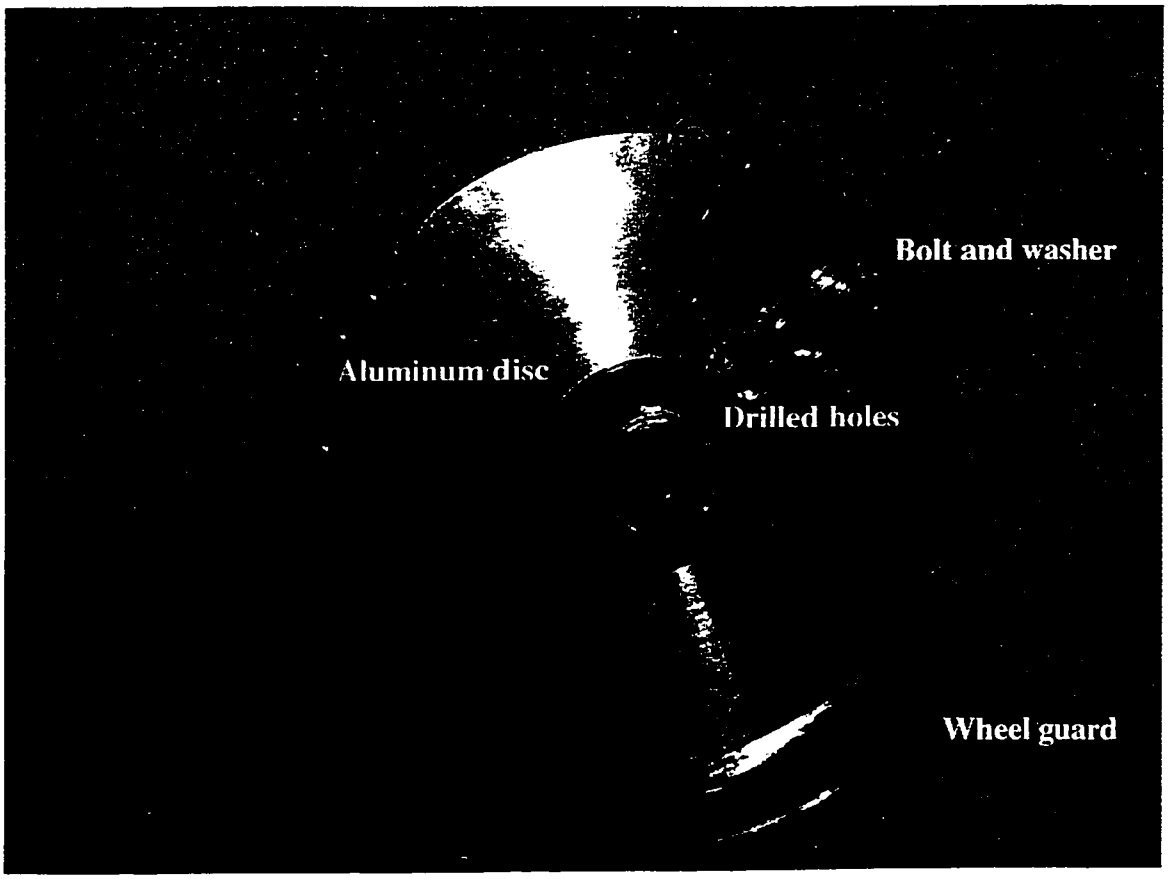

Figure 3.5: A pictorial view of the test disc showing holes and attached unbalance mass.

3.4 Experiment Design and Test Matrix

Figure 3.6 shows a schematic diagram of the experimental setup. The power source, which is the air supply, enters the grinder while the speed is controlled by a switch on the grinder and the source pressure. The experimental setup included three accelerometers mounted on a common block, as shown in Figure 3.7. The accelerometer signals were conditioned using charge amplifiers. The signal capture and analysis was initiated when the grinder reached its steady speed. In order to perform a test at a constant speed, the source pressure was monitored and carefully controlled. A pressure sensor was installed on the pressure line and the experiment was initiated only when the line pressure

reached the desired value of 517.10 kpa (75 psi). Two two-channel (Brüel and Kjaer 2635) signal analyzers were used to analyze the three acceleration signals. Both the analyzers were synchronized using a common trigger signal. Figure 3.8 illustrates a pictorial view of the two signal analyzers, together with the charge amplifiers. The experiments were also attempted on the grinder alone in the absence of the human hand by clamping the grinder in a vice-grip. The purpose of such experiments was to study the grinder vibration in the absence of the human hand. These experiments, however, revealed poor repeatability due to inadequate clamping of the vice-grip and relatively large centrifugal forces and moments developed by the grinder. The experiments were conducted with two adult male subjects. Each experiment was repeated three times.

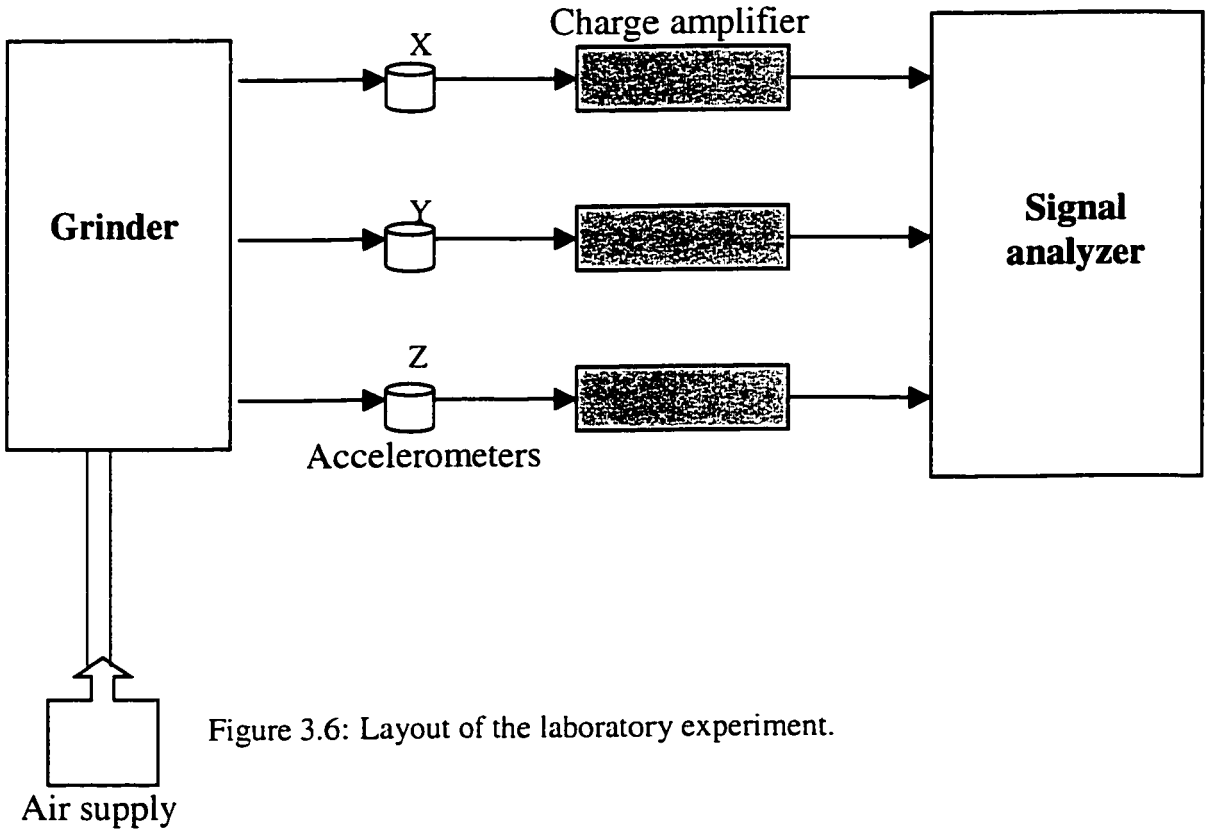

Figure 3.6: Layout of the laboratory experiment.

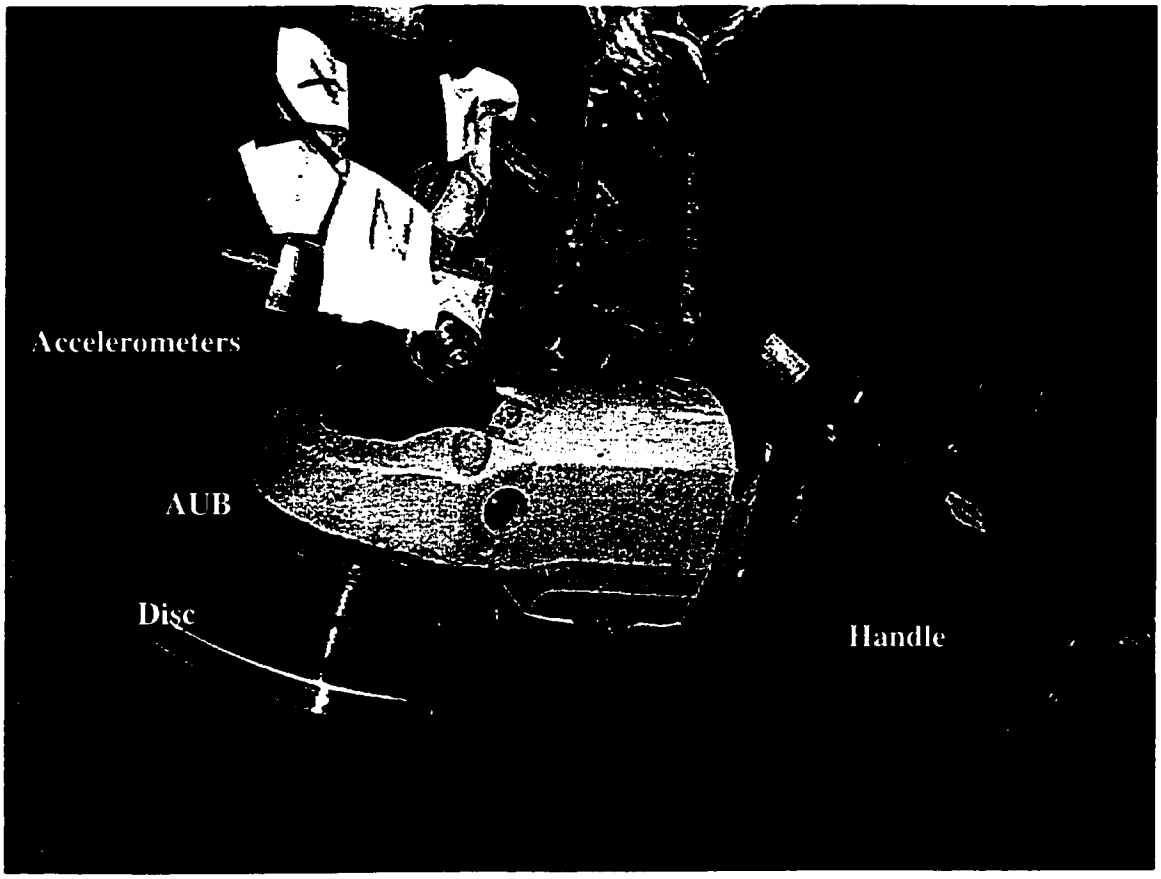

Figure 3.7: A pictorial view of the grinder with accelerometers and string hooks.

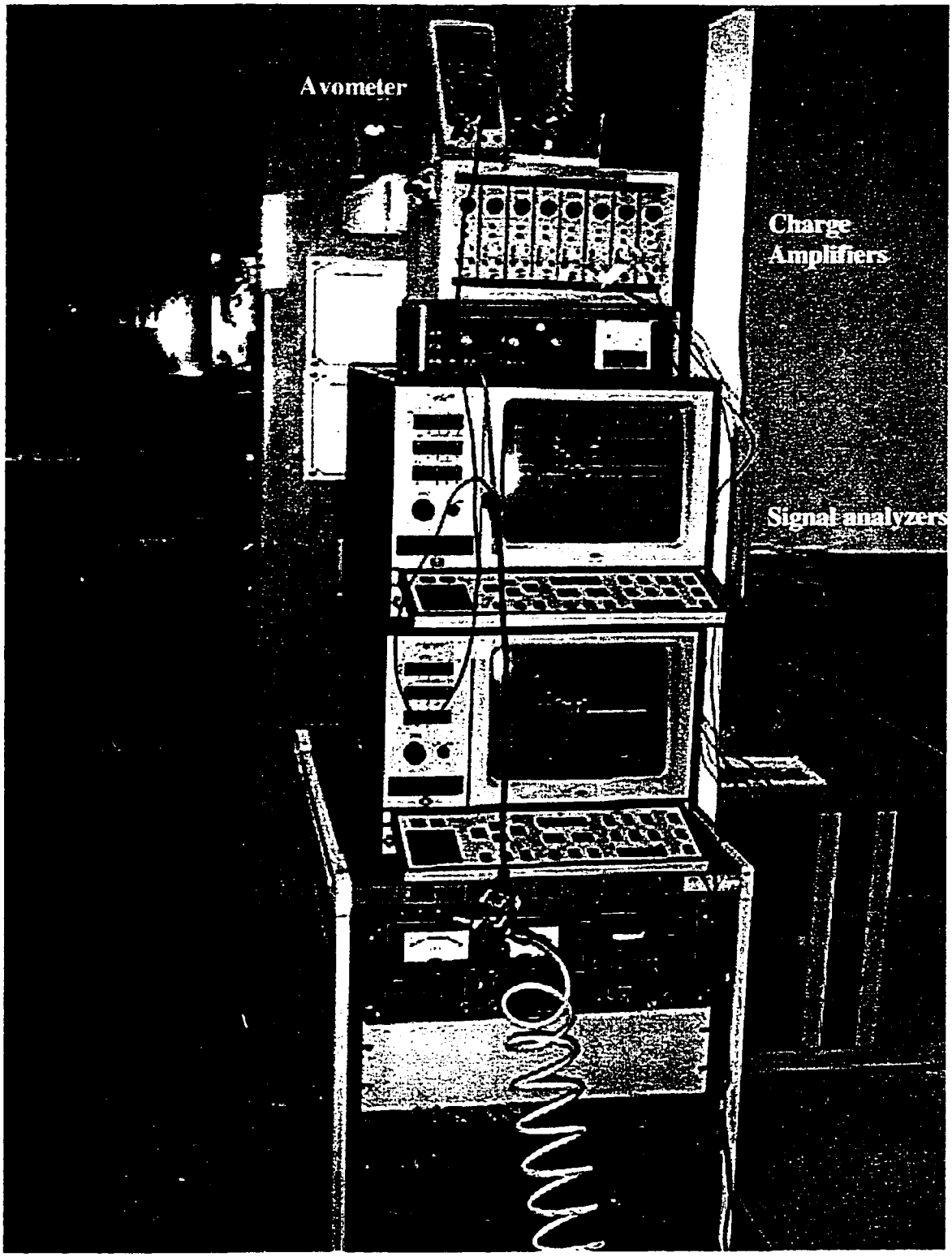

Figure 3.8: A pictorial view of the signal analyzers and charge amplifiers.

The test matrix included combinations of 4 levels of feed forces (0, 50, 75 and 100 N), 5 levels of rotating unbalance including the balanced disc (0, 76, 295, 402 and 510 gm-mm), 2 levels of balancer (on and off) and two subjects. Tables 3.2 and 3.3 summarize the test variables and test matrix.

Table 3.2: Test Matrix.

	AUB on					AUB off				
Feed force	Balanced disc	Unbalance gm-mm				Balanced disc	Unbalance gm-mm			
		76	295	402	510		76	295	402	510
0 N	✓	✓	✓	✓	✓	✓	✓	✓	✓	✓
50 N	✓	✓	✓	✓	✓	✓	✓	✓	✓	✓
75 N	✓	✓	✓	✓	✓	✓	✓	✓	✓	✓
100N	✓	✓	✓	✓	✓	✓	✓	✓	✓	✓

✓ **Experiment has been conducted along with feed force on both discs.**

Table 3.3: Test Variables.

Variable	Values
Feed Force (N)	0, 50, 75, and 100
Mass unbalance gm-mm	0, 76, 295, 402, and 510
Subjects	S1, S2
Balancer	On, Off
Speed rpm	7,500 at 75 psi air pressure

3.5 Automatic Balancing Unit

Balancing of rotating imbalance varying in time is best accomplished by autobalancing masses. The type of imbalance can be static, dynamic or a combination of both. Depending on the design of the autobalancers, continuous or discrete balancing can be achieved. The discrete balancing usually involves some sort of locking mechanism of the correction masses (Adolfsson, 1997). The most noticeable system parameter, regarding continuous balancing, is the rotational speed.

The term auto in autobalancing refers to the fact that it is a passive system, where no active forces or controllers are applied to move the correction masses. The concept of autobalancers has been introduced over 80 years ago and the first patent exists from the 1920's (Agafonov, 1976). Although the use of autobalancers in rotary power tool is not widespread, there exist many different patents on the subject, mostly regarding the design of the locking mechanism of the moving correction masses (Adolfsson, 1997). The limited applications of autobalancers may be attributed to many factors. For example, the magnitude of forces that move the correction masses to their adequate location are relatively small compared to the centrifugal forces.

3.5.1 Principle of AUB

Figure 3.9 shows a schematic of the automatic balancing unit, (AUB). As shown in the Figure, the center of mass 'M_C' and the geometrical center 'G_C' do not coincide, while the disc is rotating under a mass unbalance. Operating at over-critical speeds, as in the case of hand-held tools, the disc rotates around its mass center. When the auto balancer is fitted on the drive spindle, these forces would affect the position of the balls inside the race or groove within the AUB. In Figure 3.9, F_c is the centrifugal force with

origin at the mass center of the unbalanced disc, and F_n is the normal force acting between the moving masses and the guide within the AUB.

Since the above two forces do not counteract exactly, a resulting force, F_r, is developed making the balls move along the raceway. The balls will stop when a state of equilibrium is reached, which yields a balanced disc using the masses of the balls. At this state, 'M_C' and 'G_C', describing the mass center and geometric center, respectively, coincide and the magnitude of F_c approaches equal and opposite to F_n. Balancing usually takes not more than 100 ms (Nilsagard, 1993). The total balancing capacity of an AUB depends on the number and the sizes of the balls and the diameter of the raceway. With imbalance changes during operation, the balls tend to continuously adapt to their counteracting positions. Low friction between the balls and raceways is therefore essential for adequate response. The AUB used with the grinder in this study consists of 7 balls with high surface-finish that rotate freely within the raceway. A lubricant of high viscosity is also used in the AUB to overcome the friction between the balls and the runway path. Only a few reported studies have been found in the literature, which on the basis of measured data have established that the use of an AUB can reduce the magnitudes of HTV considerably (Nilsagard, 1993; Lindell, 1993).

3.6 Data Analysis

The important factors that greatly affect the human exposure to hand-transmitted vibration in a working environment include: (i) the frequency components of vibration; (ii) the magnitudes of vibration; (iii) the duration of exposure in a working day; and (iv) the cumulative exposure to date. Some other factors, which may influence the effects of

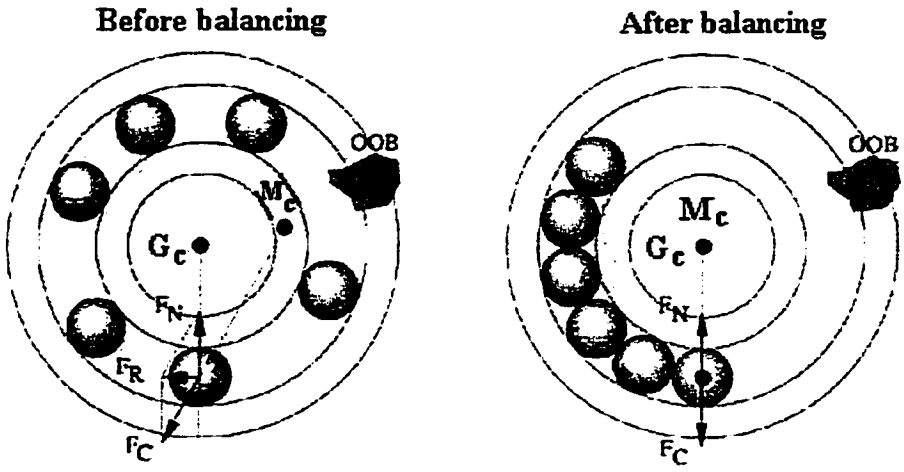

Figure 3.9: Orientations of the moving masses in the race of the AUB unit (Nilsagard, 1993).

vibration exposure, are the direction of vibration transmitted to the hand, the method of working and operator's skill, the individual's age and health, and feed and grip forces imparted on the tool. The current standards on hand-arm vibration provide guidelines to the measurement and assessment of the severity of vibration in the immediate vicinity of the hand (ISO-5349-1, 2001; ANSI, and ACGIH, and NIOSH, 1989). This is based upon the findings of the epidemiological studies that provided dose-response relationship to describe the risk of VWF as a function of the vibration measured on the handle near the hands. The current standard proposed by ISO recommends that the vibration be measured and analyzed in the 5-1500 Hz frequency range (ISO-5349-1, 2001). All of the reported standards recommend the use of rms acceleration to characterize the magnitude of HTV. The ISO-5349-1 (2001) provides a frequency weighting function to derive the overall frequency weighted rms acceleration. Figure 3.10 illustrates the frequency variation of the recommended weighting function.

The measured data in this study are analyzed to derive the rms acceleration spectra in the 1/3-ocatve frequency bands to study the dominant frequency contents of the HTV. The overall unweighted rms accelerations are computed from:

$$a_{rms} = \sqrt{\frac{1}{N}\sum_{i=1}^{N} a^2(f_i)} \tag{3.1}$$

where $a(f_i)$ is the vector sum of the three components of rms accelerations along x, y, and z directions corresponding to the center frequency of the *ith* 1/3-octave band. Further, a_{rms} is the overall unweighted rms acceleration, and N is the number of third-octave bands considered.

The recommended frequency-weighting filter is applied to determine the frequency-weighted rms accelerations along the three-axes. The effective magnitude of the frequency-weighted acceleration is computed from:

$$a_{rms\_w} = \sqrt{\frac{1}{N}\sum_{i=1}^{N} a_w^2(f_i)} \tag{3.2}$$

where a_w is the frequency-weighted rms acceleration derived from the weighting-function corresponding to center frequency f_i of the *ith* third-octave band, and a_{rms_w} is the overall frequency-weighted rms acceleration due to HTV in m/s^2.

When evaluation of exposure to hand-transmitted vibration is carried out in accordance with (ISO 5349, 1986), the following information must be available: (i) the total value of vibration for each operation as determined from the effective frequency-weighting magnitude in Equation (3.2); (ii) the daily vibration exposure; (iii) the location and orientation of the transducers; (iv) the total daily duration for each operation; (v) the

power tools, inserted tools and/or work pieces involved; (vi) the subject of the exposure evaluation; and (vii) the operations causing exposures to vibration.

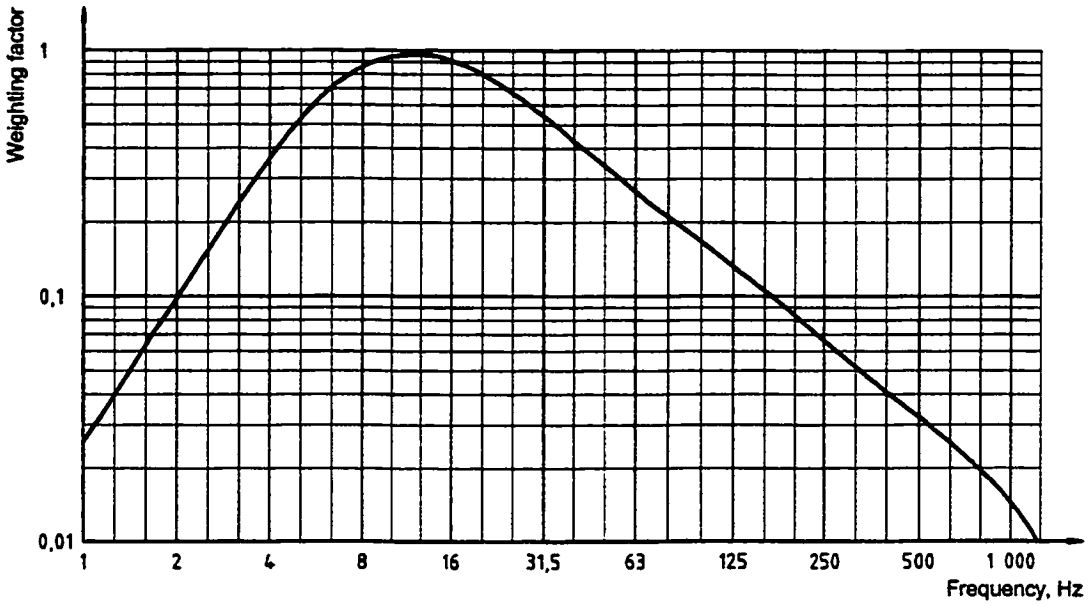

Figure 3.10: Frequency variation of the weighting function recommended in (ISO-5349-1, 2001).

3.6.1 Daily Vibration Exposure and Assessment

Vibration exposure is dependent on the magnitude of the vibration and on the duration of the exposure. Daily exposure duration is the total time for which the hands are exposed to vibration during a working day. The exposure duration may be shorter than the time for which the person is working with the power tools or work pieces. It is important to base estimates of total daily exposure duration on appropriate representative sample for various operating conditions, and durations and their intermittency. Daily vibration exposure is derived from the magnitude of the vibration (vibration total value) (ISO-5349-1, 2001) and the daily exposure duration. In order to facilitate comparison between daily exposures of different durations, the daily exposure shall be expressed in

terms of the 8-h energy-equivalent frequency-weighted vibration total value, $A(8)$, which is computed from:

$$A(8)=a_{rms\_w}\sqrt{\frac{T}{T_o}} \tag{3.3}$$

where T is the total daily duration of exposure to vibration a_{rms_w} and T_o is the reference duration of 8 h (28,800 sec).

In the event that the total daily vibration exposure consists of several intermittent operations with different vibration magnitudes, the daily vibration exposure, $A(8)$, is obtained from:

$$A(8)=\sqrt{\left(\frac{1}{T_o}\sum_{i=1}^{n} a_{rms\_wi}^2 T_i\right)} \tag{3.4}$$

where a_{rms_wi} is the frequency weighted vibration total for the *ith* operation, n is the number of individual vibration exposures, and T_i is the duration of the *ith* operation. In this study the measured data is analyzed to derive the 8-hour equivalent energy, $A(8)$, for assessment of severity of vibration exposure. The standard further provides a dose-response relationship relating the 8-hour equivalent value to the number of years of exposure over which 10% of the population may acquire VWF. The computed values of $A(8)$ are therefore used to assess the risk as a function of the mass unbalance. It is essential to note that no attempts were made to study the inter-subject variability due to small subject sample. The repeatability of the measured data, however, was examined for selected experiments. The measured data for each experiment is analyzed to derive rms

acceleration spectra, and overall unweighted and frequency-weighted rms acceleration, using Equations (3.1) and (3.2). The data acquired during the three trials are analyzed to examine the mean and standard deviations for each subject. The data revealed relatively large values of coefficients of variation for both subjects. These values were similar to those reported in the literature and could be attributed to an array of operating factors, such as variations in the hand-arm posture, variations in hand positions on the handles, and variations in the orientation of the tool and the hands.

It is known that on most power tools, the vibration entering the hand contains contributions from all three-measurement directions. It is assumed that vibration in each of the three directions is equally detrimental. The evaluation of vibration exposure is based on the vibration total value or the vector sum, a_v, is defined as the root-sum-of-squares of the three component values:

$$a_v = \sqrt{(a_x^2 + a_y^2 + a_z^2)} \tag{3.5}$$

where $a_x = \sqrt{\left(\frac{1}{T} \int_0^T \ddot{x}^2 \, dt \right)}$; $a_y = \sqrt{\left(\frac{1}{T} \int_0^T \ddot{y}^2 \, dt \right)}$; $a_z = \sqrt{\left(\frac{1}{T} \int_0^T \ddot{z}^2 \, dt \right)}$

where a_i is the root-mean-square (r.m.s) single axis acceleration value of the hand-transmitted vibration, in m/s^2 along the direction i. $i = x, y, z$. The assessment of severity of vibration, however is based upon the total value of the frequency weighted acceleration (ISO 5349-1, 2001), given by:

$$a_{vw} = \sqrt{(a_{wx}^2 + a_{wy}^2 + a_{wz}^2)} \tag{3.6}$$

Figures 3.11 to 3.14 illustrates a comparison of the rms acceleration spectra of the vibration measured during three independent trials with one subject under a feed force of 50 N and different values of mass unbalance with the AUB. The figures illustrate the intra-subject variability, as an example, from the three trials of measurements along the x, y, and z directions. The three trials are designated as x1, x2, and x3, respectively, for the x-direction. The results show reasonably good repeatability in the majority of the measurements. The large variations in the rms acceleration response can be seen by comparing Figure 3.11, which represents a mass unbalance of 76 gm-mm and Figure 3.14, which represents a mass unbalance of 510 gm-mm. The dominant frequency was around 125 Hz. The measured data reveals that the mass unbalances of 295 and 402 gm-mm, imparts considerably higher levels of vibration along the x-axis when compared to that along the y and z axes as shown in Figures 3.12 and 3.13. The magnitude of vibration corresponding to the fundamental frequency of 125Hz along all the directions tends to increase with increase in the mass unbalance. The lowest rms accelerations are observed to occur along the z-axis, which is along the human hand-arm system.

The intra-subject variability is further assessed in terms of mean and standard deviations of the rms accelerations corresponding to each third-octave frequency bands. Figures 3.15 through 3.18, illustrate the standard deviations of measurements for both subjects for the four values of mass unbalance, when the automatic balancer is on. Each of the following figures represent the standard deviation of the data obtained along the three axes, x, y, and z through the three trials of each experiment. The standard deviation of the measurements in general is low in view of the high magnitude mean values, which suggest good repeatability of the measurements.

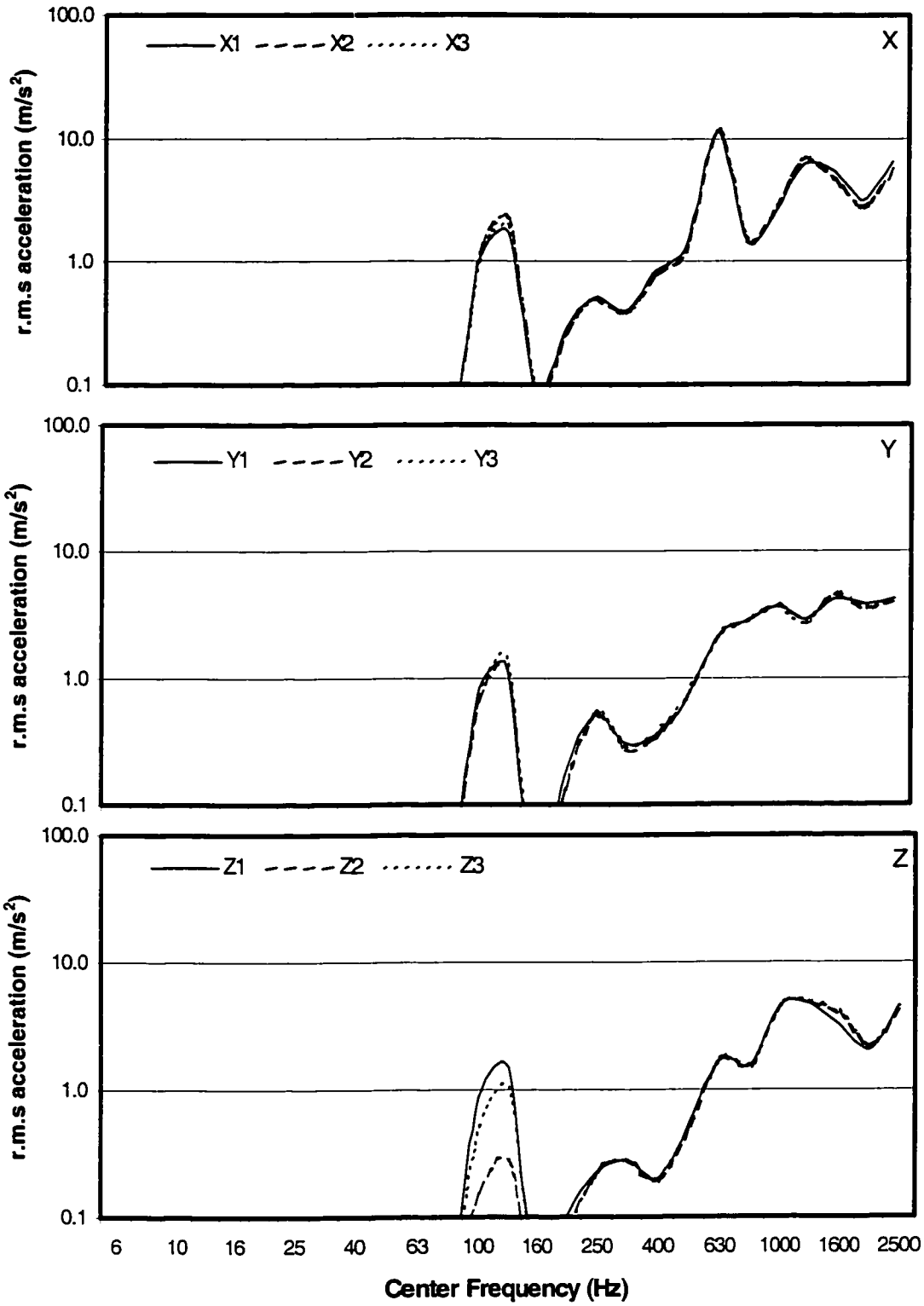

Figure 3.11: The rms acceleration spectra of measured vibration during three trials (mass unbalance = 76 gm-mm; Feed force = 50 N).

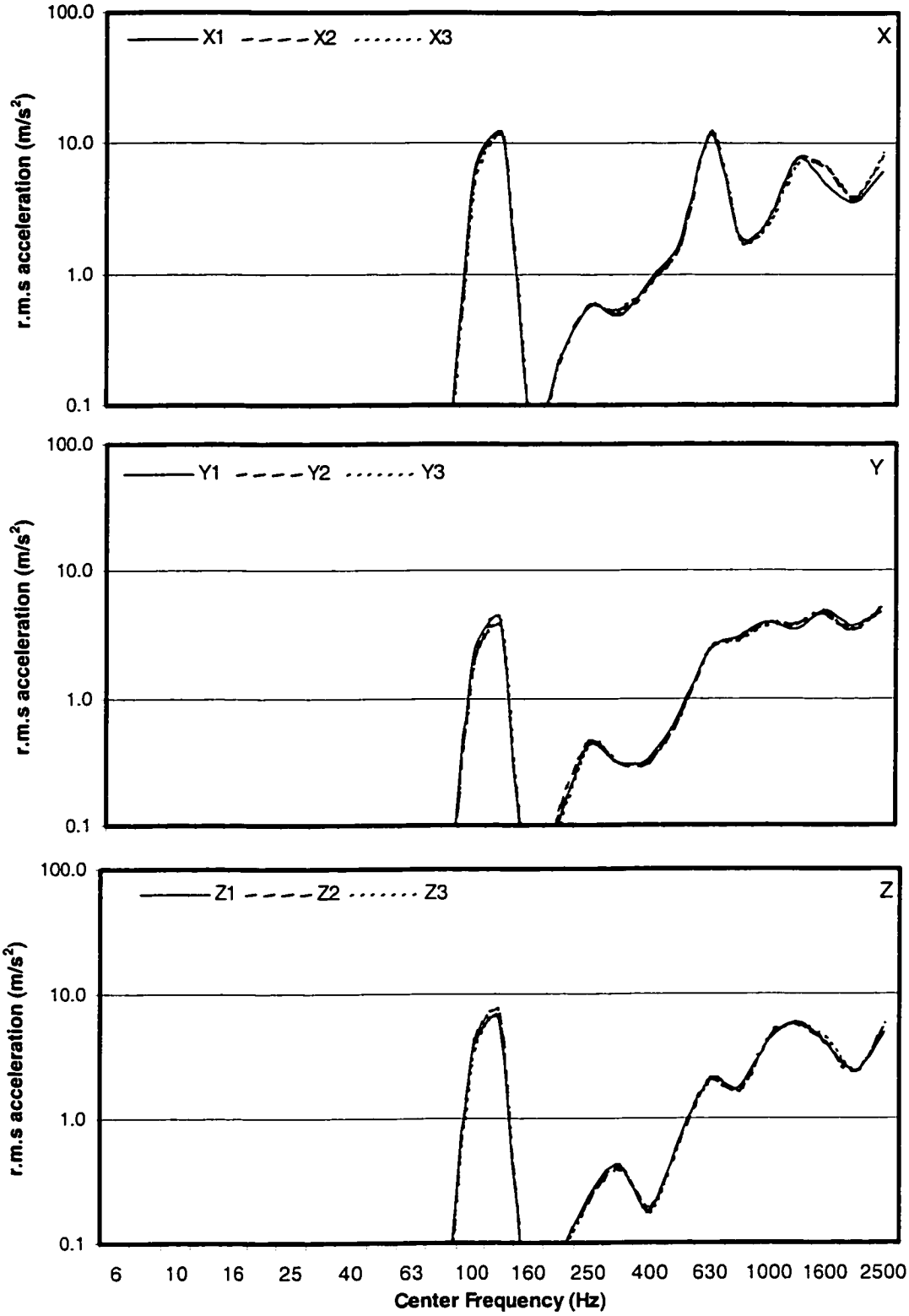

Figure 3.12: The rms acceleration spectra of measured vibration during three trials (mass unbalance = 295 gm-mm; Feed force = 50 N).

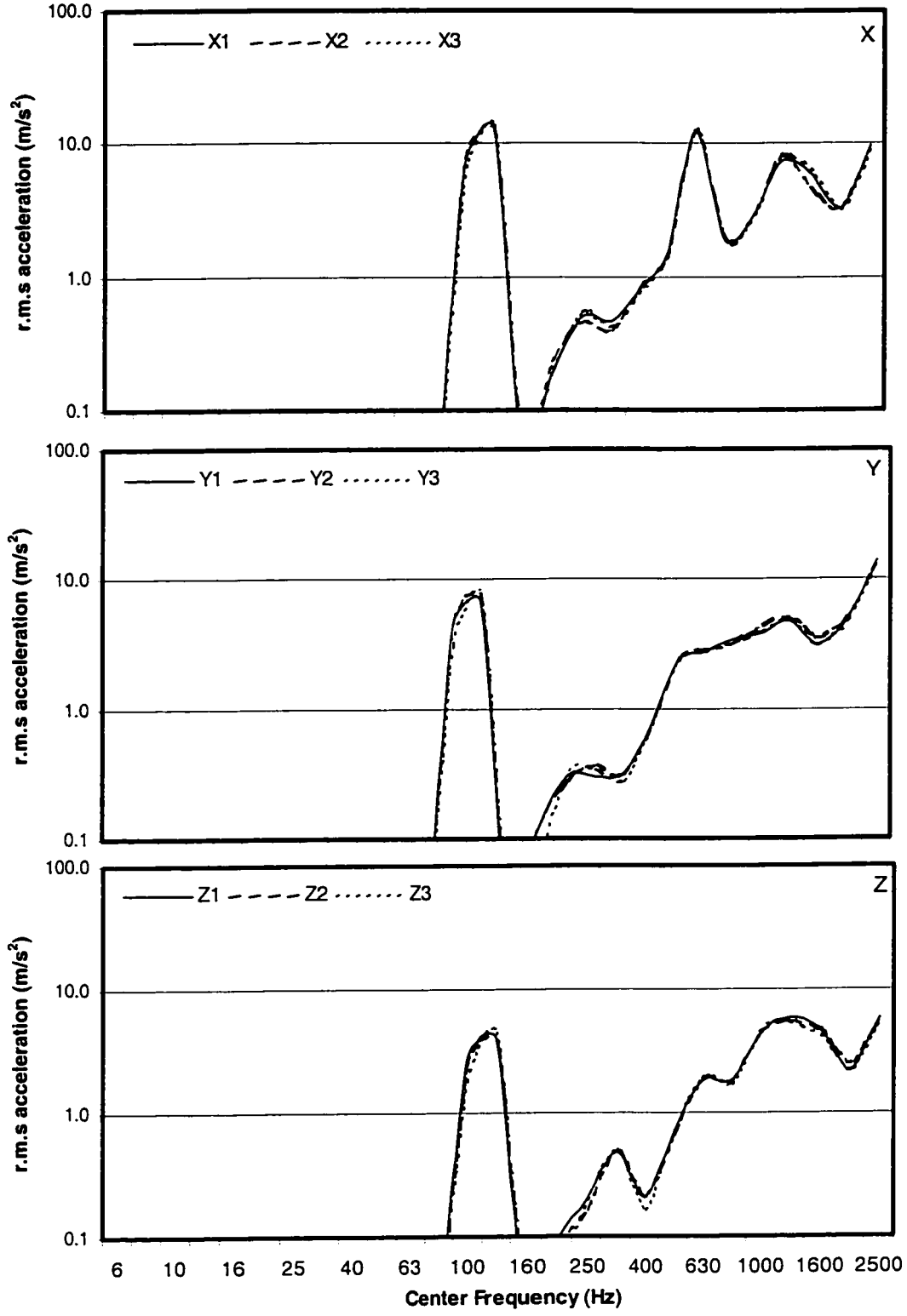

Figure 3.13: The rms acceleration spectra of measured vibration during three trials (mass unbalance = 402 gm-mm; Feed force = 50 N).

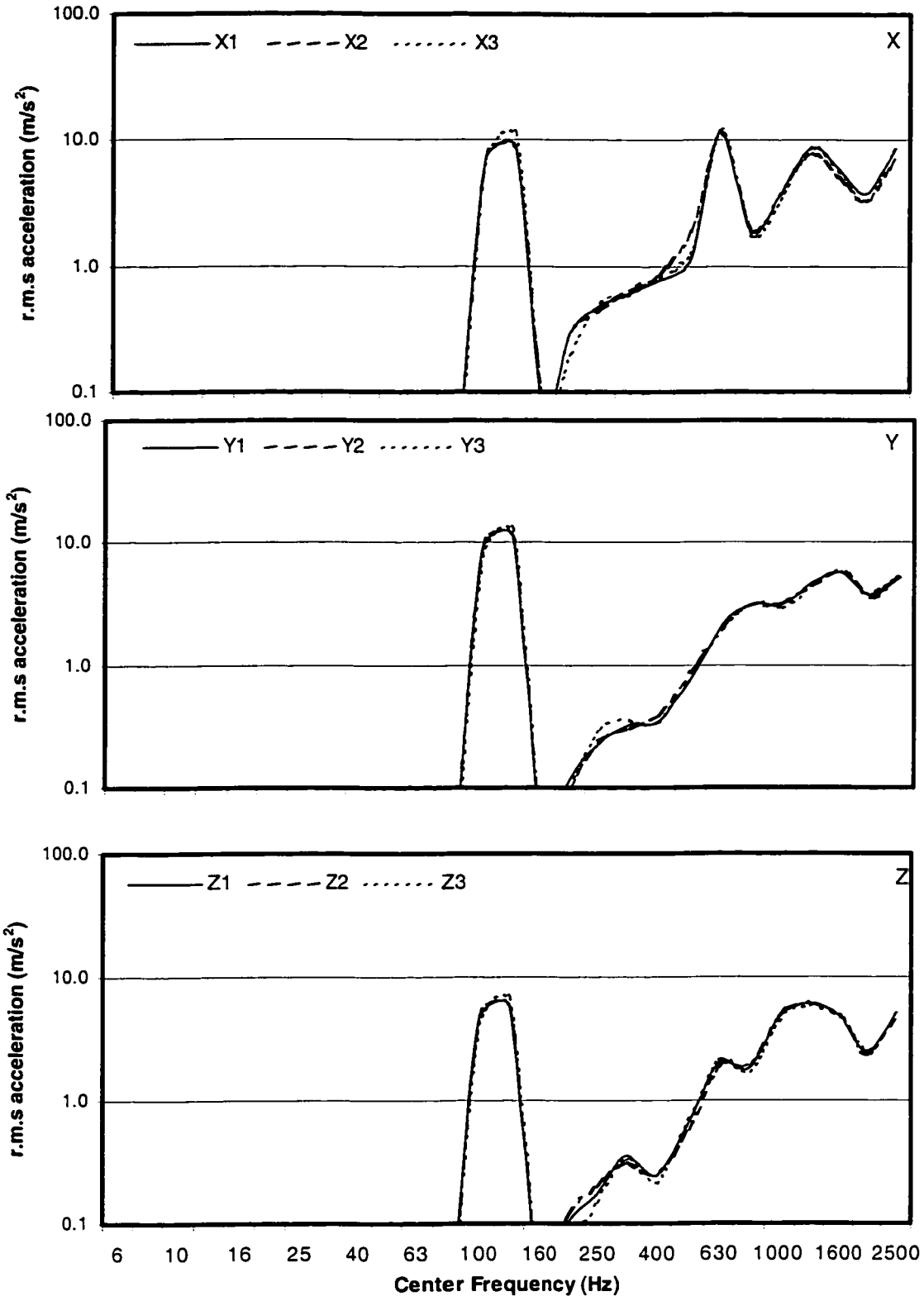

Figure 3.14: The rms acceleration spectra of measured vibration during three trials (mass unbalance = 510 gm-mm; Feed force = 50 N).

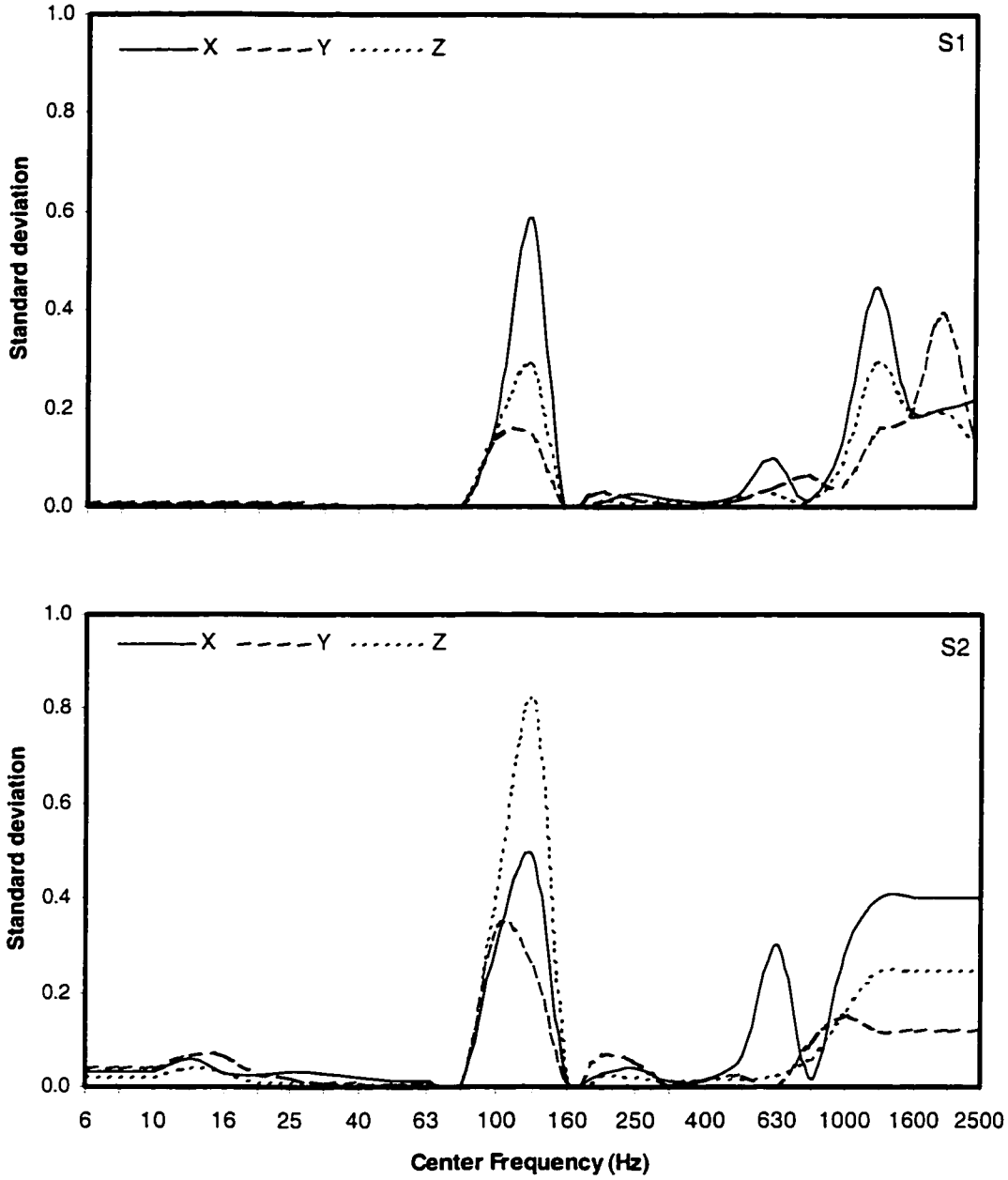

Figure 3.15: Standard deviation of the rms acceleration attained during three trials corresponding to each third-octave band center frequency (mass unbalance = 76 gm-mm unbalance; Feed force = 100 N).

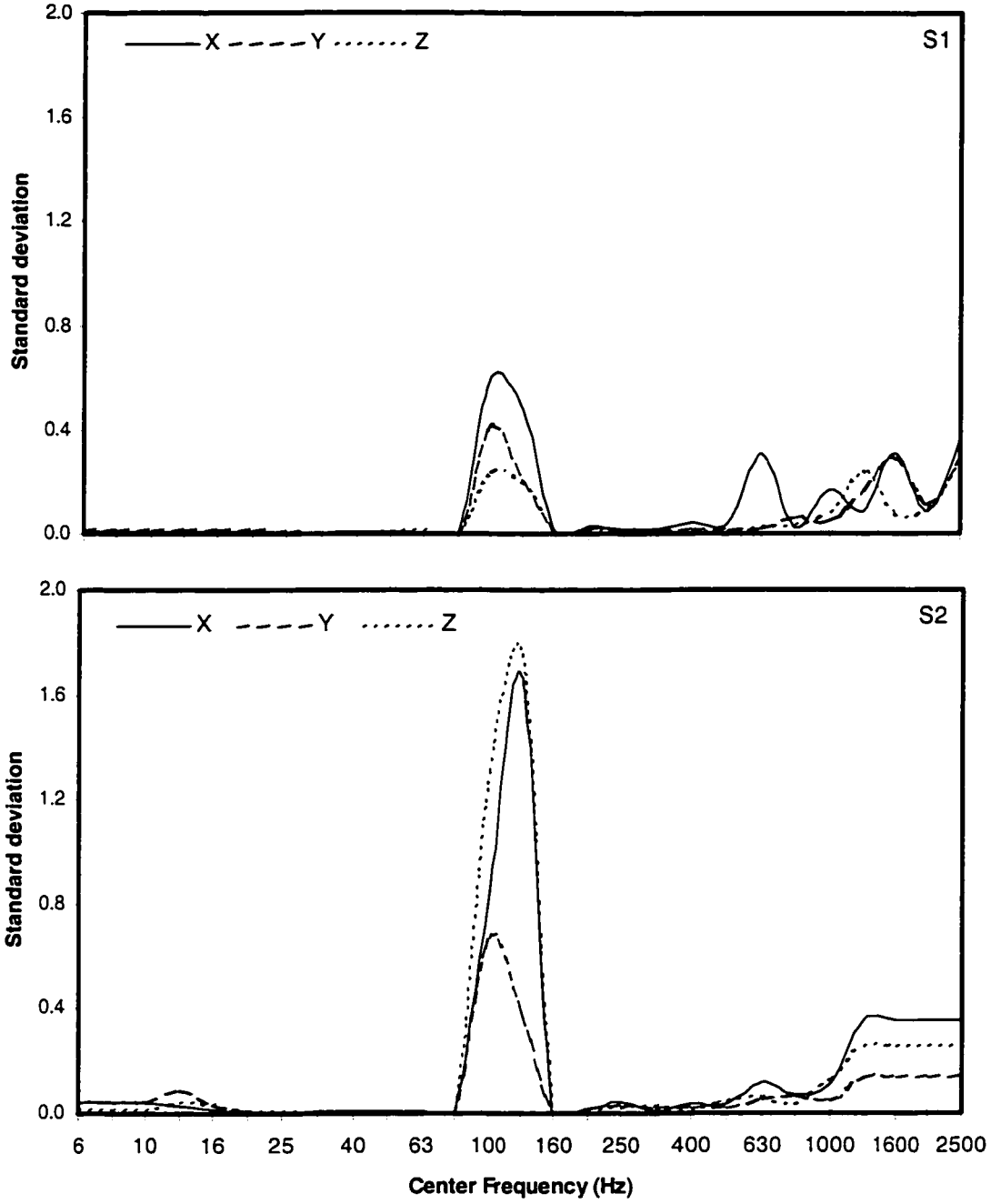

Figure 3.16: Standard deviation of the rms acceleration attained during three trials corresponding to each third-octave band center frequency (mass unbalance = 295 gm-mm unbalance; Feed force = 100 N).

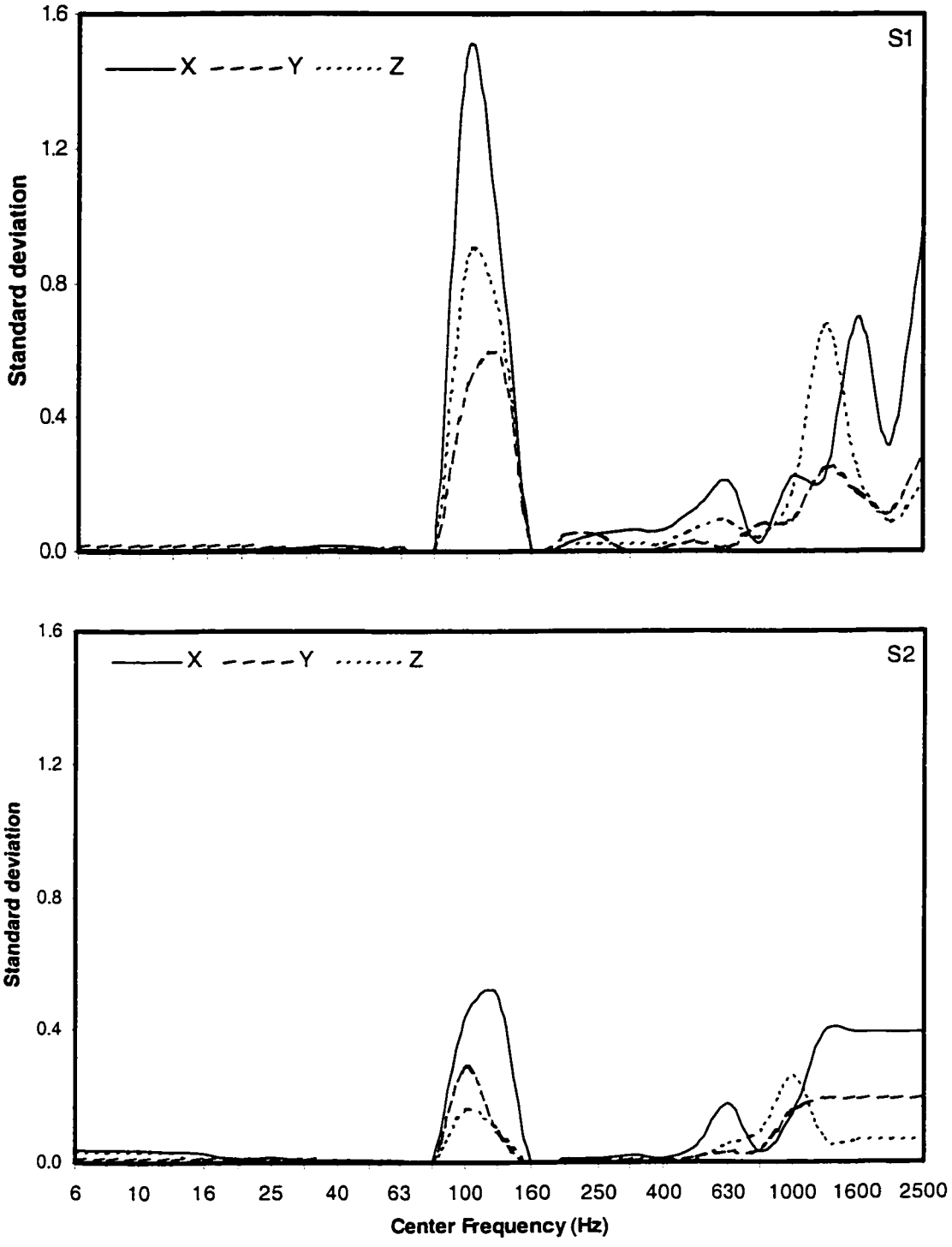

Figure 3.17: Standard deviation of the rms acceleration attained during three trials corresponding to each third-octave band center frequency (mass unbalance = 402 gm-mm; Feed force = 100 N).

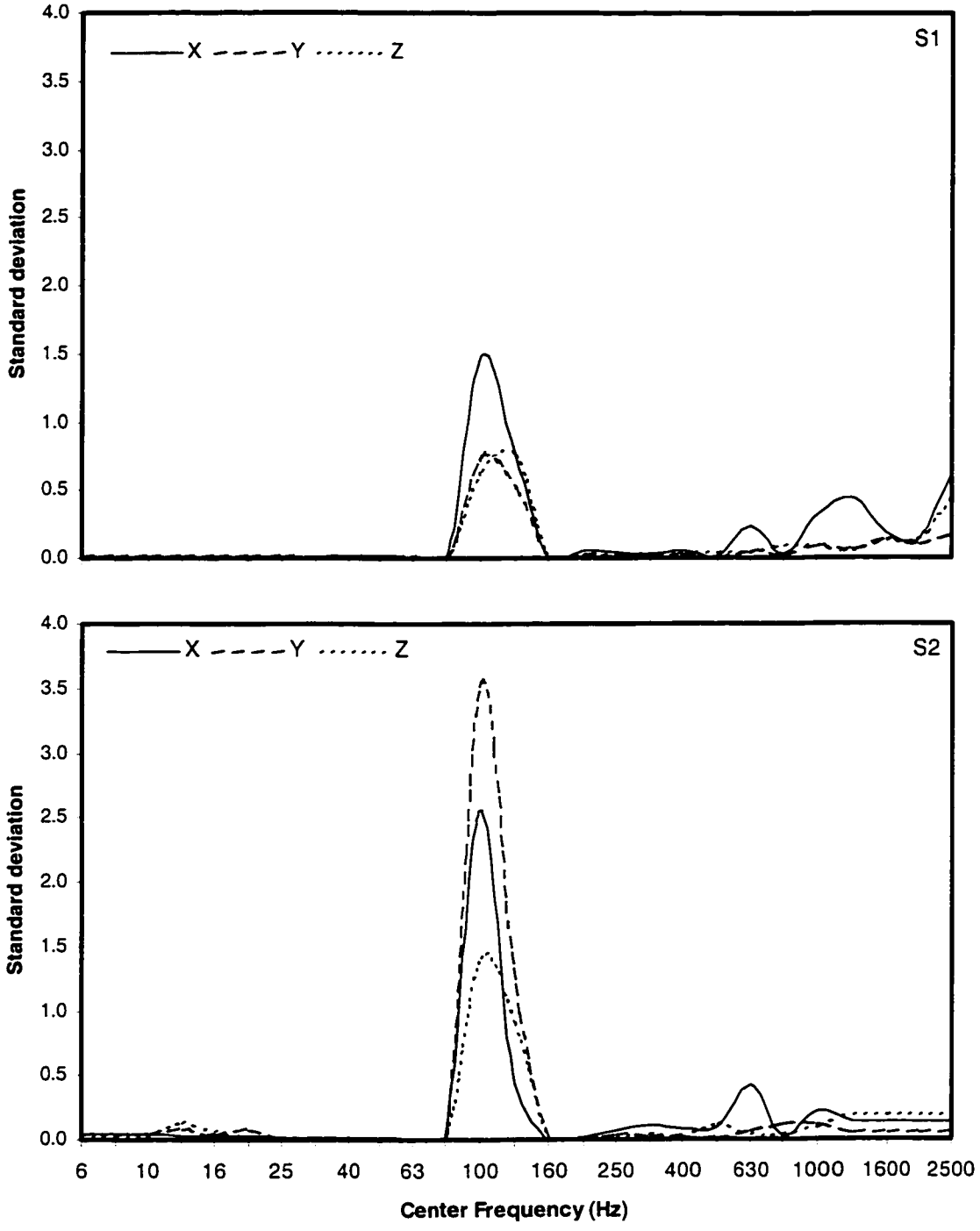

Figure 3.18: Standard deviation of the rms acceleration attained during three trials corresponding to each third-octave band center frequency (mass unbalance = 510 gm-mm; Feed force = 100 N).

3.7 Results and Discussion

The measured data are initially evaluated to study the effects of variations in the feed force and the mass unbalance. Figure 3.19 to 3.24 illustrates the mean spectra of rms accelerations measured along the x, y, and z-axes, respectively, for both subjects, as functions of the 4 levels of the feed force. The results are shown for 76, 295, 402, 510 gm-mm of mass unbalance, in the presence of the auto-balancer. The results show that the rms accelerations along the three-axes are predominant in the 100-125 Hz bands, which correspond to the rotating speed of 7500 rpm of the grinding wheel. The effects of mass-unbalance and feed force on the spectra of measured accelerations are discussed below.

3.7.1 Variation in the Feed Force

The results presented in Figures 3.19 through 3.24, in general, suggest minimal influence of variations in the feed force. The rotational speed of the grinder during operation was 7500 rpm (785 rad/sec). The spectra of measured vibration reveal dominant peak in the 125 Hz frequency band, irrespective of the direction of measurement and the feed force. The spectra also exhibit additional peaks at considerably higher frequencies. In general the variations in the feed force could alter the cutting force and thus the vibration. The variations in the feed force considered in this study, do not influence the rotor response vastly in all the three axes, which could be attributed to the absence of the cutting forces. The vibration response is observed to be the highest along the x-axis. The magnitudes of vibration tend to increase with increase in the unbalance. The spectra also exhibit two distinct peaks, likely to appear around 120 Hz, and 630 Hz.

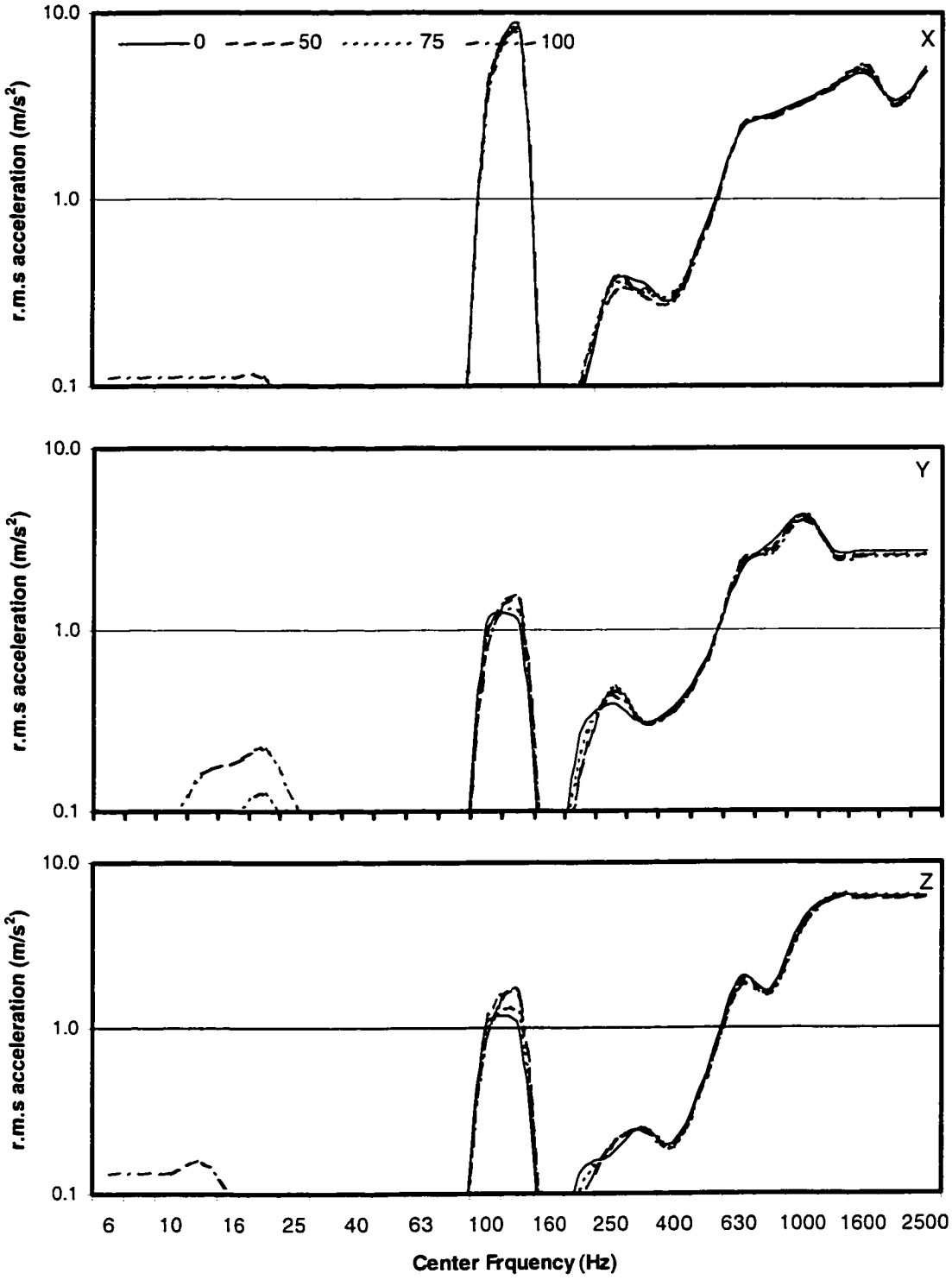

Figure 3.19: Mean spectra of rms acceleration measured along the three axes (S1; mass unbalance = 76 gm-mm; AUB on).

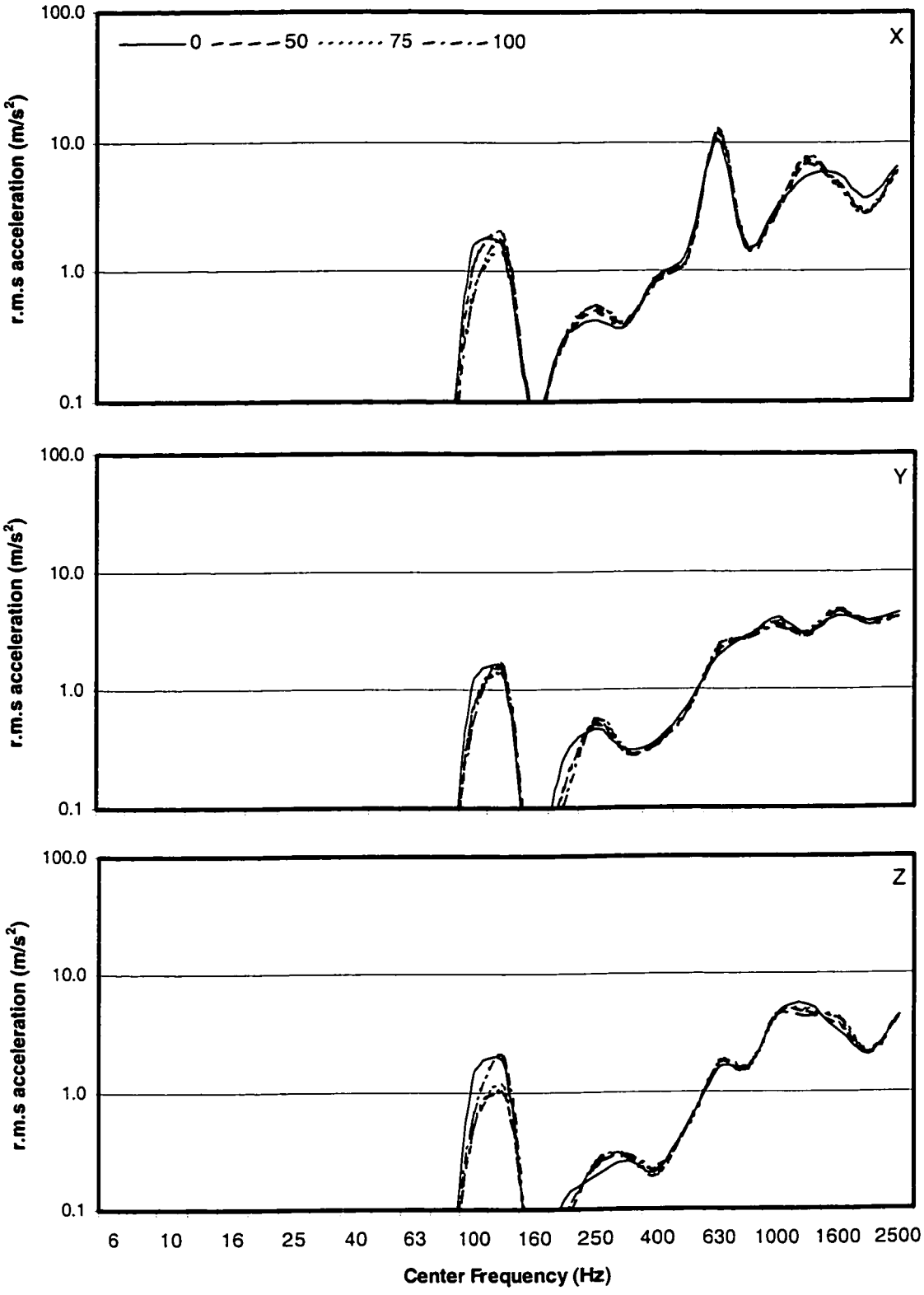

Figure 3.20: Mean spectra of rms acceleration measured along the three axes (S2; mass unbalance = 76 gm-mm; AUB on).

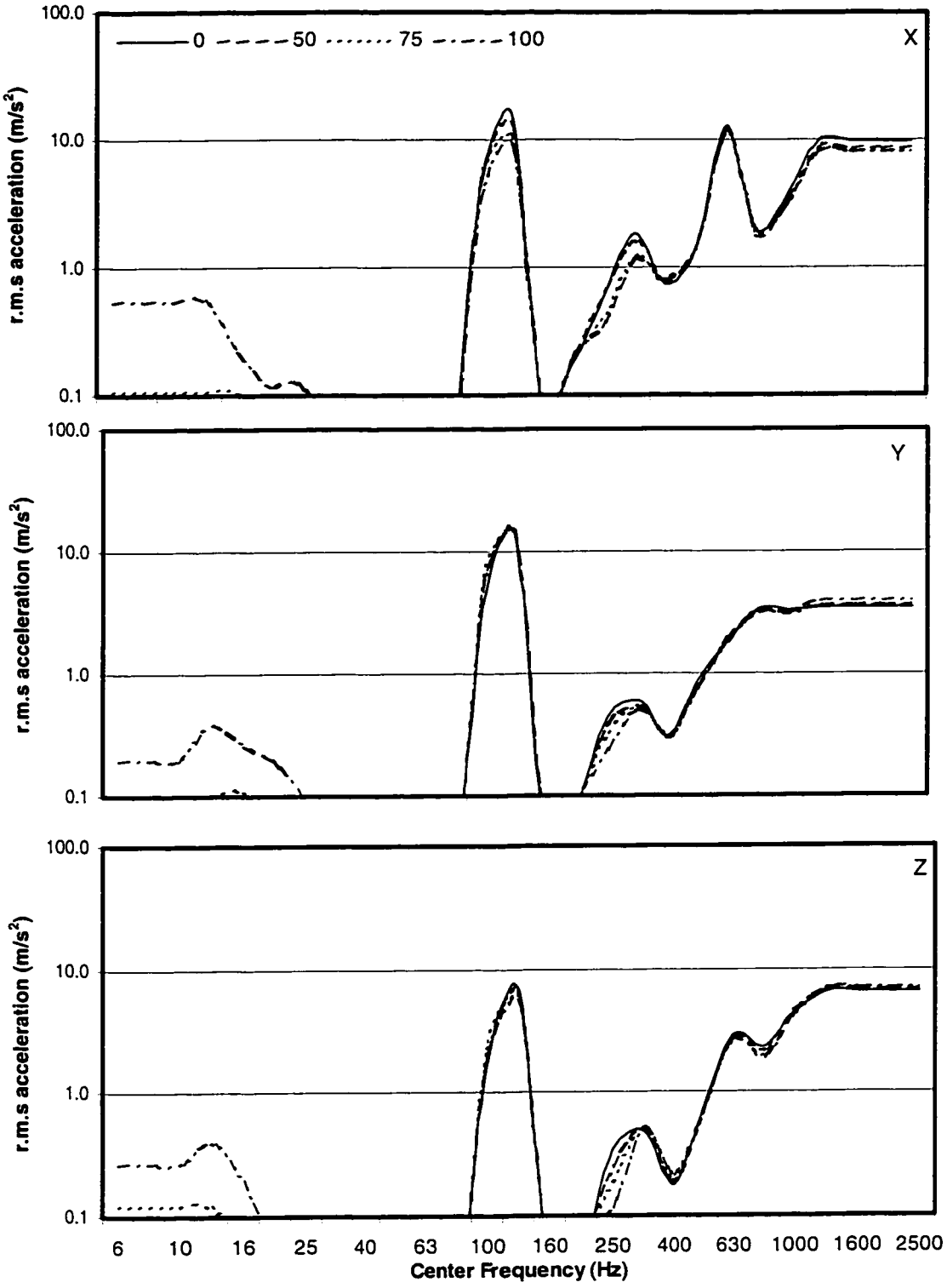

Figure 3.21: Mean Spectra of rms acceleration at measured along the three axes (S1; mass unbalance = 402 gm-mm; AUB on).

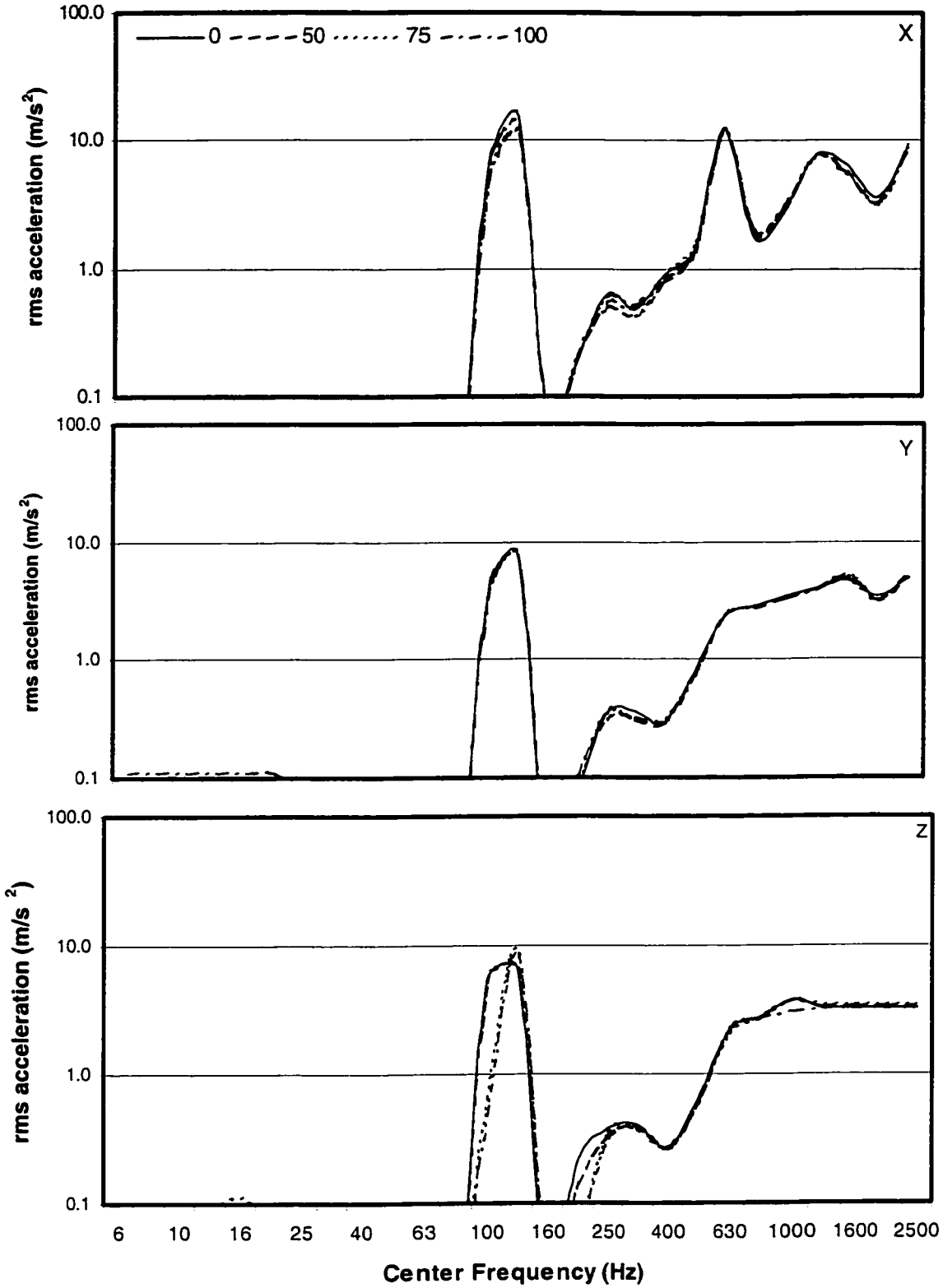

Figure 3.22: Mean Spectra of rms acceleration measured along the three axes (S2; mass unbalance = 402 gm-mm; AUB on).

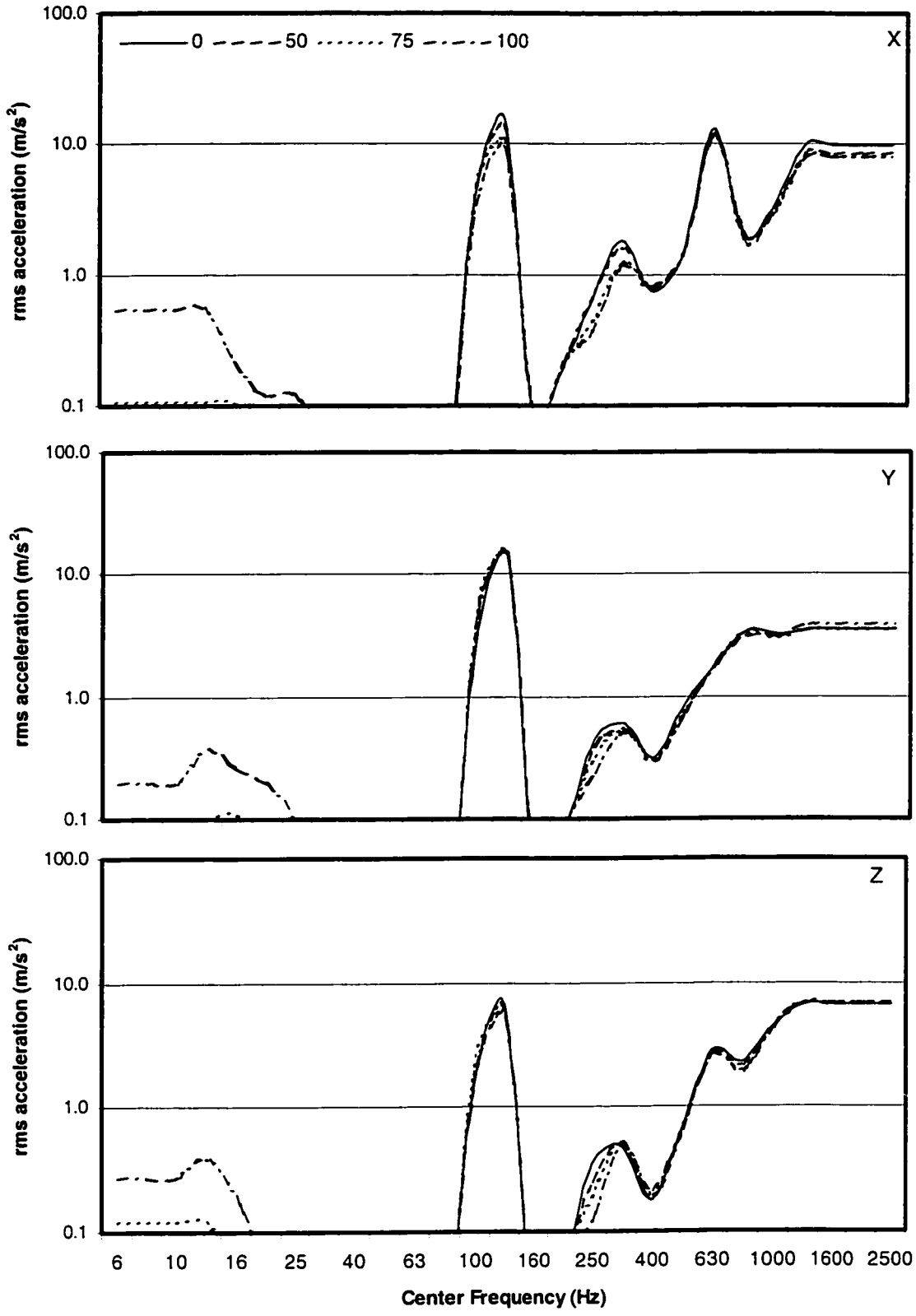

Figure 3.23: Mean Spectra of rms acceleration measured along the three axes (S1; mass unbalance = 510 gm-mm; AUB on)

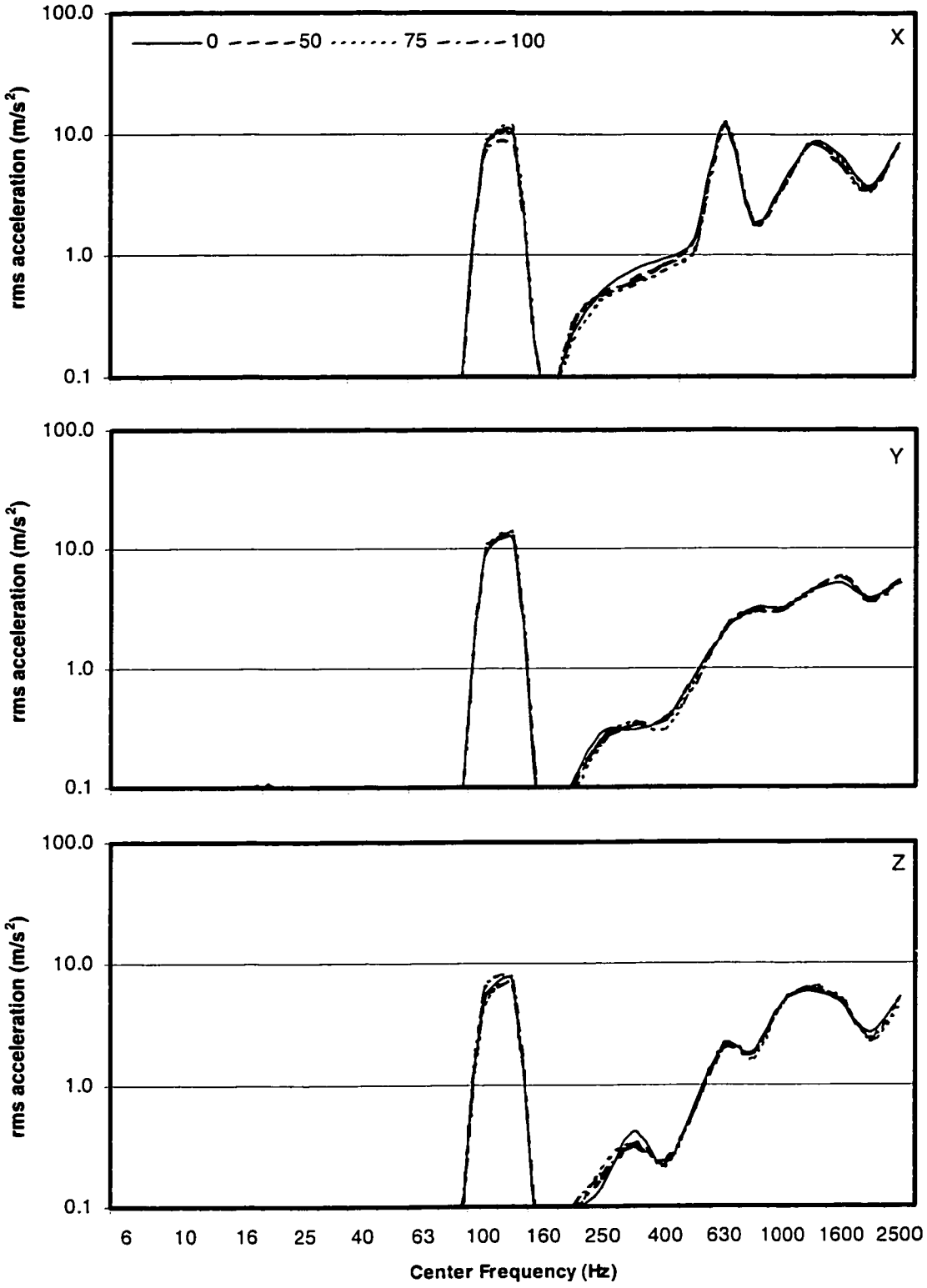

Figure 3.24: Mean Spectra of rms acceleration measured along the three axes (S2; mass unbalance = 510 gm-mm; AUB on)

3.7.2 Variation in mass-unbalance

Figures 3.25 and 3.26 illustrate the rms spectra of the measured accelerations along the x, y and z-axes as a function of the mass unbalance. The magnitudes of mass unbalance are indicated as 'U1', 'U2', 'U3', 'U4', respectively, representing mass unbalances of 76, 295, 402, and 510 gm-mm. The results are shown for 0 N and 100 N feed forces in conjunction with the autobalancer unit. The results show that the mass unbalance contributes considerably to the rms acceleration corresponding to the third-octave band centered at 125 Hz. The magnitude of rms acceleration in this band increases significantly as the mass-unbalance increases from U1=76 gm-mm to U2=295 gm-mm, irrespective of the axis of vibration and the feed force. The rms acceleration along the x-axis, however, does not vary significantly as the mass unbalance is further increased. The most significant variations in the rms acceleration with increasing mass-unbalance are observed to occur along the y-axis. The influence of mass unbalance on the rms acceleration response in the higher frequency bands is observed to be relatively insignificant, which may be attributed to the presence of the autobalancer.

Figures 3.27 and 3.28 illustrate the mean acceleration spectra measured in the absence of the autobalancer for 0 N and 100 N feed forces. A comparison of these results with those presented in Figures 3.25 and 3.26 clearly illustrates the effectiveness of the autobalancer in the higher frequency bands. The magnitudes of rms accelerations tend to be significantly higher in the absence of the autobalancer. The influence of the mass-unbalance of the transmitted vibration in the vicinity of the 125 Hz band is similar to that observed in Figures 3.25 and 3.26, while the magnitudes are considerably higher.

Overall resultant rms accelerations are further computed for different values of mass unbalance using Equation (3.5). Figures 3.29(a) and (b) illustrates the overall rms accelerations due to transmitted vibration for both subjects at feed force of 100 N and for different unbalance masses with and without AUB unit. The rms acceleration for subject 1 range from 14.996 to 31.432 m/s^2 for the balanced disc and the mass unbalance 510 gm-mm with the AUB 'on'. The rms acceleration for the same subject while the AUB is 'off' revealed a considerable increase in the rms acceleration from 65.810 to 508.951 m/s^2. For subject 2, the rms acceleration range from 24.190 to 32.828 m/s^2 when the AUB is 'on', while for the AUB 'off' the values is from 66.371 to 305.254 m/s^2. Figures 3.30(a) and (b) illustrate the overall weighted rms accelerations due to transmitted vibration with and without the balancer for both subjects. As evident from the results, the overall rms acceleration increase considerably with increasing mass unbalances. The presence of an autobalancer tends to suppress the magnitudes of transmitted vibration significantly, irrespective of the mass-unbalance. The effectiveness of the balancer is more pronounced for higher degree of mass unbalance. Comparing the balanced disc with the mass unbalance U1, the vibration response did not affect adversely. Figure 3.30(a) the weighted rms acceleration range from 0.913 to 2.827 m/s^2 for the balanced disc and mass unbalance U1 when the AUB is 'on'. The corresponding values for the same subject ranges from 1.733 to 19.297 m/s^2 when the AUB is 'off'. In Figure 3.27 the rms acceleration occurred at 175 Hz instead of 125 Hz, this is due to the air pressure increase while conducting the experiments.

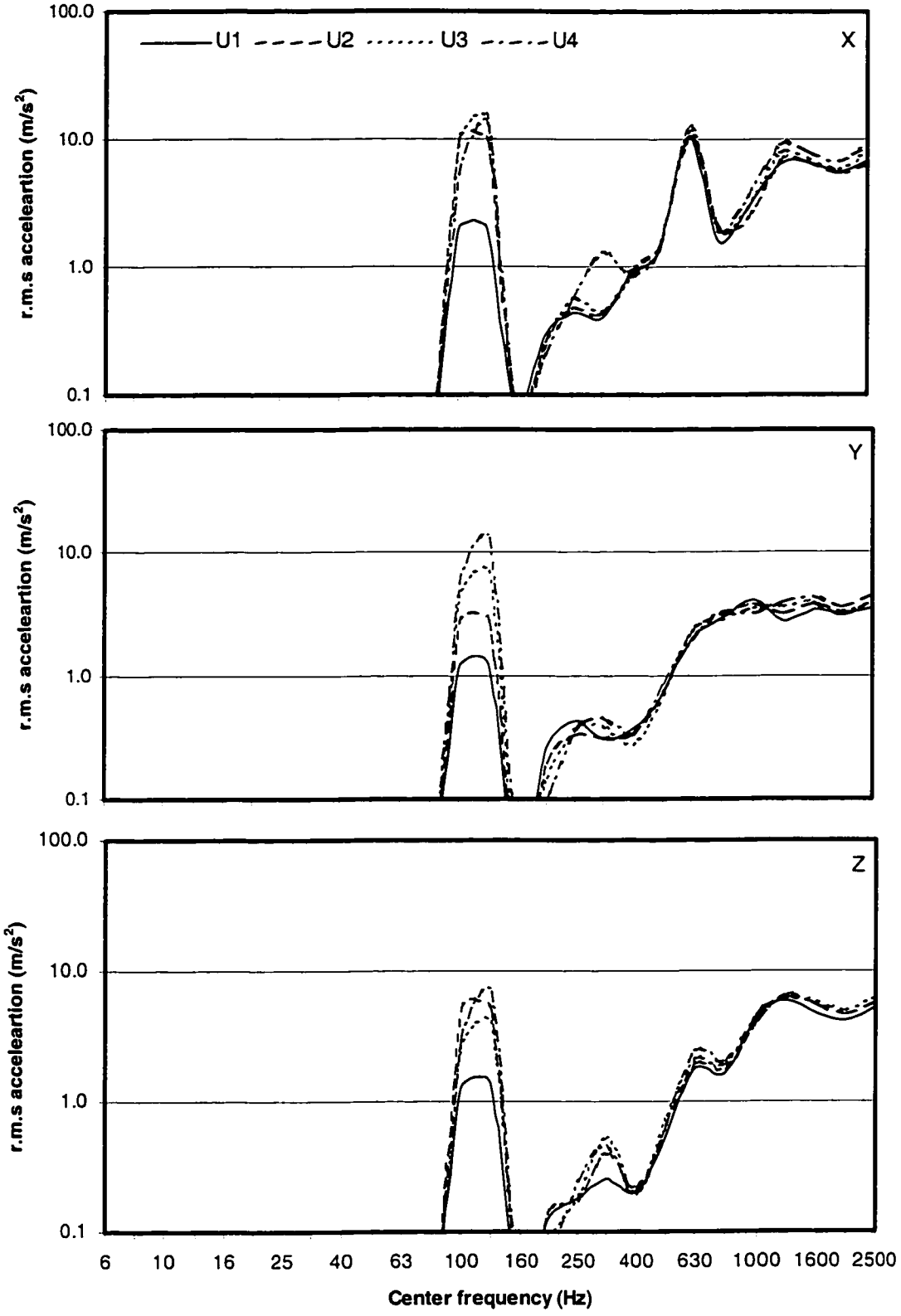

Figure 3.25: Mean rms acceleration response as a function of the mass unbalance (Feed force = 0 N; AUB on).

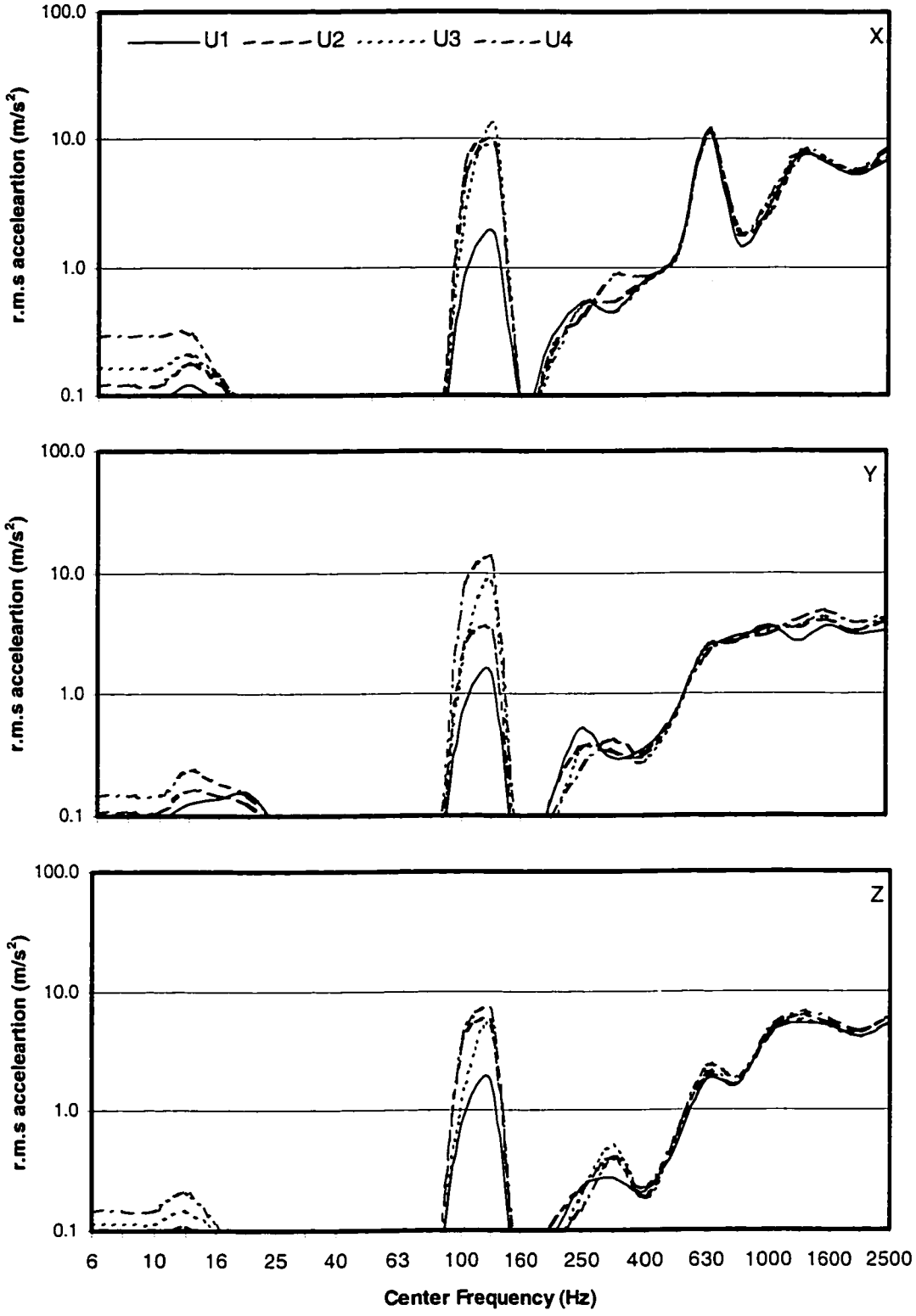

Figure 3.26: Mean rms acceleration response as a function of the mass unbalance (Feed force = 100 N; AUB on).

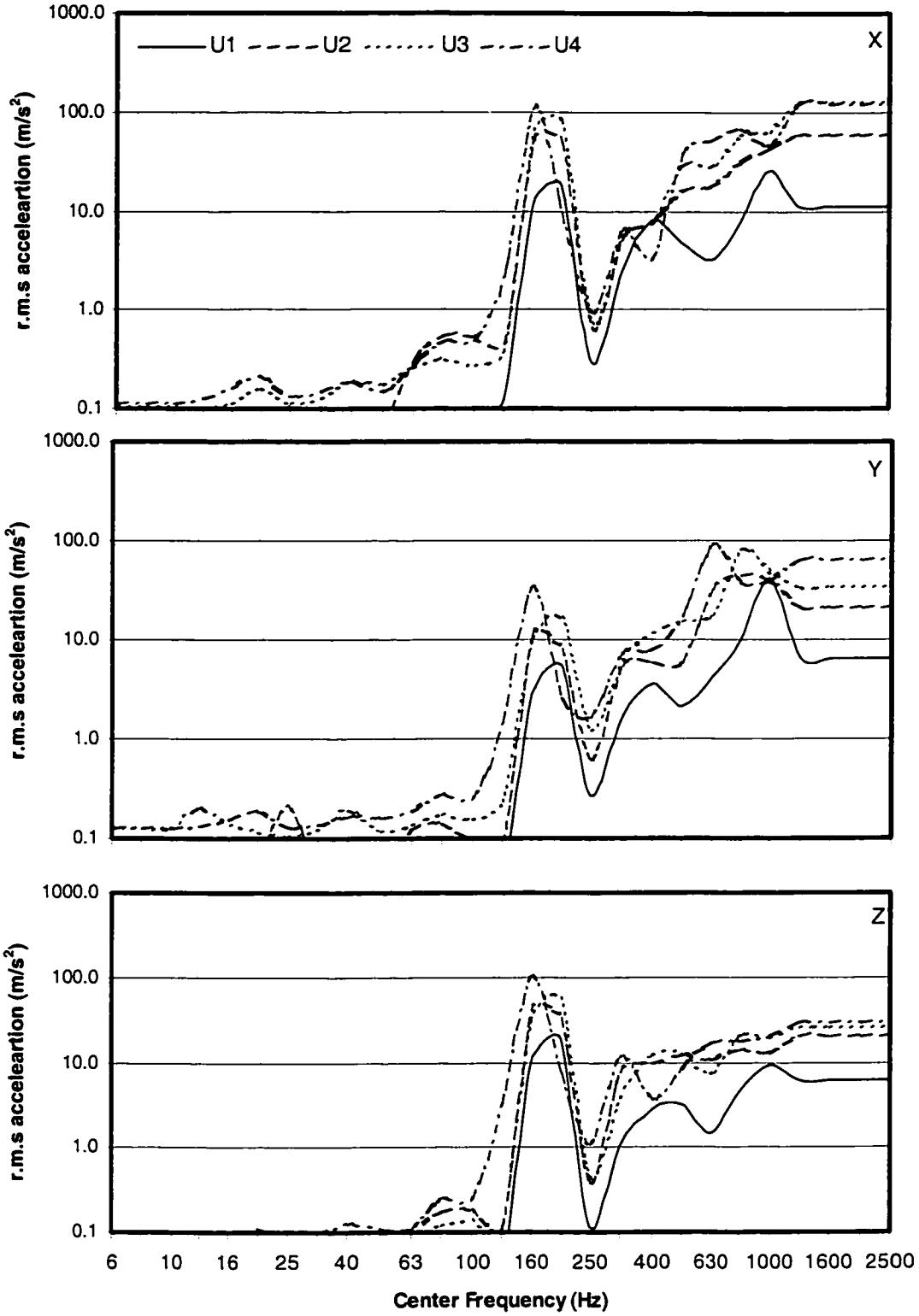

Figure 3.27: Mean rms acceleration response as a function of the mass unbalance (Feed force = 0 N; AUB off).

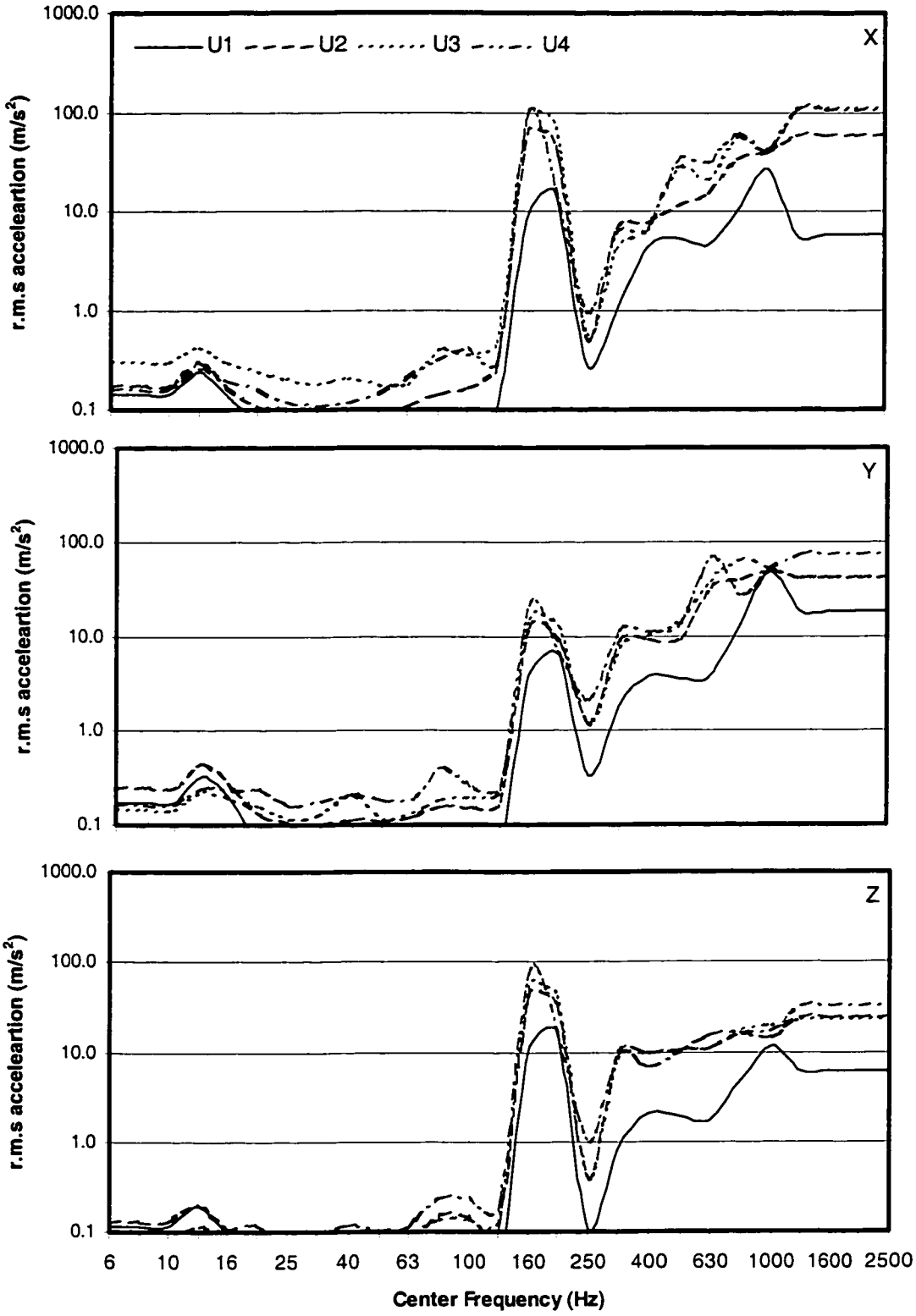

Figure 3.28: Mean rms acceleration response as a function of the mass unbalance (Feed force = 100 N; AUB off).

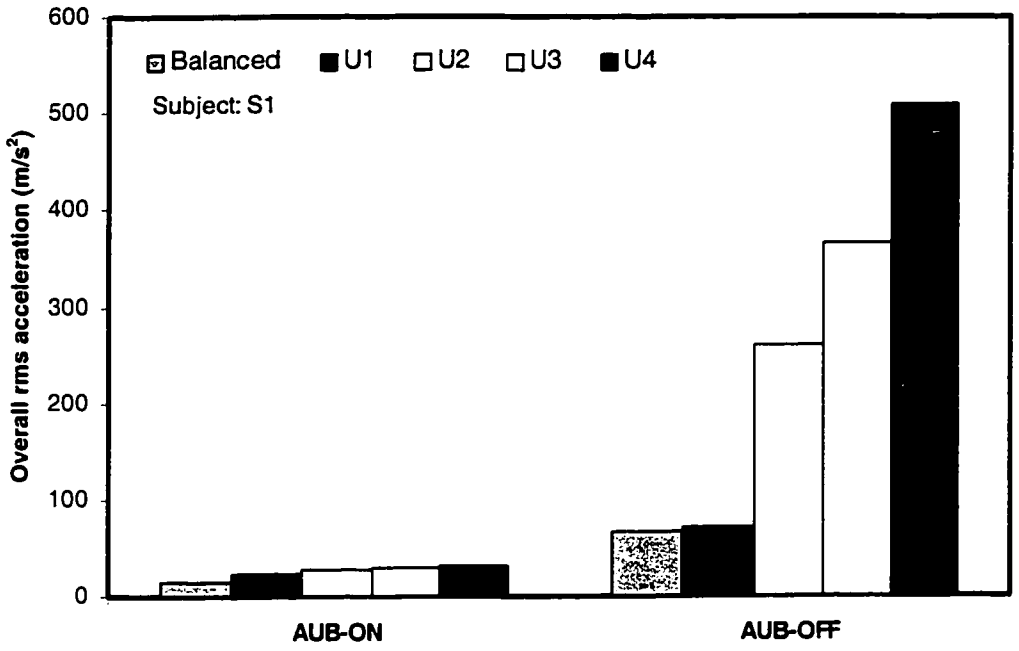

force = 100 N)

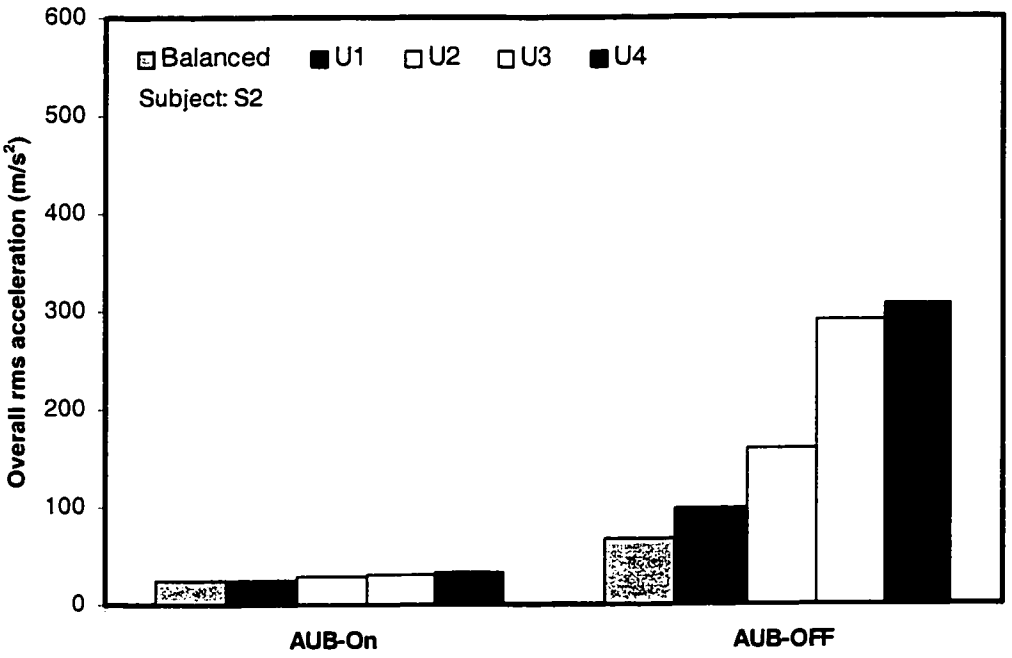

Figure 3.29.b: Influence of mass unbalance on the mean overall rms acceleration (Feed force = 100 N)

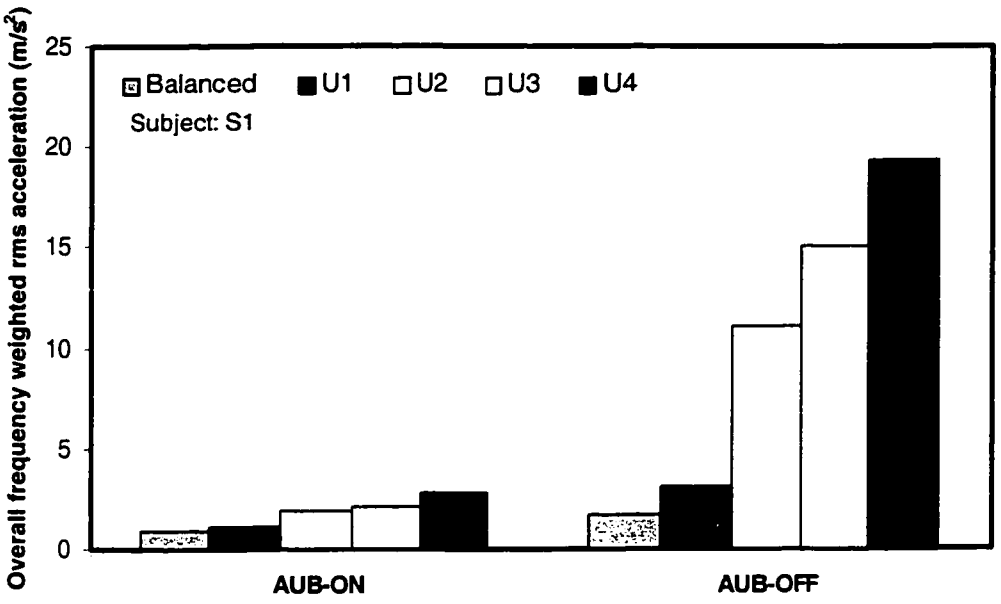

Figure 3.30.a: Influence of mass unbalance on the mean overall rms acceleration (Feed force = 100 N)

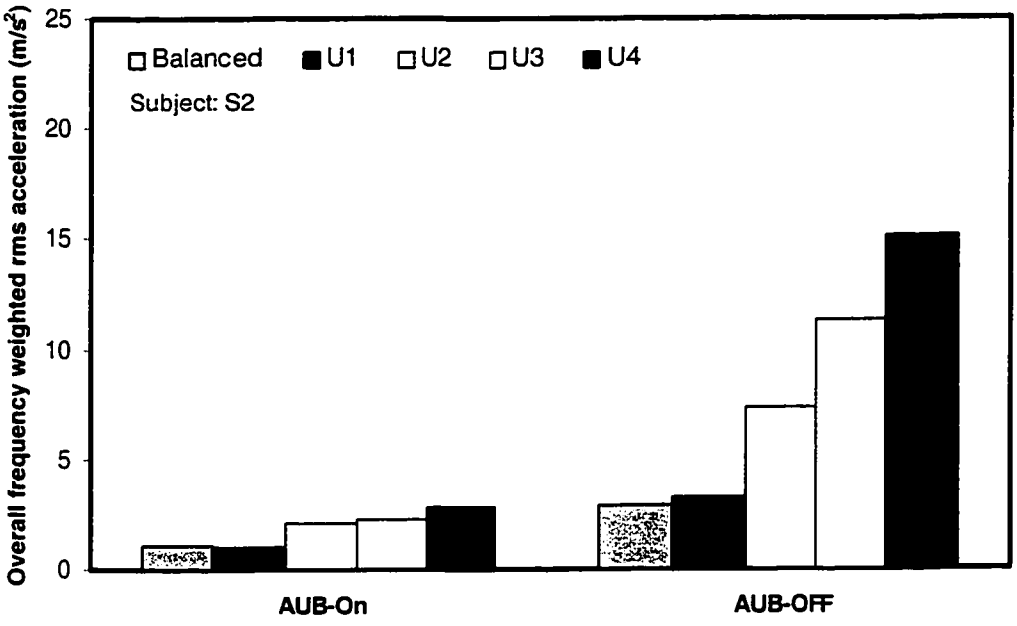

Figure 3.30.b: Influence of mass unbalance on the mean overall rms acceleration (Feed force = 100 N)

3.7.3 Effect of Automatic Balancer

Figure 3.31 further shows the effect of the automatic balancing unit on the magnitudes of the transmitted vibration for the highest mass unbalance of 510 gm-mm and 100 N feed force for the subject 1. The results are presented in terms of overall rms accelerations along x, y, and z-axis, and the resultant overall rms acceleration computed using Equation (3.5). It is evident that the presence of an AUB reduces the magnitudes of transmitted vibration to half of its original value. Figure 3.32 shows the same results obtained with subject S2. The Figure shows that the AUB reduces the vibration from 234.16 m/s^2 to 22.547 m/s^2 along the x-axis, from 153.852 m/s^2 to 17.437 m/s^2 along the y-axis and 121.157 m/s^2 to 16.286 m/s^2 along the z-axis. The resultant rms acceleration can be reduced from 305.254 m/s^2 to approximately 32.828 m/s^2.

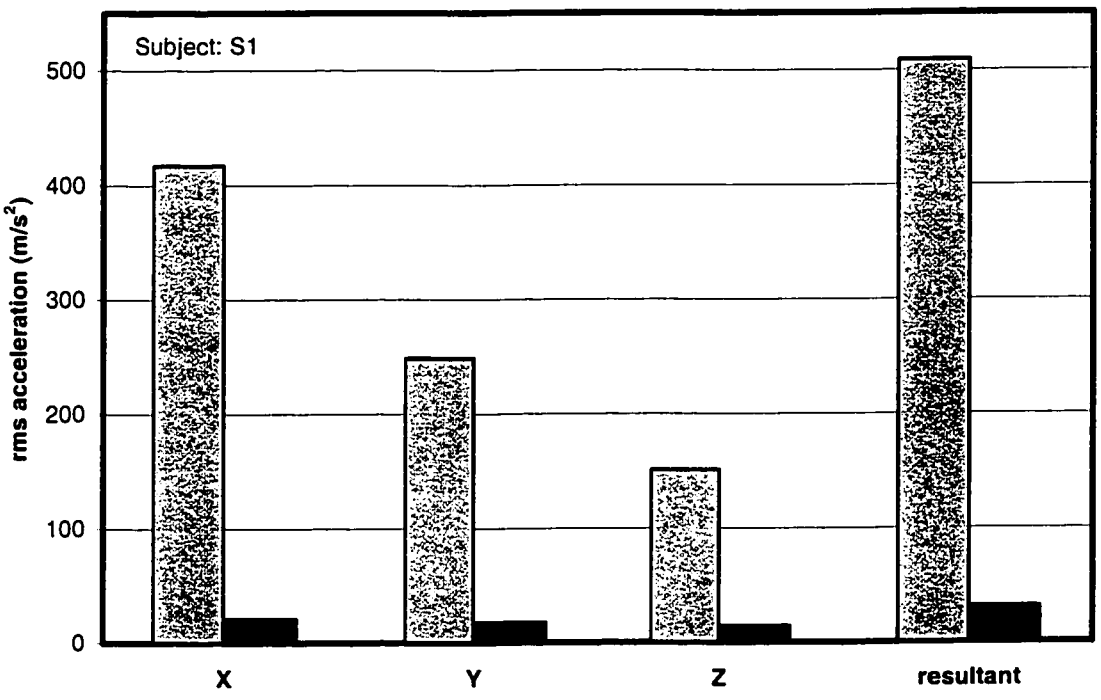

Figure 3.31: Influence of autobalancer on the overall rms accelerations due to transmitted vibration (mass unbalance = 510 gm-mm; Feed force = 100 N).

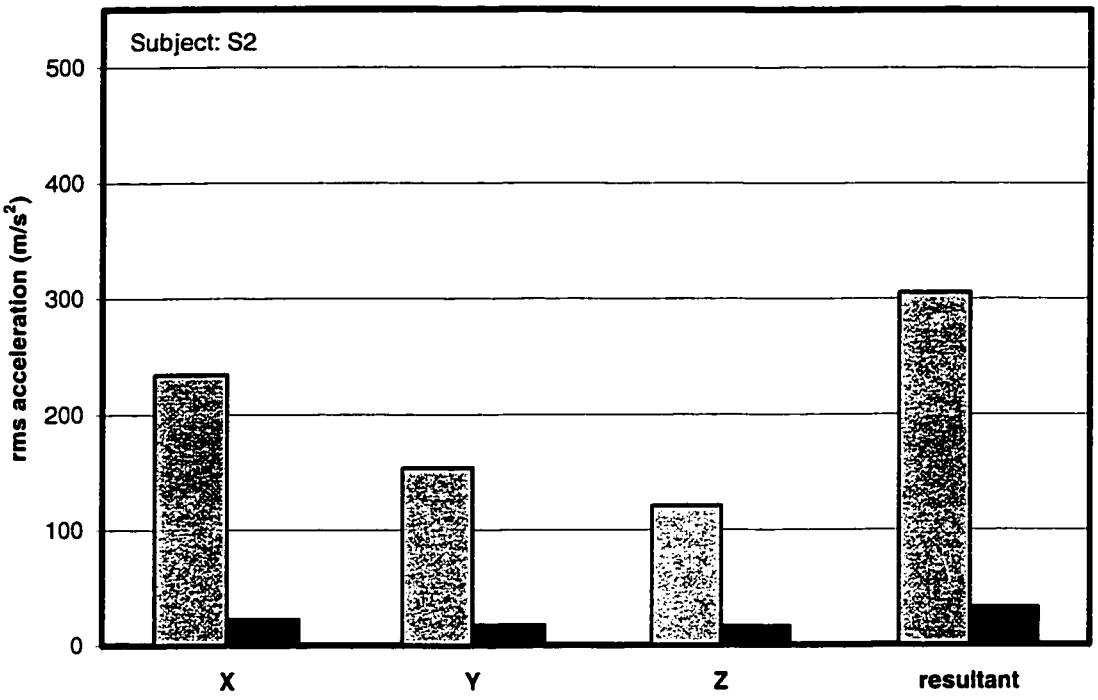

Figure 3.32: Influence of autobalancer on the overall rms accelerations due to transmitted vibration (mass unbalance = 510gm-mm; Feed force = 100 N).

3.7.4 Eight Hour Energy Equivalent and Assessment of Transmitted Vibration

There have been attempts to estimate the vibration exposure that would produce finger blanching in groups of persons performing equivalent work involving similar tools, or industrial processes. Table 3.4 shows the daily vibration exposure, $A(8)$, which may be expected to produce episodes of finger blanching in 10% of population for persons exposed for a given number of years D_y (ISO 5349-1, 2001). The international standard, ISO-5349, utilizes the concept of equal energy. A complex exposure pattern of any duration during a day can be evaluated in terms of an equivalent value for an exposure of eight hours. The recent revision of the standard suggests the use of 8-hour equivalent

energy instead of 4 hours as it was stated previously in its previous version (ISO-5349, 1986).

The current standard provides guidelines for assessment of HTV based upon the expected occurrence of finger blanching or VWF. A relation between the years of exposure D_y, the eight-hour energy equivalent frequency weighted acceleration $A(8)$, and the predicted prevalence of finger blanching has been proposed in the standard;

$$C = 100\left[\frac{A(8) * D_y}{95}\right]^2 \qquad (3.7)$$

The factor C in the above equation refers to the percentage of population that could be affected by finger blanching. The British standard (BS-6842, 1987) and (ISO-5349-1, 2001) further provide a relationship between exposure time before blanching could occur and the 8-hour equivalent acceleration in m/s^2 for predicted prevalence of 10%. The eight hour equivalent energy is computed using Equations (3.3) or (3.4). The number of years of exposure that could cause finger blanching among C % of population may thus be derived from

$$D_y = \sqrt{\frac{C}{100}} * \frac{95}{A(8)} \qquad (3.8)$$

The number of years of exposure that could cause finger blanching among 10% of population may thus be simply derived from $D_y \approx \frac{30.04}{A(8)}$. The relationship in Equation (3.8) does not predict the risk of finger blanching occurring in any particular individual within the group.

Table 3.4: Values of the 8-hour equivalent energy $A(8)$ that may produce finger blanching in 10% of the population exposed to vibration for a given number of years D_y (ISO-5349-1, 2001)

D_y, Years	1	2	4	8
$A(8)$, m/s^2	26	14	7	3.7

The measured data are analyzed to compute the eight-hour energy equivalent, $A(8)$, using Equation (3.3) assuming daily exposure durations of 240 minutes. Figure 3.33 illustrates the eight-hour equivalent due to vibration measured for the two subjects corresponding to 0 N feed force. The results are computed for different values of mass unbalance and with and without the balancer. Figure 3.33 shows the eight-hour energy equivalent value from the experimental data for both subjects at 0 N feed force and for the balanced disc and the four values of mass unbalance with and without the AUB unit installed. The figures show a significant reduction in the $A(8)$ values when the AUB unit is 'on'. The values of $A(8)$ vary between 0.645 and 1.999 m/s^2 for the AUB 'on', depending upon the magnitude of the mass unbalance for subject 1. The corresponding values of the eight-hour equivalent energy without the autobalancer range from 1.225 to 13.645 m/s^2. The values of $A(8)$ vary between 0.749 and 1.985 m/s^2 for the AUB 'on', depending upon the magnitude of the mass unbalance for subject 2. The corresponding values of the eight-hour equivalent energy without the autobalancer range from 2.058 to 10.67 m/s^2. The use of an automatic balancer can help reduce the transmitted vibration to nearly 17%. The inter-subject variation in Figure 3.33 reveals that subject 1 experienced higher values of $A(8)$ around 13.645 m/s^2 compared to 10.67 m/s^2 for subject 2.

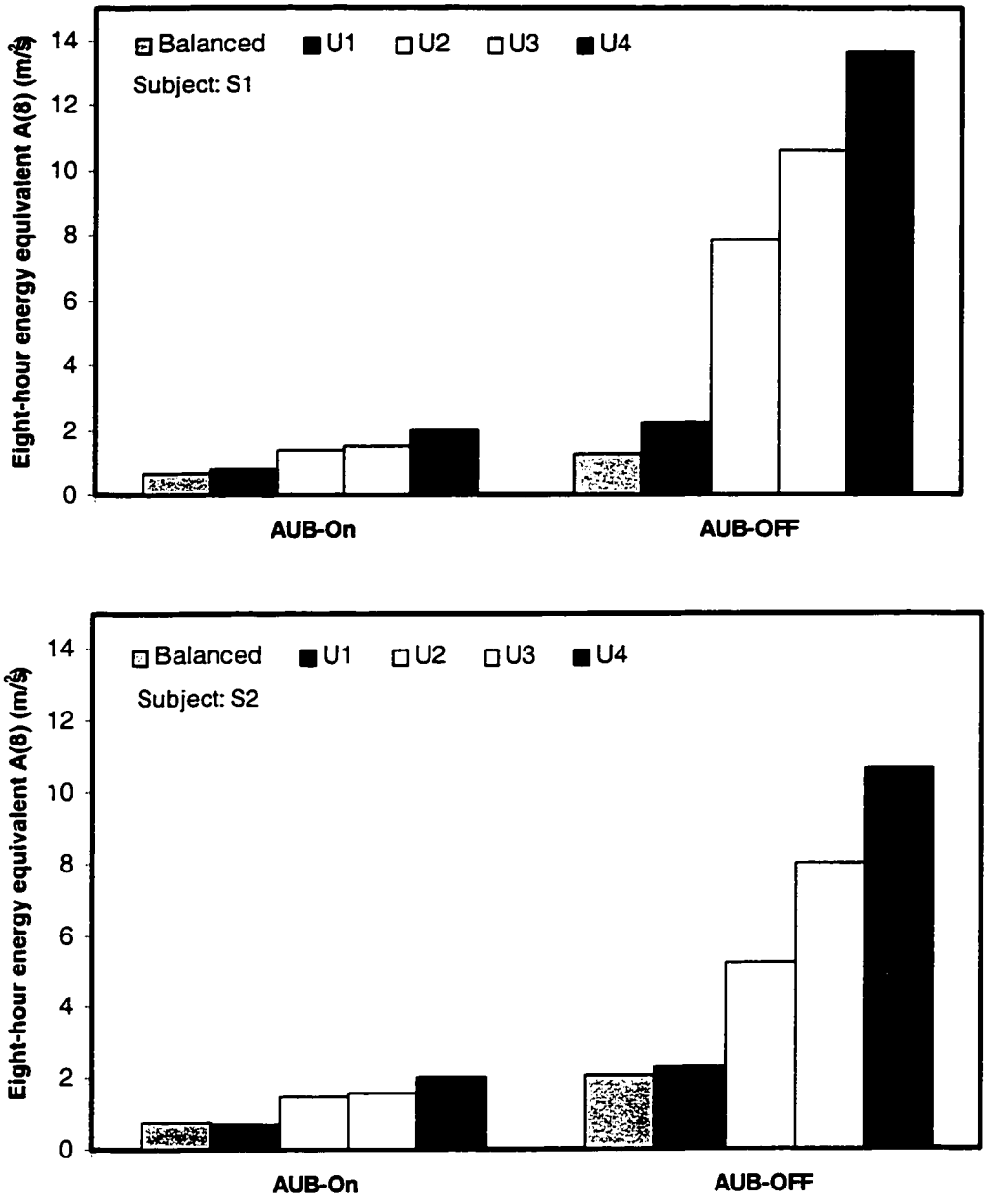

Figure 3.33: $A(8)$ values due to transmitted vibration for both subjects (Feed force = 0N).

Table 3.5: Eight-hour equivalent energy and number of exposure years for 10% prevalence of VWF (Subject 2, Balancer On).

Mass unbalance gm-mm	**Overall rms acceleration m/s^2**		$A(8)$ **m/s^2**	D_y **(Years); C=10%**
	a_{rms}	a_{rms_w}		
0	24.190	1.060	0.749	43.139
76	25.424	1.009	0.713	45.468
295	28.561	2.093	1.480	20.986
402	30.765	2.219	1.569	19.721
510	32.828	2.808	1.985	15.367

Table 3.6: Eight-hour equivalent energy and number of exposure years for 10% prevalence of VWF (Subject 2, Balancer Off).

Mass unbalance gm-mm	**Overall rms acceleration m/s^2**		$A(8)$ **m/s^2**	D_y **(Years); C=10%**
	a_{rms}	a_{rms_w}		
0	66.371	2.911	2.058	14.793
76	97.076	3.255	2.302	13.139
295	159.982	7.360	5.204	5.533
402	289.033	11.333	8.014	3.748
510	305.254	15.097	10.675	2.814

The results obtained from the measurements are further analyzed to compute the 8-hour equivalent energy and number of years of exposure for predicted 10% prevalence of finger blanching. The results obtained for varying magnitudes of mass unbalance with and without balancer are presented in Tables 3.5 and 3.6. Owing to negligible influence of the feed force, results represent the mean values obtained for all the feed forces considered in the analysis. Tables 3.5 and 3.6 summarize the overall unweighted and frequency-weighted rms accelerations, eight-hour energy equivalent value and the number of years of exposure before the symptoms of VWF could be observed in the 10% of the exposed workers. The two tables represent the mean values for the tool vibration with and without the balancer, respectively, attained for subject 1. The results suggest that the increased mass-unbalance could considerably reduce the number of years of exposure for the symptoms to appear in the 10% of the exposed population. The addition of the automatic balancer tends to suppress the adverse effects of the rotating mass unbalance. Figure 3.34 shows the plot for the eight-hour energy equivalent and the corresponding number of years for the symptoms to appear in the 10% of the operators. The figure shows the duration of vibration exposure in number of years as a function of the 8-hour equivalent energy $A(8)$, as described in ISO 5349-1, (2001). The figure indicates the severity of exposure to the measured hand-transmitted vibration corresponding to different mass unbalances in the absence of an automatic balancer. The results obtained with the automatic balancer suggest that the number of years of exposure is well above 13 years. Figure 3.34 shows the results obtained from the practical experiments and presented in Table 3.6 on the eight-hour energy equivalent chart. The results that fall within the chart range are plotted.

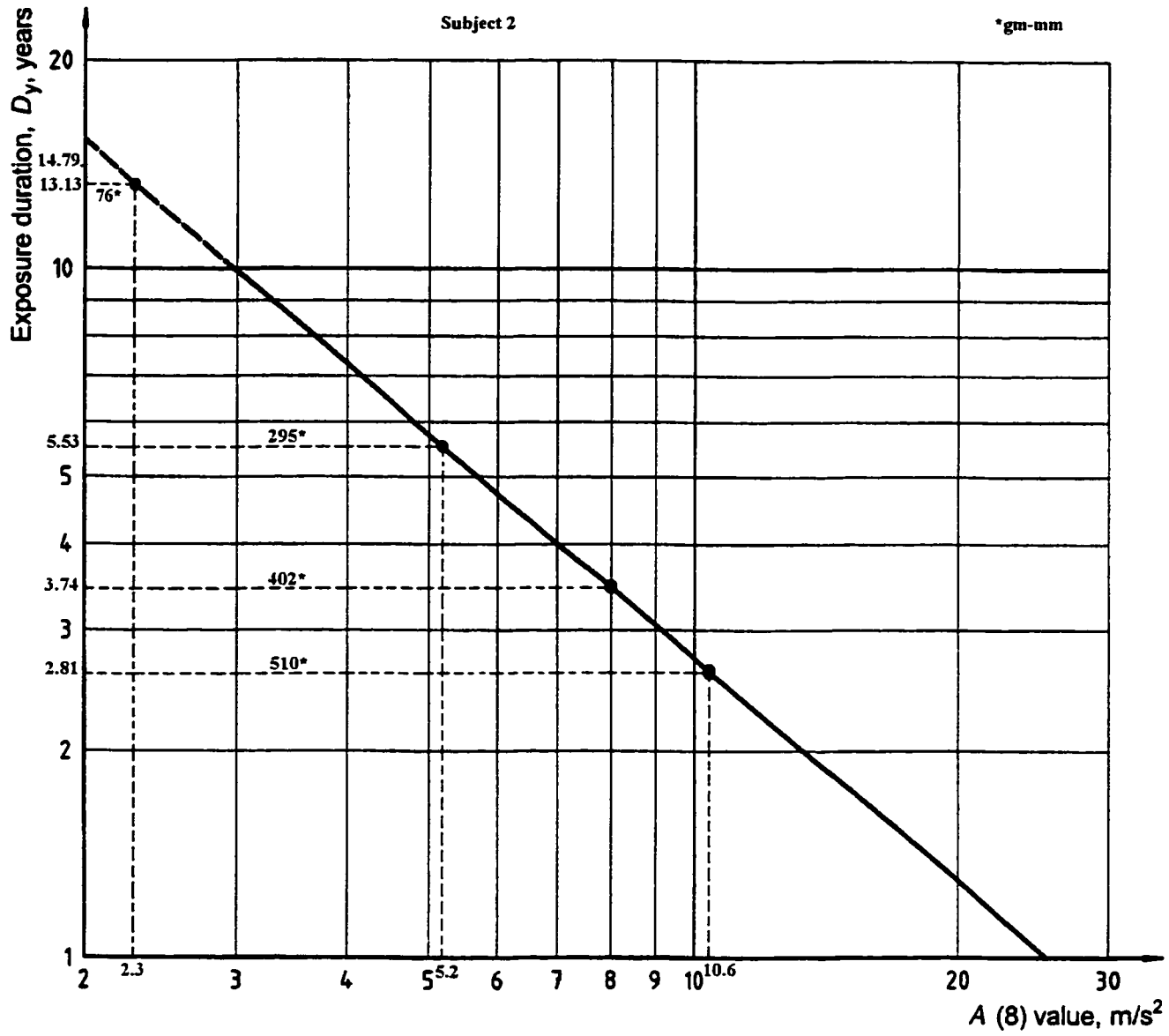

Figure 3.34: Number of exposure years D_y versus the eight-hour energy equivalent $A(8)$ for the measured conditions.

3.8 Summary

The results of the experimental investigations are reported in this chapter. The results show that the feed force does not have a significant effect on the rms acceleration values due to hand-transmitted vibration. However, it must be noted that the feed force simulated in the experiment acts only on the hand and does not affect the cutting forces. The mass unbalances; however, affect the magnitude of hand-transmitted vibration quite significantly. A simple analytical model of the grinder, represented by a disc on a rigid shaft, is developed in the next chapter in order to obtain an insight into the response of the hand-arm power tool system subject to rotary unbalance excitation. Measurements performed with two subjects revealed considerable deviations, the inter-subject variability was observed to be relatively low. The measured data are analyzed in terms of unweighted and frequency weighted overall rms accelerations, eight-hour energy equivalent and number of years of exposure before the symptoms could occur in 10% of the population. The results clearly suggest that the use of an automatic balancer could counter the adverse effects of mass-unbalance, thereby could enhance the safety of the hand-held grinder, and reduce the vibration transmitted to the hand of the operator.

Chapter 4

Development of the Hand-Grinder Model

4.1 Introduction

The characteristics of the hand-transmitted vibration are mainly dependant upon the type of power tool and nature of the task performed by the operators. The vibration characteristics of various tools, measured at the handle, have been reported in the literature (Reynolds, 1982; Radwin, 1985, 1990). A study of the reported data shows that the handle vibration characteristics of different tools are considerably different (Rakheja et al., 2002a). The assessment of severity of hand-transmitted vibration necessitates appropriate consideration of vibration characteristics of specific tools.

Grinding machines are one of the primary tools used in the industry, and may lead to VWF over years of occupational use, as evident from the previous chapter. Especially the workers in the welding and foundry industry are subjected to high risk of vibration injuries due to long exposure times and high vibration levels transmitted to the workers' hands. The residual unbalance in the grinding wheel is one of the primary causes of high magnitudes of HTV. The unbalance also changes as the grinding wheel wears during grinding. Automatic balancing device has been developed to reduce the magnitude of HTV (Agafonov, 1976; Lindell, 1996; Rajalingham et al., 1998).

A simple model of the hand-held grinder is developed using the theory presented in chapter 2 to study the vibration behavior of the grinder in the presence of a mass unbalance. The hand-grinder model consists of the grinder represented by a cantilevered rotor supported on two bearings, the tool body that includes the rigidly connected handle,

and a single degree-of-freedom representation of the human hand. The bearings are characterized by linear stiffness and damping elements. The axis system, which is used in defining the motion of the tool, is the basicentric system, where z-axis is along the human hand and arm and y-axis along the handle of the tool.

4.2 Hand-Grinder Model

The vibration characteristics of hand-held grinders have been extensively measured in the laboratory and the field for the purposes of assessment in relation to the vibration exposure of the human hand-arm (Lindell, 1996, ISO-8662-4, 1994). No attempts, however, have been reported on the analytical modeling of such grinders. An analytical model and its analysis could yield significant insight into many desirable design features and vibration isolation mechanisms to reduce the severity of HTV. The lack of efforts in the modeling and analysis is most likely attributed to the complexities involving characterization of highly complex cutting forces and torques, uneven wear of the grinding discs, non-uniform distributions of the cutting forces, varying degree of mass-unbalance during a grinding task, nonlinear properties of bearings, structural flexibility of the grinding wheel and the spindle, etc. While the characterization of cutting forces is quite complex, the role of mass-unbalance alone on the grinder vibration can be investigated using a simple model.

In this study, a simple mathematical model is developed for the coupled hand-grinder system in order to study its vibration behaviour due to mass unbalance. The contributions due to flexibility of the disc and spindle are neglected in the model. Such contributions are evident from the measured data presented in chapter 3. While the measured data, invariably, reveal dominant responses near frequencies corresponding to

the angular speed of the disc, considerable vibration magnitudes are also evident at higher frequencies. These high frequency components are mostly attributed to the flexibility of the shaft-rotor system and nonlinear properties of the bearings. The proposed simplified model, however, could predict the behaviour due to mass unbalance in the vicinity of frequencies corresponding to the angular speed, and is thus considered as a preliminary attempt in deriving an analytical model of the grinder. Furthermore, no attempts are made to compare the simulation results with the measured data due to extreme simplicity of the model. The rotor and shaft assembly is represented by a rigid rotor supported on a cantilever shaft, which is also considered to be rigid. The tool body together with the handles is considered as a rigid body with two-degrees-of-freedom along the y and z-axes, while the motion along the x-axis is not considered in the plane model. Each bearing is represented by a parallel combination of a linear spring and a viscous damper connecting the shaft to the tool body. Representative values for the bearing stiffness were taken from published literature on bearings employed in similar applications (Tiwari, 2000; Gargiulo, 1980; Tamura, 1985). The values for the damping coefficients were adjusted to realize response magnitudes comparable with those attained from the measurements.

A large number of lumped-parameter models of the hand-arm system have been proposed on the basis of measured driving-point mechanical impedance of the human hand arm. These models range from single to four-degrees-of-freedom models with linear stiffness and damping elements. The properties of the reported models have been compared in a recent study with one of the objective being the identification of a suitable model for applications in the hand-tool system modeling (Rakheja et al., 2002c). The

study concluded that none of the reported models is suited for such applications primarily due to very low stiffness of some of the spring elements. A single-degree-of-freedom hand-arm model is implemented to the tool model to represent the visco-elastic hand-handle contact and the hand-arm mass m_h. An identical model of the hand-arm system is employed along both axes of vibration, z and y-axes. The damping and stiffness of the human hand are obtained from the earlier studies on hand-arm vibration (Radwin, 1985).

Figure 4.1a illustrates the analytical model of the coupled hand-tool model in the z-axis. Identical bearing properties and hand-arm models are also considered in the y-axis as shown in Figure 4.1b. The disc is represented by its mass m_d and mass moment of inertia I_p. K_{b1} and K_{b2} represent the constant spring rates due to lower and upper bearings, respectively, and C_{b1} and C_{b2} are their respective damping coefficients. The tool housing together with the handles is represented by a lumped mass m_b, while m_h represents the hand-arm mass. K_{h1} and C_{h1} are the stiffness and damping coefficients of hand in contact with the tool body, and K_{h2} and C_{h2} are the coefficients of the hand-arm system. The gyroscopic effect is not considered in this model because of its insignificant effect.

4.3 Equations of motion for the Model

The equations of motion of the coupled hand-tool system are derived along the z and y-axes, considering four-degrees-of-freedom along each axis. These include the motion of the tool body (y_3, z_3), motion of hand-arm mass (y_4, z_4), translational motion of the disc (y_d, z_d) and rotational motions of the disc (β, α).

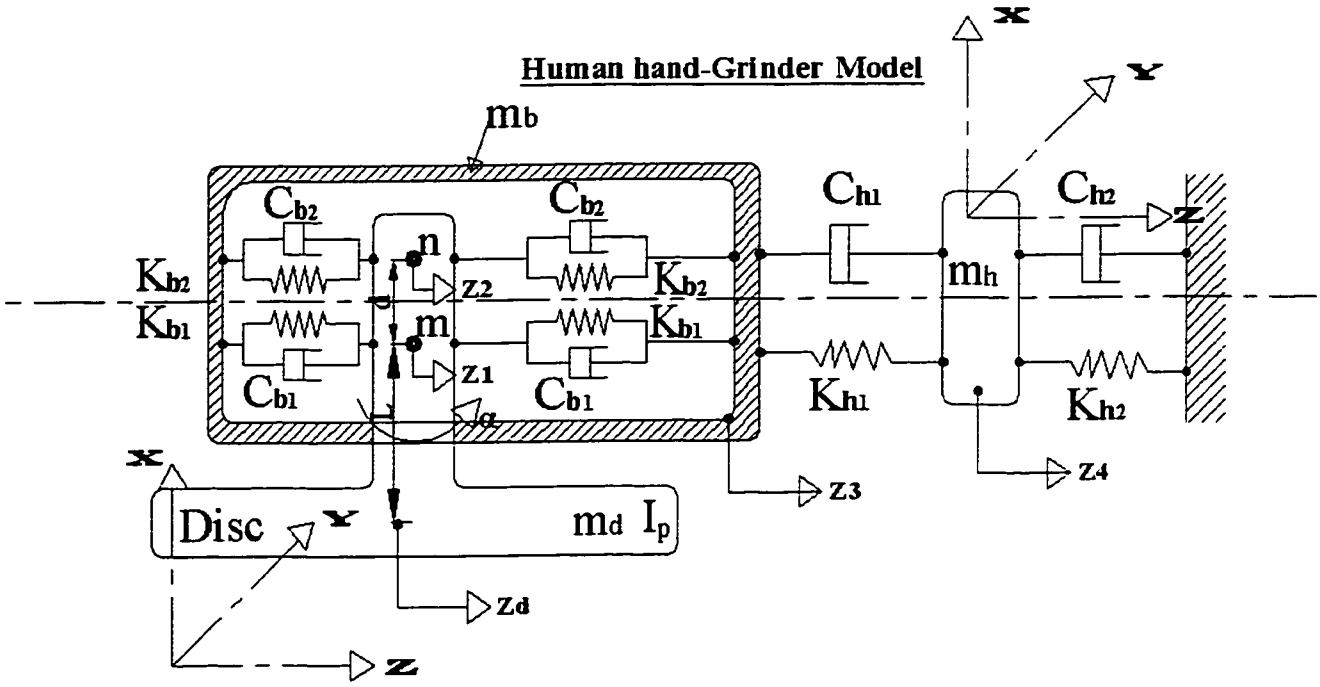

Figure 4.1.a: Analytical model for a human hand and power tool in the z-axis.

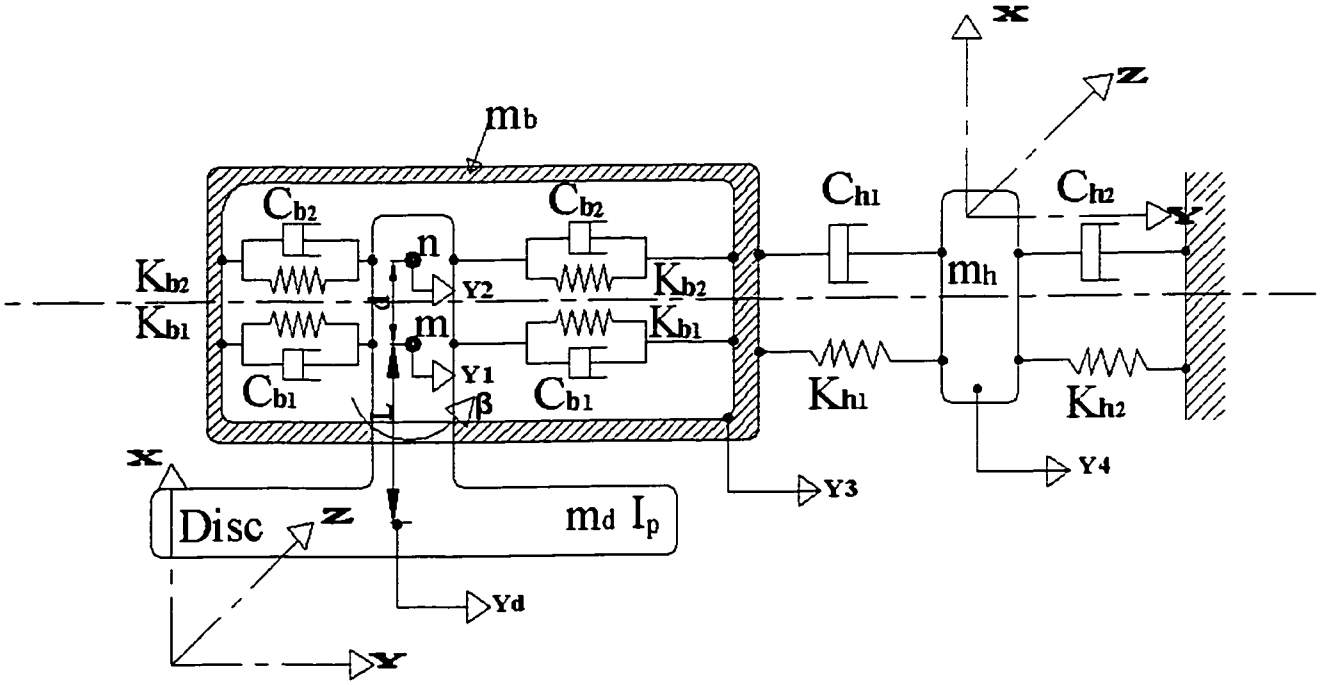

Figure 4.1.b: Analytical model for a human hand and power tool in the y-axis.

4.3.1 Equations of motion along the z-axis

The centroidal motion of the grinding wheel can be related to the motions of the shaft in the vicinity of the bearings support, such that:

$$z_d = z_1 + \alpha l$$

where z_d is the centroidal motion of the disc and α is the angular motion of the shaft-disc assembly, as shown in Figure 4.1.a. The translation of the shaft in the vicinity of the upper bearing support can be expressed as:

$$z_2 = z_1 - \alpha d$$

Consequently, the rotation of the shaft-wheel assembly is described by the parameter α as:

$$\alpha = \frac{z_1 - z_2}{d}$$

Time differentiation of the above equations yields the following expressions for the acceleration of the disc:

$$\ddot{\alpha} = \frac{\ddot{z}_1 - \ddot{z}_2}{d}; \text{ and } \ddot{z}_d = \ddot{z}_1 + \frac{\ddot{z}_1 l}{d} - \frac{\ddot{z}_2 l}{d}$$

Let m_u represent the mass-unbalance of the grinding wheel with an eccentricity e, such that the total mass of the shaft-disc assembly is $m_T = m_d + m_u$. The equation of motion for the translational motion of the assembly may thus be derived as:

$$\ddot{z}_d = \frac{1}{m_T}[-2c_{b1}\dot{z}_d + 2c_{b1}l\dot{\alpha} + 2c_{b1}\dot{z}_3 - 2c_{b2}\dot{z}_d + 2c_{b2}(l+d)\dot{\alpha} + 2c_{b2}\dot{z}_3 - 2k_{b1}z_d + 2k_{b1}l\alpha + 2k_{b1}z_3 - 2k_{b2}z_d + 2k_{b2}(l+d)\alpha + 2k_{b2}z_3 + m_u e\omega^2 \cos\omega t] \quad (4.1)$$

The equation of motion describing the rotational motion of the disc is derived as:

$$\ddot{\alpha} = \frac{1}{I_p}[-2c_{b1}\, l\dot{z}_d + 2c_{b1}\, l^2\, \dot{\alpha} + 2c_{b1}\, l\, \dot{z}_3 - 2c_{b2}(l+d)\dot{z}_d + 2c_{b2}(l+d)^2\, \dot{\alpha} + 2c_{b2}(l+d)\, \dot{z}_3$$
$$-2k_{b1}\, lz_d + 2k_{b1}l^2\, \alpha + 2k_{b1}lz_3 - 2k_{b2}(l+d)\, z_d + 2k_{b2}(l+d)^2\, \alpha + 2k_{b2}(l+d)z_3\,] \qquad (4.2)$$

The equations of motion describing the motions of the tool body (z_3) and the hand-arm mass (z_4) are derived in a similar manner and given by:

$$\ddot{z}_3 = \frac{1}{m_b}[-2c_{b1}\, \dot{z}_d + 2c_{b1}l\dot{\alpha} + 2c_{b1}\dot{z}_3 - 2c_{b2}\, \dot{z}_d + 2c_{b2}\,(l+d)\dot{\alpha} + 2c_{b2}\dot{z}_3 - 2k_{b1}\, z_d + 2k_{b1}l\alpha$$
$$+ 2k_{b1}z_3 - 2k_{b2}\, z_d + 2k_{b2}(l+d)\alpha + 2k_{b2}z_3 - c_{h1}\, \dot{z}_3 + c_{h1}\dot{z}_4 - k_{h1}z_3 + k_{h1}z_4\,] \qquad (4.3)$$

$$\ddot{z}_4 = \frac{1}{m_h}[-c_{h1}\dot{z}_4 + c_{h1}\dot{z}_3 - k_{h1}z_4 + k_{h1}z_3 - c_{h2}\, \dot{z}_4 - k_{h2}\, z_4] \qquad (4.4)$$

4.3.2 Equations of motion along the y-axis

The centroidal motion of the disc along the y-axis is related to its rotation about the x-axis, β:

$$y_d = y_1 + \beta l$$

where $y_1 = y_2 + \beta d$, is the motion of the shaft in the vicinity of lower bearing support. The time differentiation of the above yields following expressions for the accelerations;

$$\ddot{\beta} = \frac{\ddot{y}_1 - \ddot{y}_2}{d}; \text{ and } \ddot{y}_d = \ddot{y}_1 + \frac{\ddot{y}_1\, l}{d} - \frac{\ddot{y}_2\, l}{d}$$

Considering an unbalance mass m_u with an eccentricity of e, the equations of motion describing the motions of disc, tool body and hand-arm mass along the y-axis are described as follows:

$$\ddot{y}_d = \frac{1}{m_T}[-2c_{b1}\dot{y}_d + 2c_{b1}l\dot{\beta} + 2c_{b1}\dot{y}_3 - 2c_{b2}\dot{y}_d + 2c_{b2}(l+d)\dot{\beta} + 2c_{b2}\dot{y}_3 - 2k_{b1}y_d$$
$$+2k_{b1}l\beta + 2k_{b1}y_3 - 2k_{b2}y_d + 2k_{b2}(l+d)\beta + 2k_{b2}y_3 + m_u e\omega^2 \sin\omega t] \quad (4.5)$$

$$\ddot{\beta} = \frac{1}{I_p}[-2c_{b1}l\dot{y}_d + 2c_{b1}l^2\dot{\beta} + 2c_{b1}l\dot{y}_3 - 2c_{b2}(l+d)\dot{y}_d + 2c_{b2}(l+d)^2\dot{\beta} + 2c_{b2}(l+d)\dot{y}_3$$
$$-2k_{b1}ly_d + 2k_{b1}l^2\beta + 2k_{b1}ly_3 - 2k_{b2}(l+d)y_d + 2k_{b2}(l+d)^2\beta + 2k_{b2}(l+d)y_3] \quad (4.6)$$

$$\ddot{y}_3 = \frac{1}{m_b}[-2c_{b1}\dot{y}_d + 2c_{b1}l\dot{\beta} + 2c_{b1}\dot{y}_3 - 2c_{b2}\dot{y}_d + 2c_{b2}(l+d)\dot{\beta} + 2c_{b2}\dot{y}_3 - 2k_{b1}y_d + 2k_{b1}l\beta$$
$$+2k_{b1}y_3 - 2k_{b2}y_d + 2k_{b2}(l+d)\beta + 2k_{b2}y_3 - c_{h1}\dot{y}_3 + c_{h1}\dot{y}_4 - k_{h1}y_3 + k_{h1}y_4] \quad (4.7)$$

$$\ddot{y}_4 = \frac{1}{m_h}[-c_{h1}\dot{y}_4 - c_{h2}\dot{y}_4 + c_{h1}\dot{y}_3 - k_{h1}y_4 - k_{h2}y_4 + k_{h1}y_3] \quad (4.8)$$

Equations (4.1) to (4.8) describe the motions of the coupled hand-tool system along the y and z-axes in the presence of a mass unbalance. It should be noted that the model does not allow for consideration of feed force, since it would necessitate identification of hand-arm model parameters corresponding to a selected feed force.

4.4 Model Parameters

The spindle is supported by two different ball bearings. The lower bearing located at point m on the shaft (Figure 4.1a) is larger than the upper bearing located at point n. The stiffness of such models of bearings can be taken in the order of 10^7 N/m (Tiwari et al., 2000). Table 4.1 shows the specifications of these bearings. The geometric and inertial parameters of the tool were measured for the selected tool and summarized in Table 4.2. The table also lists the hand-arm model parameters.

Table 4.1: Specifications for the ball bearings of the tool.

Basic Bearing No.	Bore diameter*	Outer diameter*	Width*	Radius*	No. of Balls
609; upper	9	24	7	0.3	7
6002; lower	15	32	9	0.3	9

* millimeter

Table 4.2: Geometric and inertial properties of the hand-tool model.

Parameter	Value	Parameter	Value
d	$86.28*10^{-3}$ m	K_{h1}	$1*10^{6}$ N/m
ℓ	$20.82*10^{-3}$ m	K_{h2}	$3.8*10^{6}$ N/m
I_p	$6.0938*10^{-4}$ kg.m^2	$K_{b1} = K_{b2}$	$6.2*10^{7}$ N/m
$C_{b1} = C_{b2}$	$2*10^{3}$ Ns/m	m_b	1.8 kg
$C_{h1} = C_{h2}$	$2*10^{4}$ Ns/m	m_h	4.5 kg
m_d	$300*10^{-3}$ kg		

4.5 Simulation Results and Discussions

4.5.1 System Natural Frequencies and Damping Ratios

Table 4.3 shows the natural frequencies for the hand-tool model, for undamped case. The two highest undamped natural frequencies correspond to the case when the tool motion is predominant and the lowest two natural frequencies correspond to the case when the predominant motion is in the hand. The equations of motion for the coupled hand-tool system are solved under different magnitudes of mass unbalance and different values of rotational speed. Four different values of mass unbalance are considered as described in the previous chapter, and these are designated as 'U1', 'U2', 'U3', and 'U4' representing mass unbalance of 76, 295, 402, 510 gm-mm. The simulations are

performed at different angular speeds ranging from 1000 rpm to the maximum speed of 12000 rpm. The responses of the disc, tool body and the hand mass are evaluated in terms of rms accelerations.

Table 4.3: Undamped system natural frequencies.

n	$\omega_n * 10^4$
1	±5.5682
2	±1.4963
3	±0.1100
4	±0.0575

It needs to be noted that the rms acceleration response of the tool body would characterize the vibration transmitted to the hand since the handles are attached rigidly to the body. This rms acceleration response would be required for assessment using the ISO-5349-1 (2001) guidelines. The rms acceleration response of the hand mass, however, would be of little significance, since the model used in this study does not represent the biomechanical character of the hand-arm system. It should also be noted that addition of vibration isolation and protective devices, such as elastic handle grips and anti-vibrations gloves, would affect the nature of hand-transmitted vibration. The presence of gloves would alter the visco-elastic properties of the hand-tool body interface.

The vibration behavior of the tool could be altered by the damping properties of the bearings, inertial properties of the tool body, and visco-elastic properties of the hand-handle interface. An increase in the tool body may yield lower vibration (Rakheja et al., 2002b), but a heavier tool would be undesirable. The influence of variations in the inertial properties is thus not attempted in this study. The effect of damping properties of the

bearings and those of the hand-handle interface on the nature of transmitted vibration is investigated by varying the damping parameters in a systematic manner. The variations in the stiffness properties of the hand-handle interface are also not attempted, as these would directly deteriorate the dexterity.

4.5.2 Effect of Variations in the Bearing Damping

The influence of damping properties of the bearings on the magnitudes of transmitted vibration is investigated by varying the viscous damping coefficients due to both bearings. The bearing damping coefficients C_b were varied in steps of 10% of the nominal values of $2*10^3$ Ns/m, while the range was limited to ± 20 %. Owing to the simplicity of the model and consideration of symmetric properties in y and z-axes, the model simulations yield similar responses along both axes. The responses along the z-axis alone are presented as a function of the rotational speed in the 1000-12000 rpm range. The simulation results yield nearly harmonic response at the frequency corresponding to the angular speed. The acceleration responses of the tool body ($\ddot{z}_3$), hand mass ($\ddot{z}_4$) and the disc ($\ddot{z}_d$) are expressed in terms of the rms accelerations, and presented in Figure 4.2.a, b, and c for different values of mass unbalance and nominal values of the bearing damping coefficients. The results show that the magnitudes of vibration transmitted to the tool body and the hand mass increases with increasing rotational speed and the mass unbalance, which can be directly attributed to the excitation due to mass unbalance. The figures also suggest that the visco-elastic properties of the hand-handle interface tend to reduce the vibration of the hand mass considerably. Since there are no system natural frequencies in the speed range of the tool (0-12000 rpm) as shown in Table 4.3, the unbalance response shows a monotonically increasing trend.

Figures 4.3 to 4.6 illustrate the tool body and hand-mass responses as function of the unbalance and the angular speed corresponding to +10%, +20%, -10%, and –20% variations in the bearing damping, respectively. In all cases, the acceleration responses increase monotonically with the rotational speed, irrespective of the damping coefficient values and the mass-unbalance. Most importantly, the results show insignificant influence of the variations in the bearing damping coefficients. The system damping is expected to have most notable influence on the resonant response. Considering the high stiffness of the two bearings (in the order of $6.2*10^7$ N/m/bearing) and relatively small mass of the shaft-rotor system, the grinder yields very high natural frequency in excess of 4575.99 Hz. Since the unbalance excitation corresponding to highest rpm could yield predominant vibration near 200 Hz, the influence of bearing damping would be very small as evident from the simulation results. The results thus suggest that the magnitudes of hand-transmitted vibration, due to mass-unbalance, cannot be reduced by varying the bearing damping.

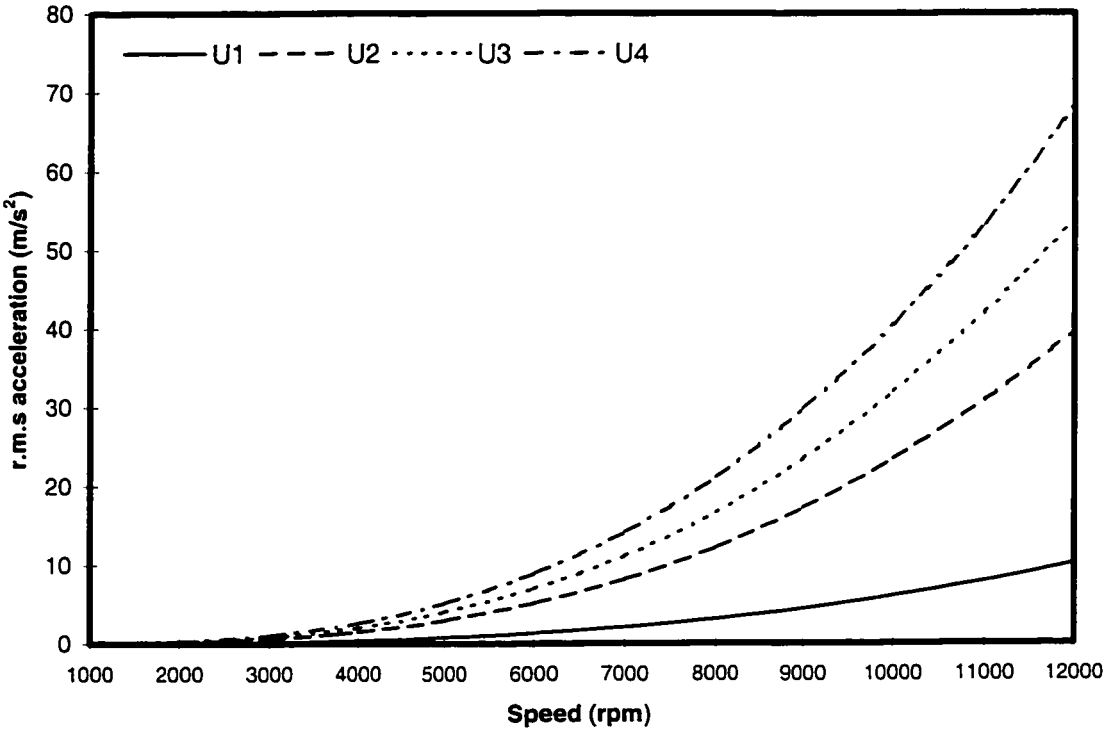

Figure 4.2.a: rms acceleration response of the tool body mass under different mass-unbalance and angular speeds ($C_b = 2*10^3$ Ns/m).

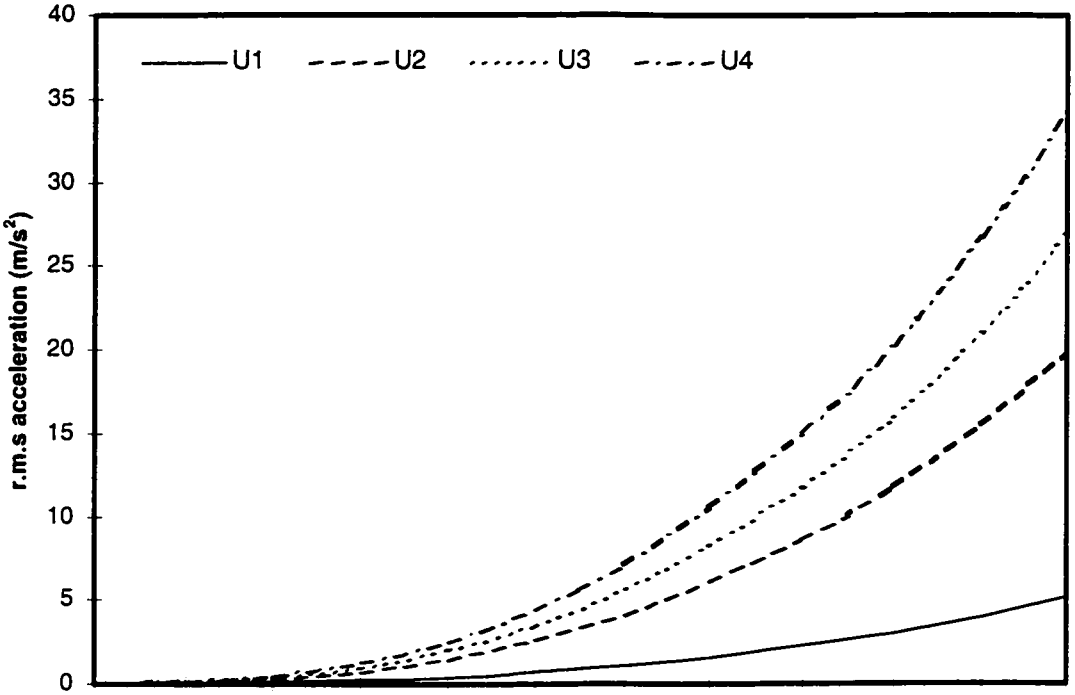

Figure 4.2.b: rms acceleration response of the hand mass under different mass-unbalance and angular speeds (C_b =2*10^3 Ns/m).

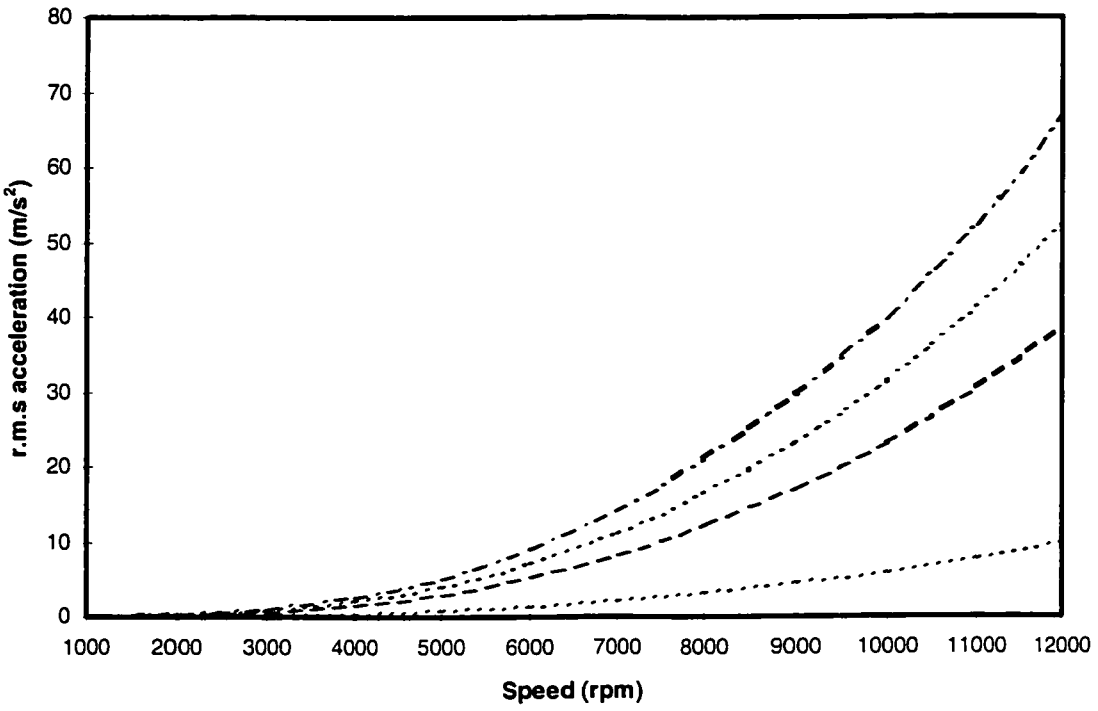

Figure 4.2.c: rms acceleration response of the disc under different mass-unbalance and angular speeds (C_b =2*10^3 Ns/m).

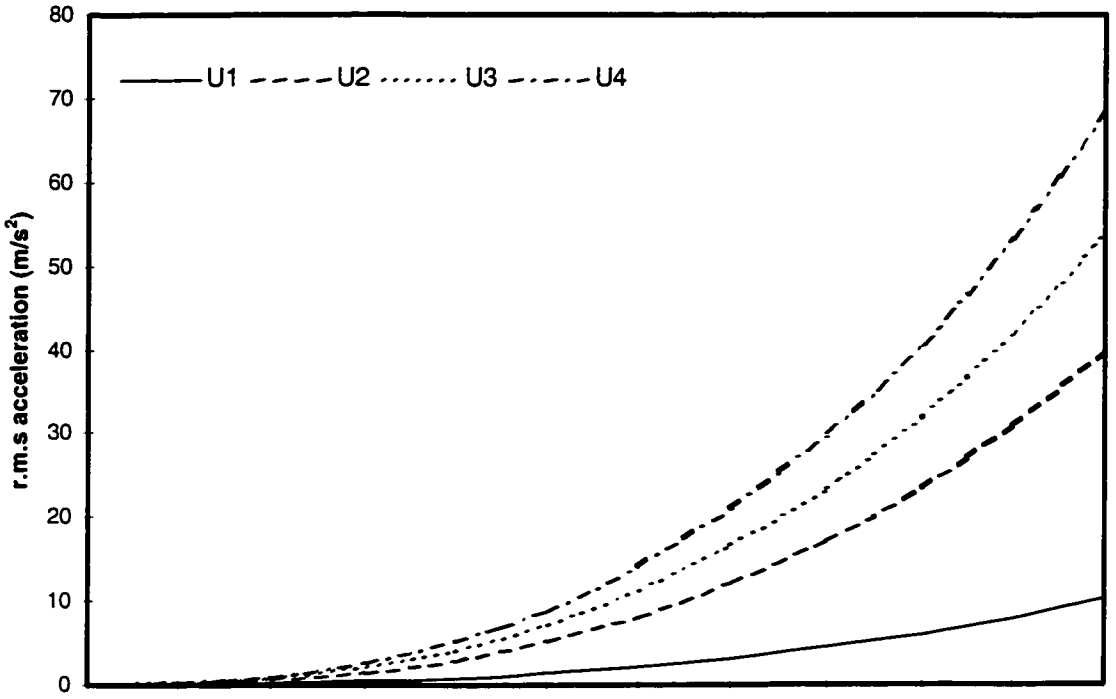

Figure 4.3.a: rms acceleration response of the tool body mass under different mass-unbalance and angular speeds ($C_b = 2*10^3$ +10% Ns/m).

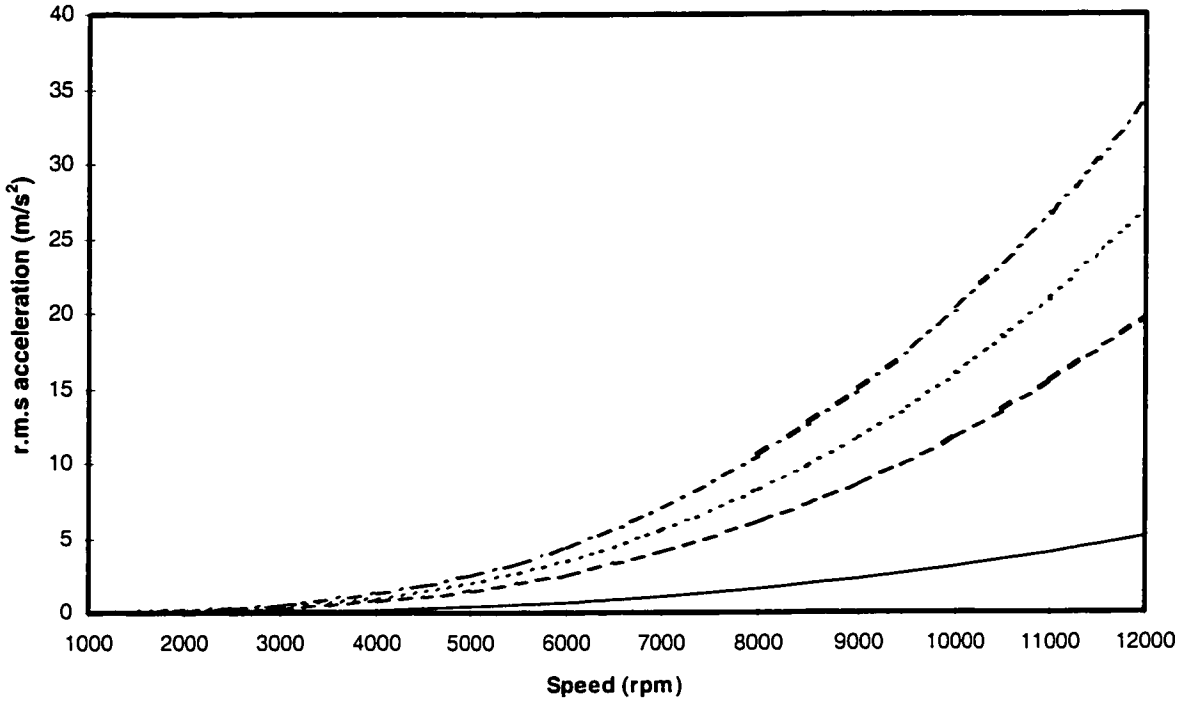

Figure 4.3.b: rms acceleration response of the hand mass under different mass-unbalance and angular speeds ($C_b = 2*10^3$ +10% Ns/m).

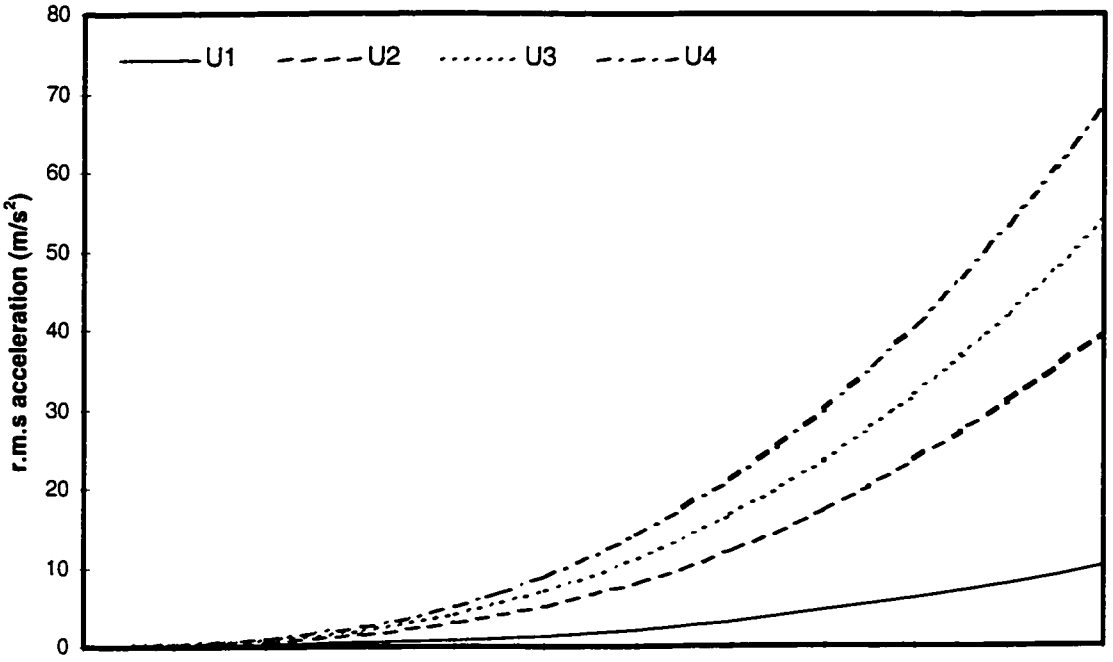

Figure 4.4.a: rms acceleration response of the tool body mass under different mass-unbalance and angular speeds ($C_b = 2*10^3$ +20% Ns/m).

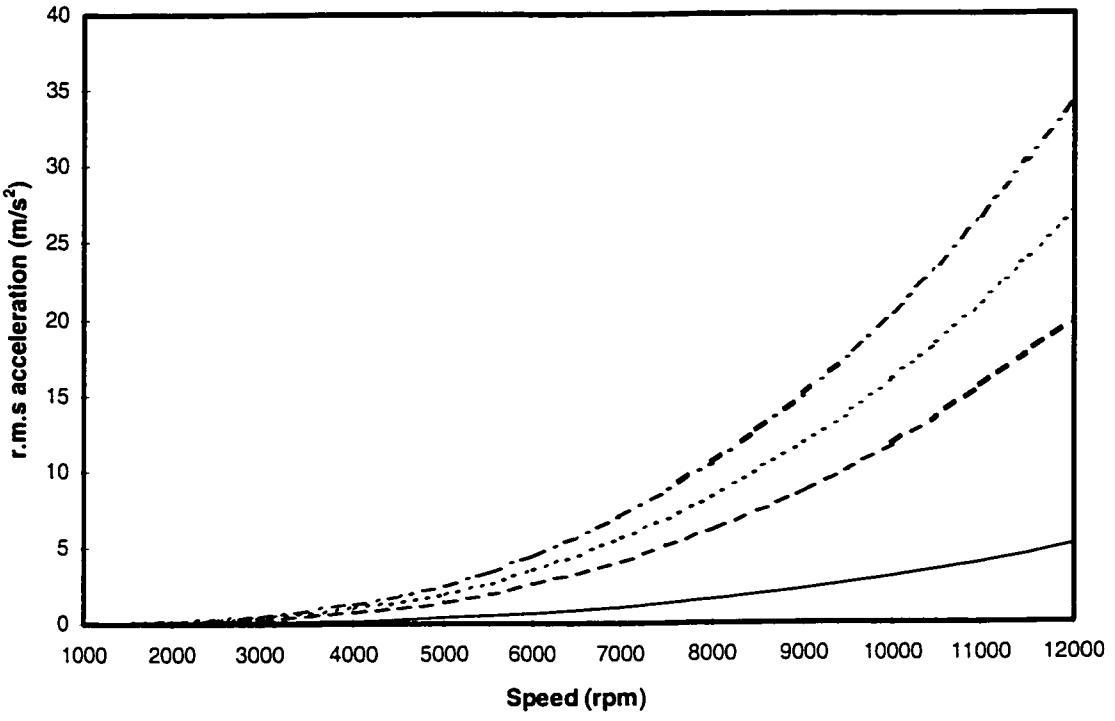

Figure 4.4.b: rms acceleration response of the hand mass under different mass-unbalance and angular speeds ($C_b = 2*10^3$ +20% Ns/m).

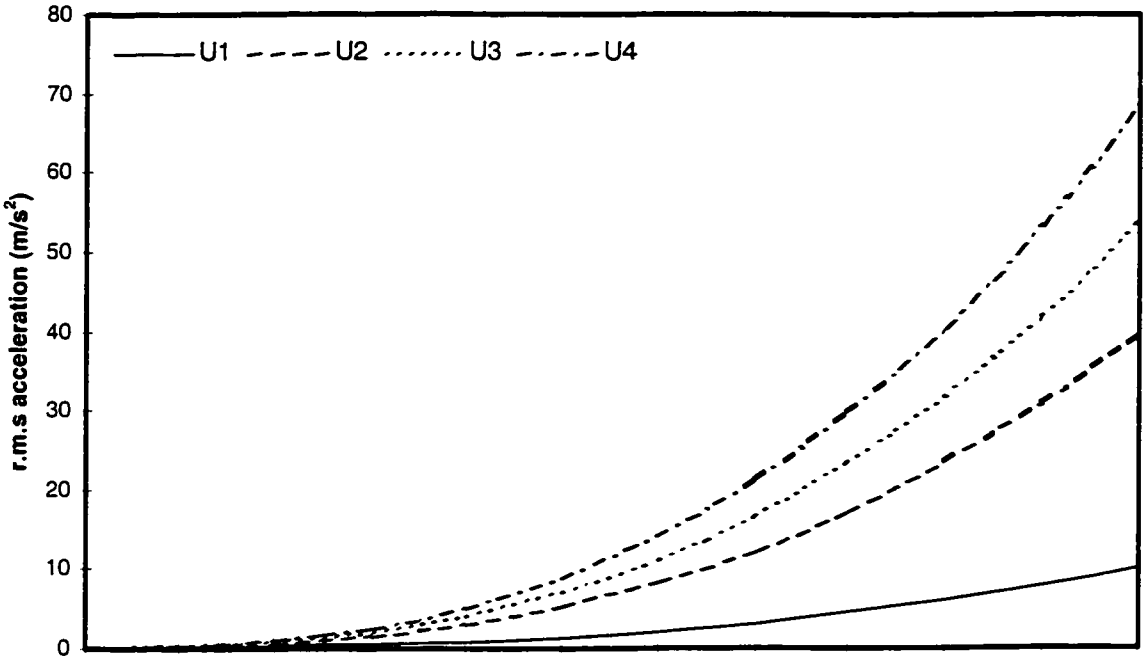

Figure 4.5.a: rms acceleration response of the tool body mass under different mass-unbalance and angular speeds ($C_b = 2*10^3$ –10% Ns/m).

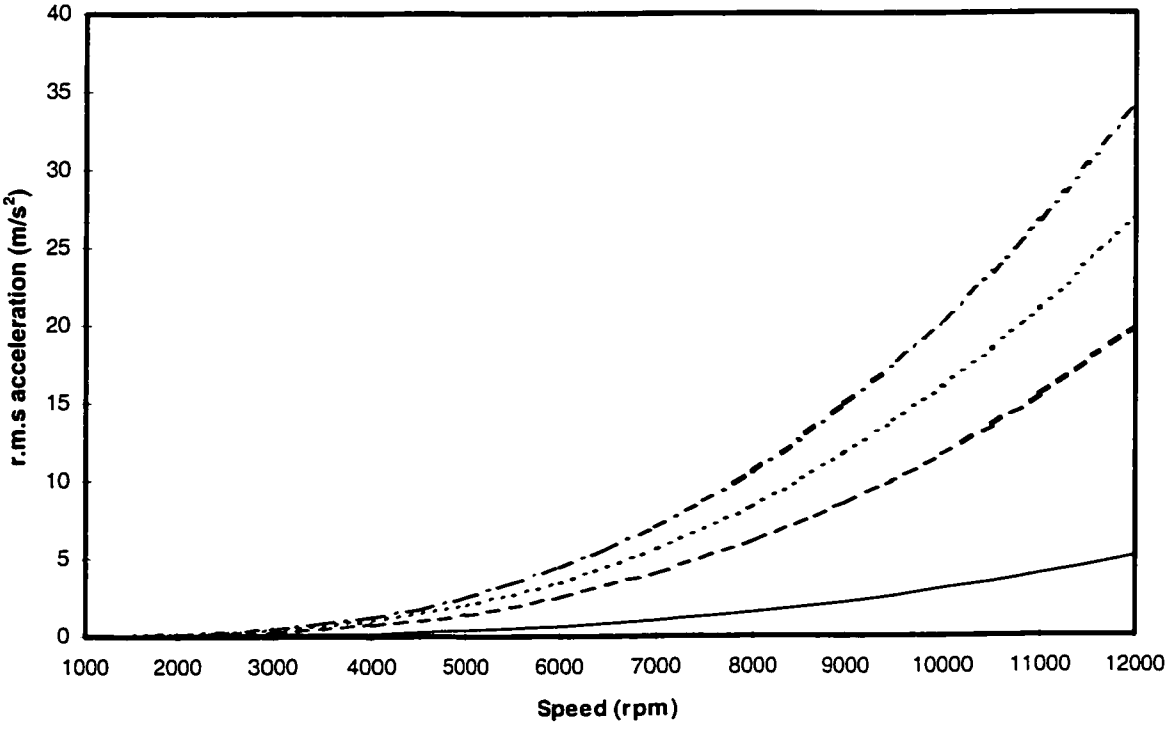

Figure 4.5.b: rms acceleration response of the hand mass under different mass-unbalance and angular speeds ($C_b = 2*10^3$ –10% Ns/m).

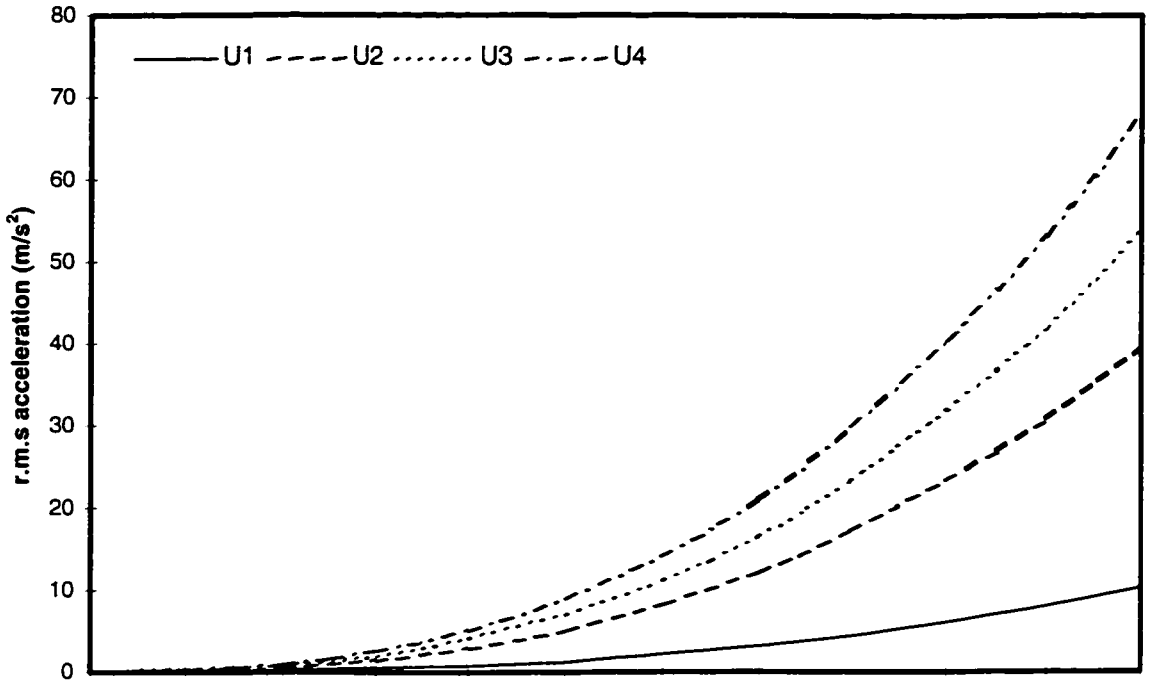

Figure 4.6.a: rms acceleration response of the tool body mass under different mass-unbalance and angular speeds ($C_b = 2*10^3$ –20% Ns/m).

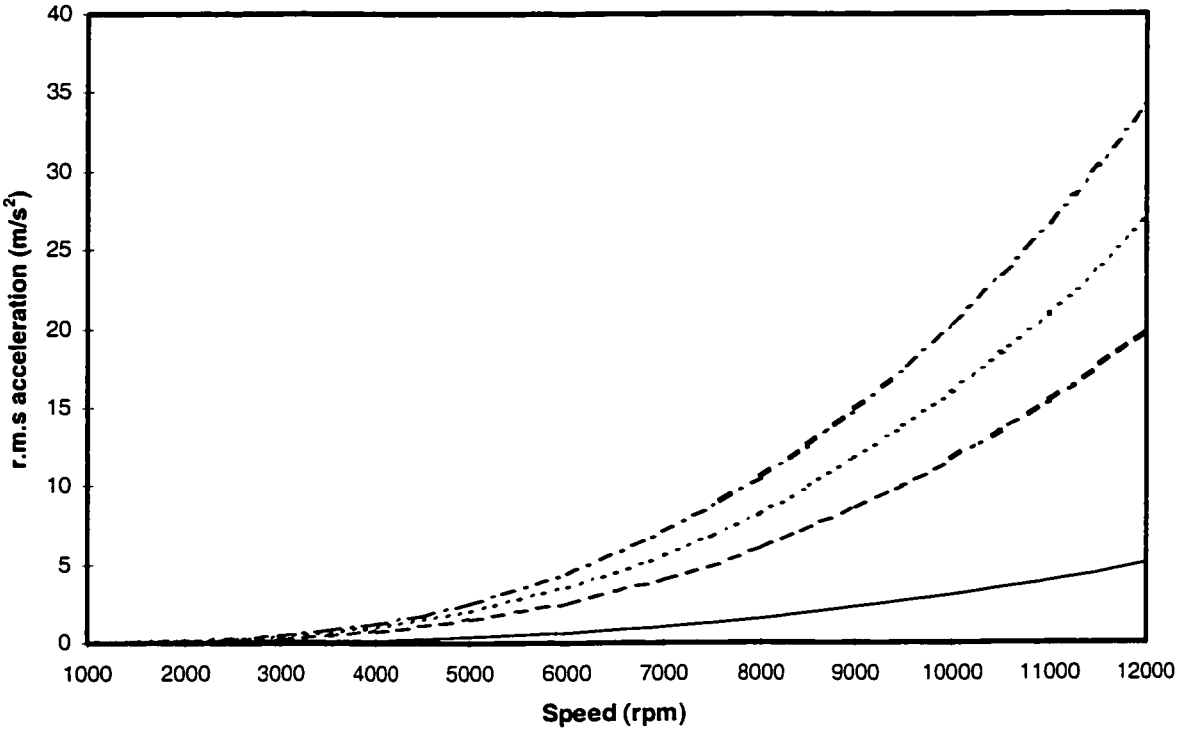

Figure 4.6.b: rms acceleration response of the hand mass under different mass-unbalance and angular speeds ($C_b = 2*10^3$ –20% Ns/m).

4.5.3 Influence of Hand-Handle Interface Properties

The tool handles are frequently designed with elastic handle grips that could effectively alter the visco-elastic properties of the hand-handle interface (K_{h1} and C_{h1}). The operators of such tools often use either protective or anti-vibration gloves, which would also affect the effective damping and stiffness coefficients of the tool body-hand interface, and thus the nature of the hand-transmitted vibration. The influence of variations in the hand-tool body interface properties are investigated by varying the stiffness and damping coefficients in the $\pm 20\%$ range of the nominal hand model parameters to study their effect on the transmitted vibration. All other model parameters are held at their nominal values.

Figures 4.7 to 4.10 illustrate the influence of variations in the interface damping coefficient (C_{h1}) on the rms acceleration responses of the tool body and the hand mass as functions of the mass-unbalance and the angular speed. The results show that the response increases monotonically with the angular speed, irrespective of the interface damping and the mass-unbalance, as observed earlier from Figures 4.2 to 4.6. The results suggest that an increase in the effective interface damping could help to reduce the magnitudes of rms acceleration responses of the tool-body and hand masses. A 20% increase in the interface damping coefficient would yield nearly 15% reduction in the tool body mass response and only 6% reduction in the hand mass response corresponds to extreme unbalance condition (U4) and 12000 rpm speed.

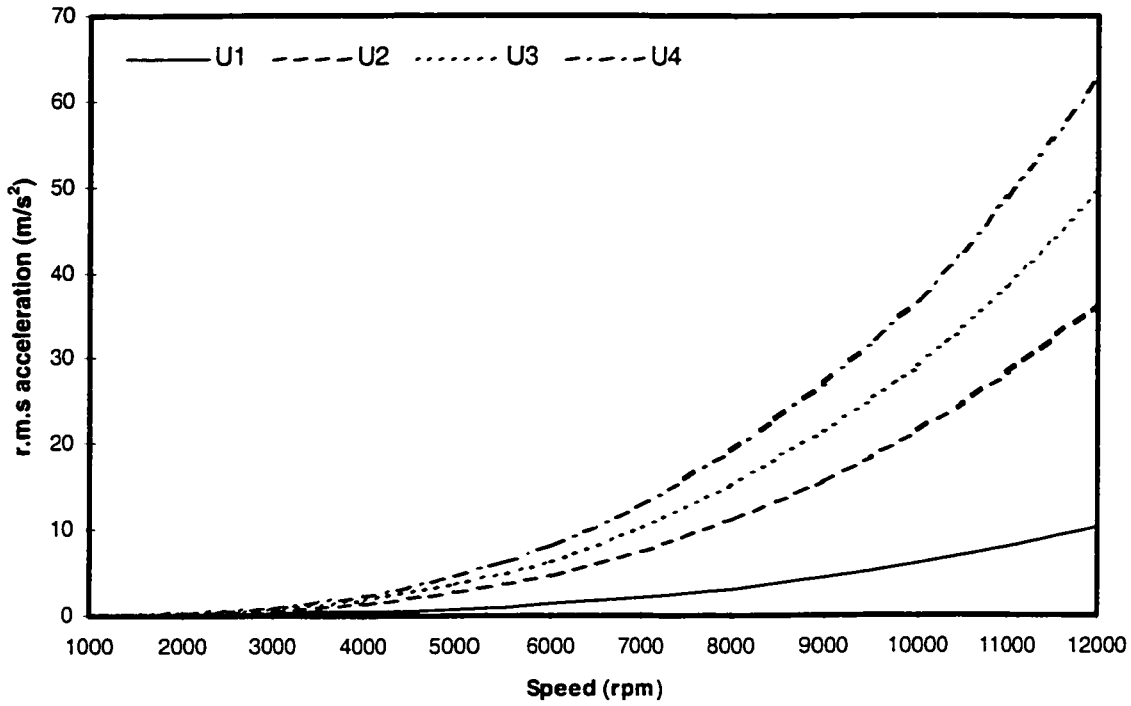

Figure 4.7.a: rms acceleration response of the tool body mass under different mass-unbalance and angular speeds ($C_{ht} = 20*10^3$ +10% Ns/m).

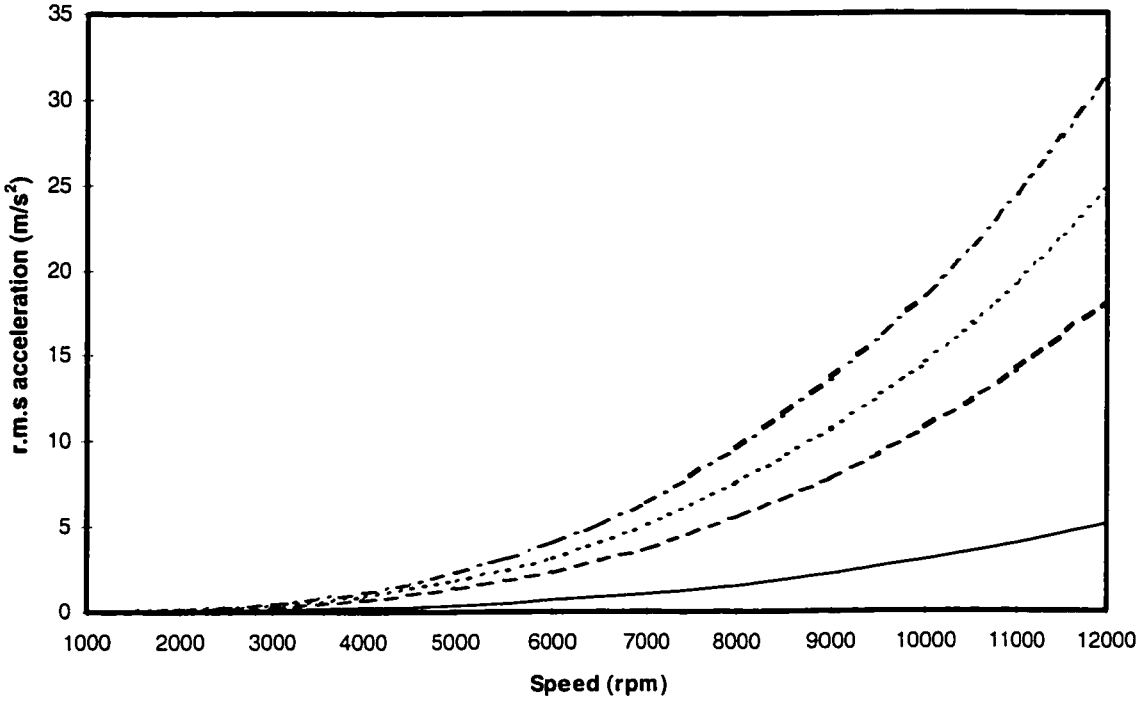

Figure 4.7.b: rms acceleration response of the hand mass under different mass-unbalance and angular speeds ($C_{ht} = 20*10^3$ +10% Ns/m).

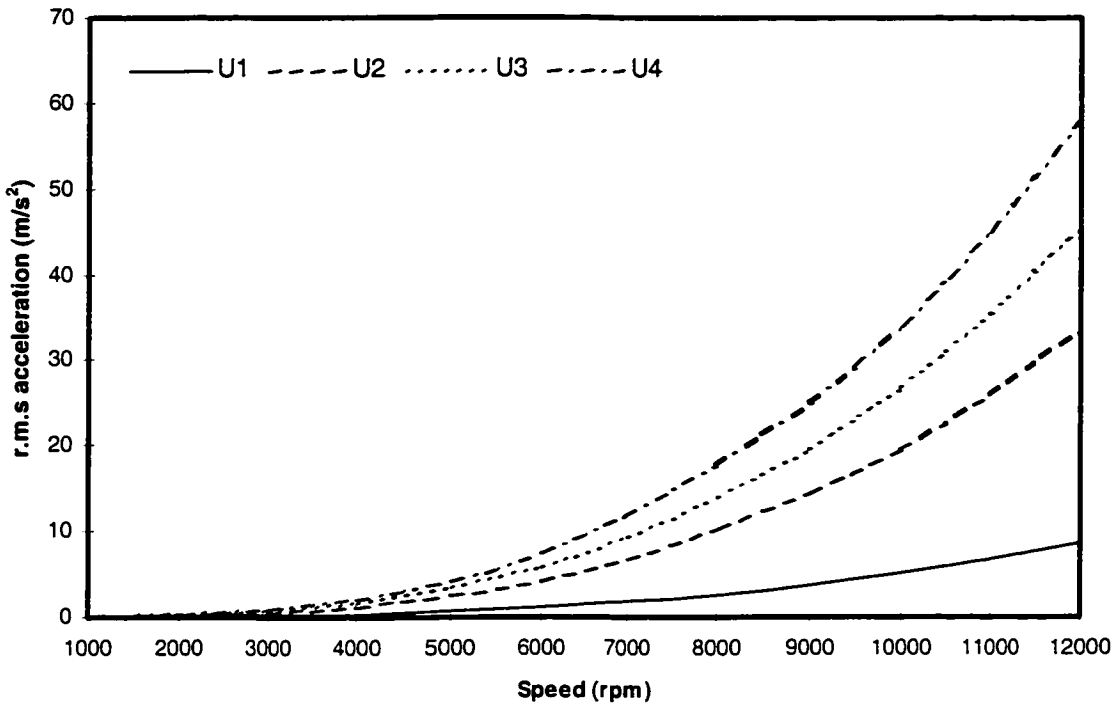

Figure 4.8.a: rms acceleration response of the tool body mass under different mass-unbalance and angular speeds ($C_h = 20*10^3$ +20% Ns/m).

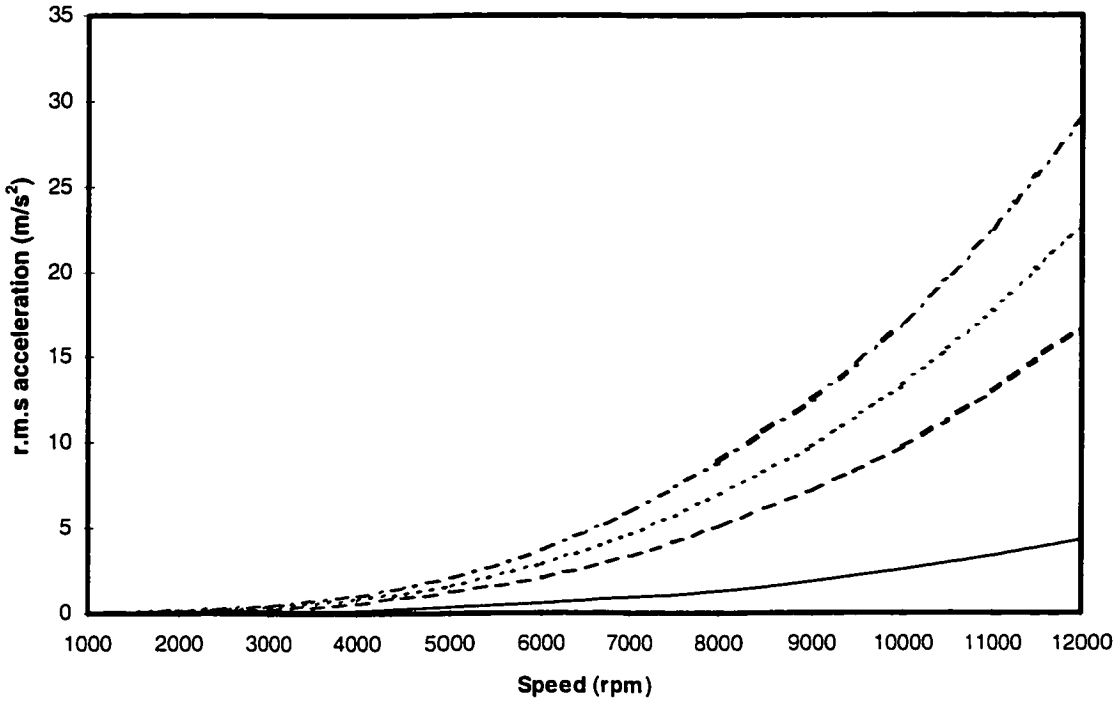

Figure 4.8.b: rms acceleration response of the hand mass under different mass-unbalance and angular speeds ($C_h = 20*10^3$ +20% Ns/m).

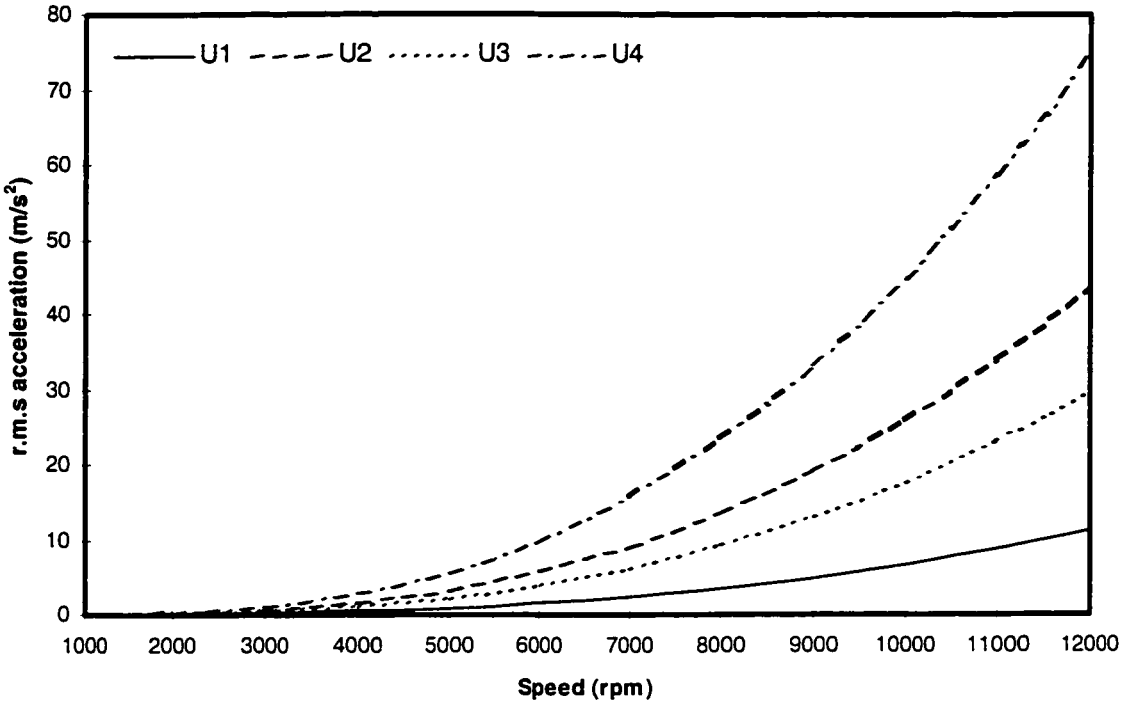

Figure 4.9.a: rms acceleration response of the tool body mass under different mass-unbalance and angular speeds ($C_h = 20*10^3$ –10% Ns/m).

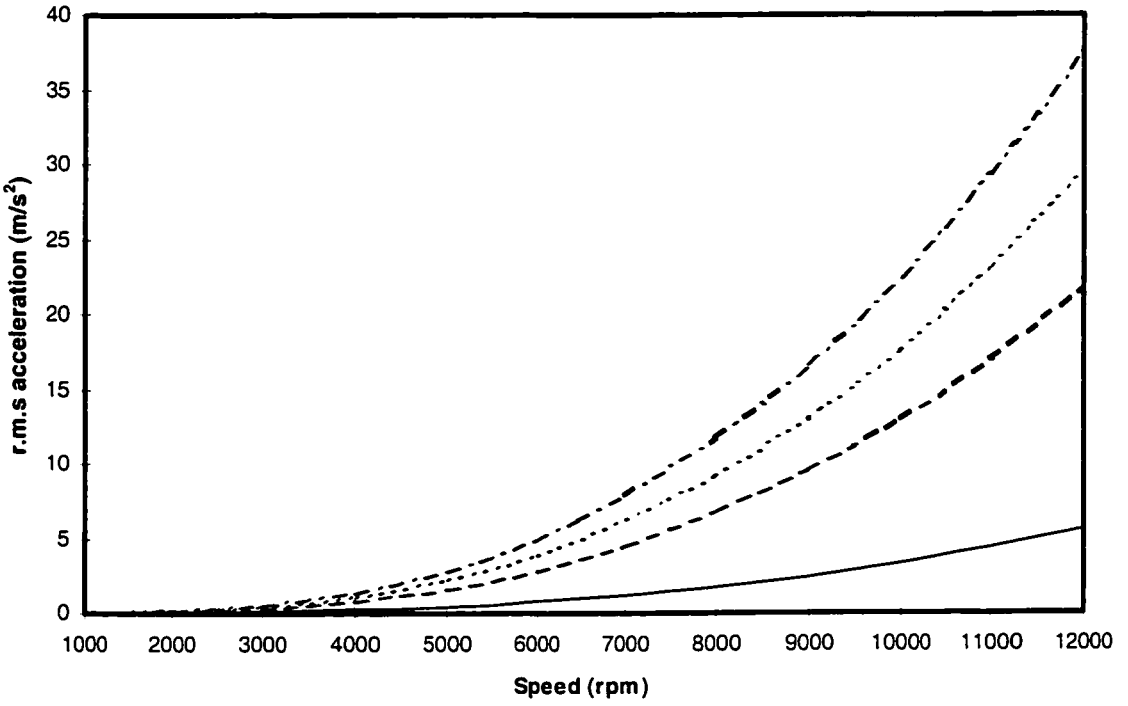

Figure 4.9.b: rms acceleration response of the hand mass under different mass-unbalance and angular speeds ($C_h = 20*10^3$ –10% Ns/m).

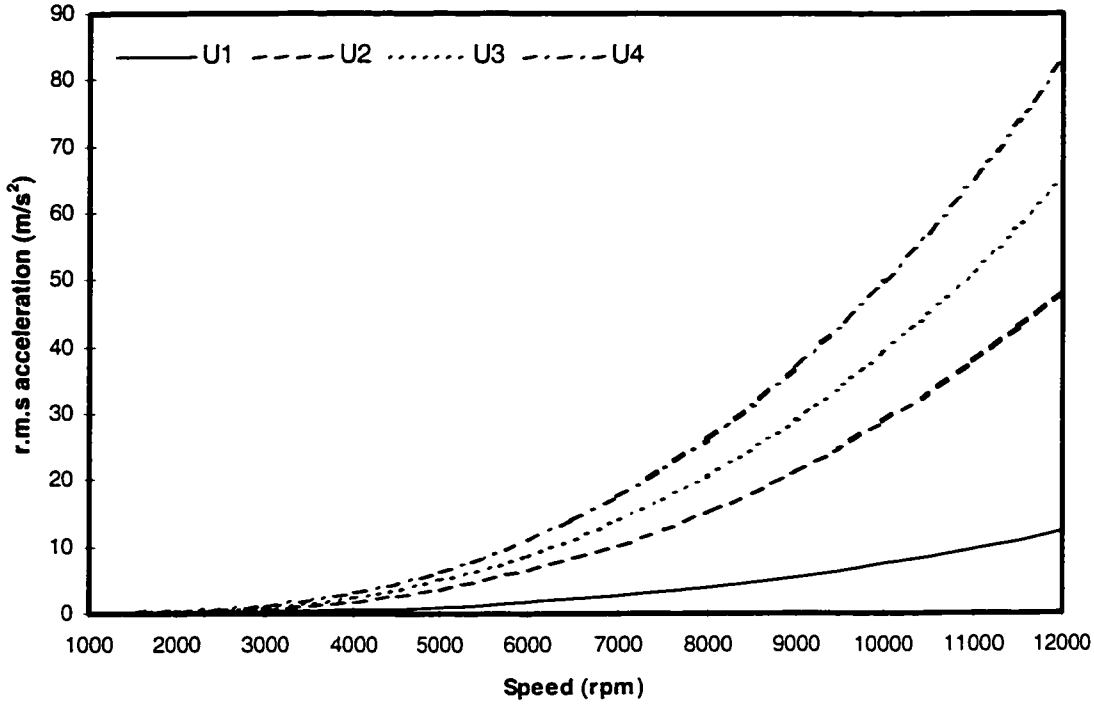

Figure 4.10.a: rms acceleration response of the tool body mass under different mass-unbalance and angular speeds ($C_h = 20*10^3$ –20% Ns/m).

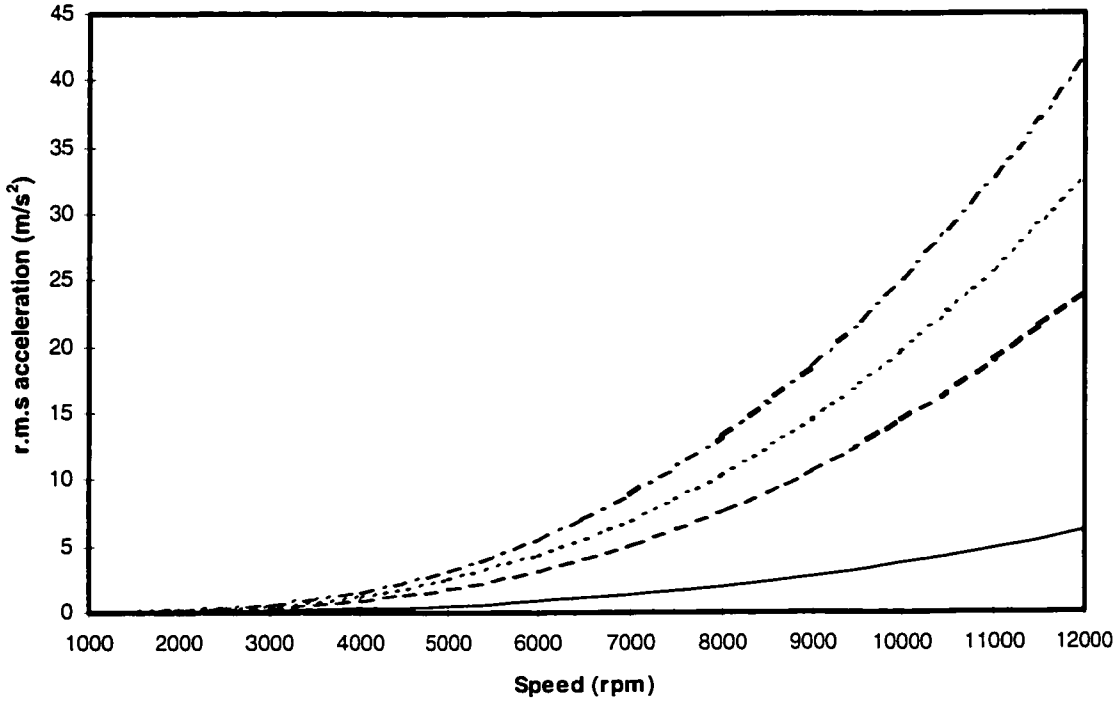

Figure 4.10.b: rms acceleration response of the hand mass under different mass-unbalance and angular speeds ($C_h = 20*10^3$ –20% Ns/m).

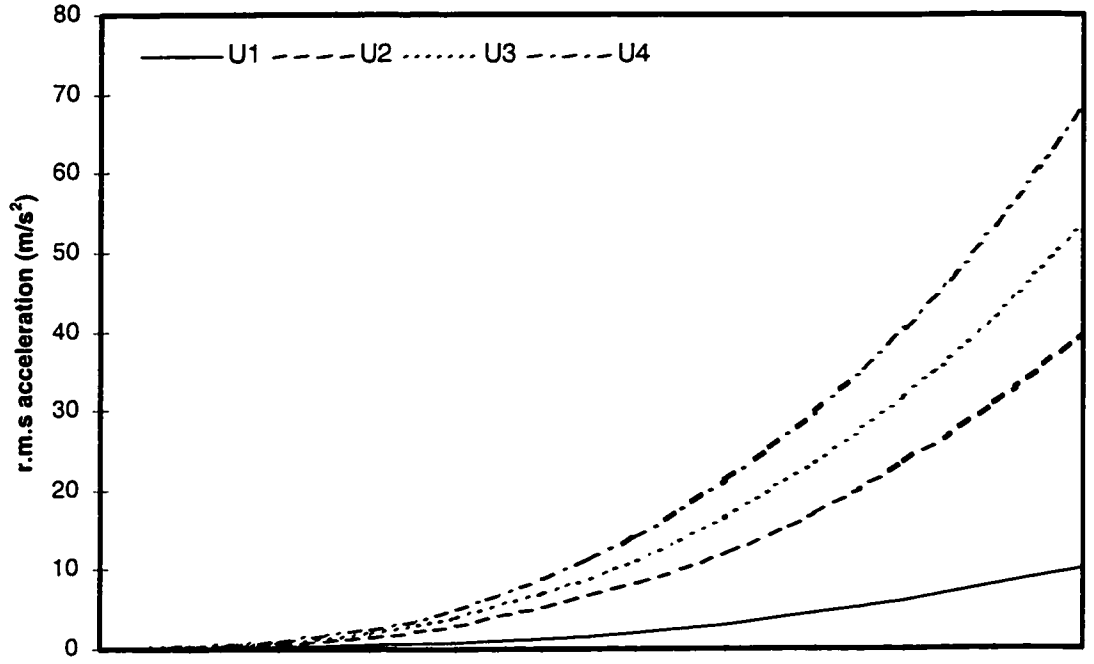

Figure 4.11.a: rms acceleration response of the tool body mass under different mass-unbalance and angular speeds ($K_{h1} = 10*10^5$ +10% N/m).

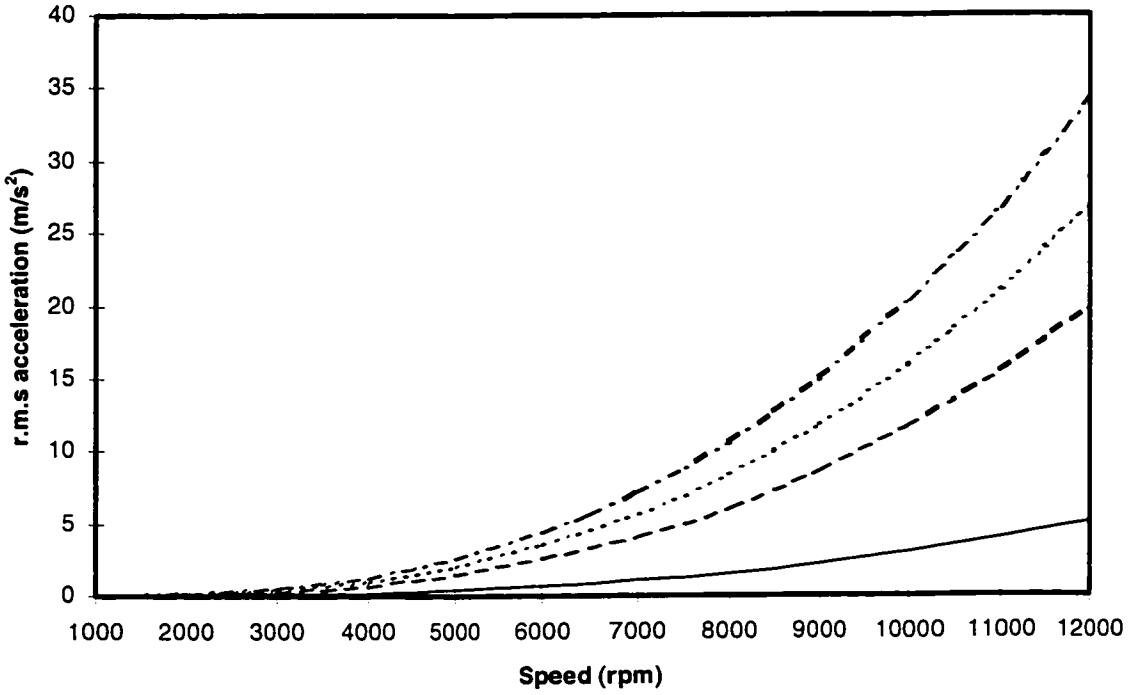

Figure 4.11.b: rms acceleration response of the hand mass under different mass-unbalance and angular speeds ($K_{h1} = 10*10^5$ +10% N/m).

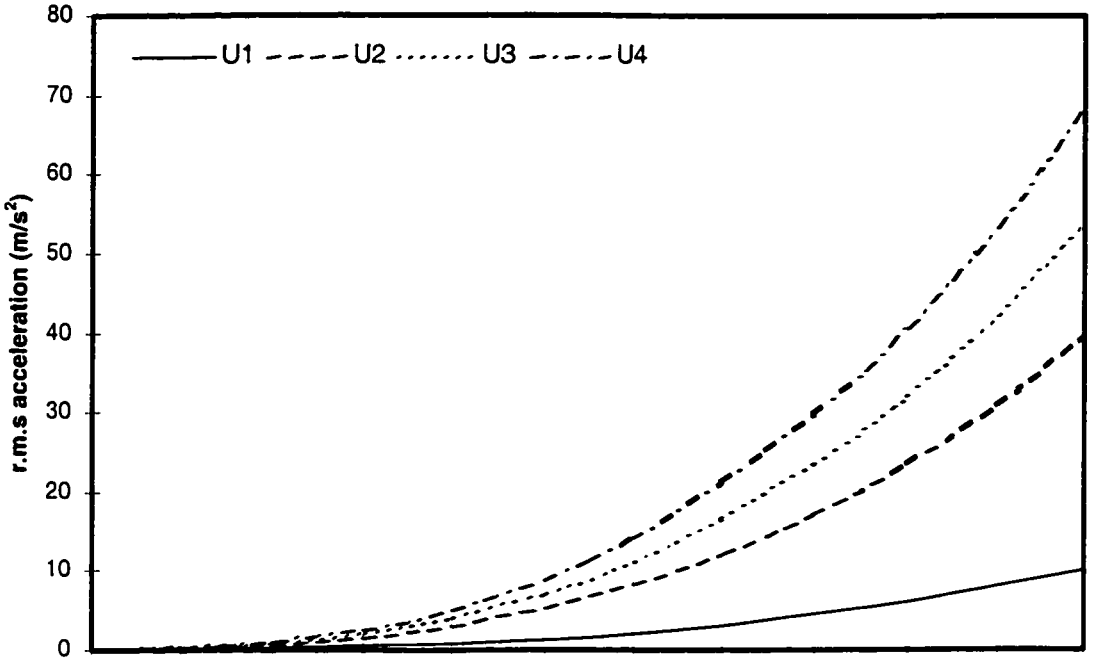

Figure 4.12.a: rms acceleration response of the tool body mass under different mass-unbalance and angular speeds (K_{h1}= 10*10^5 +20% N/m).

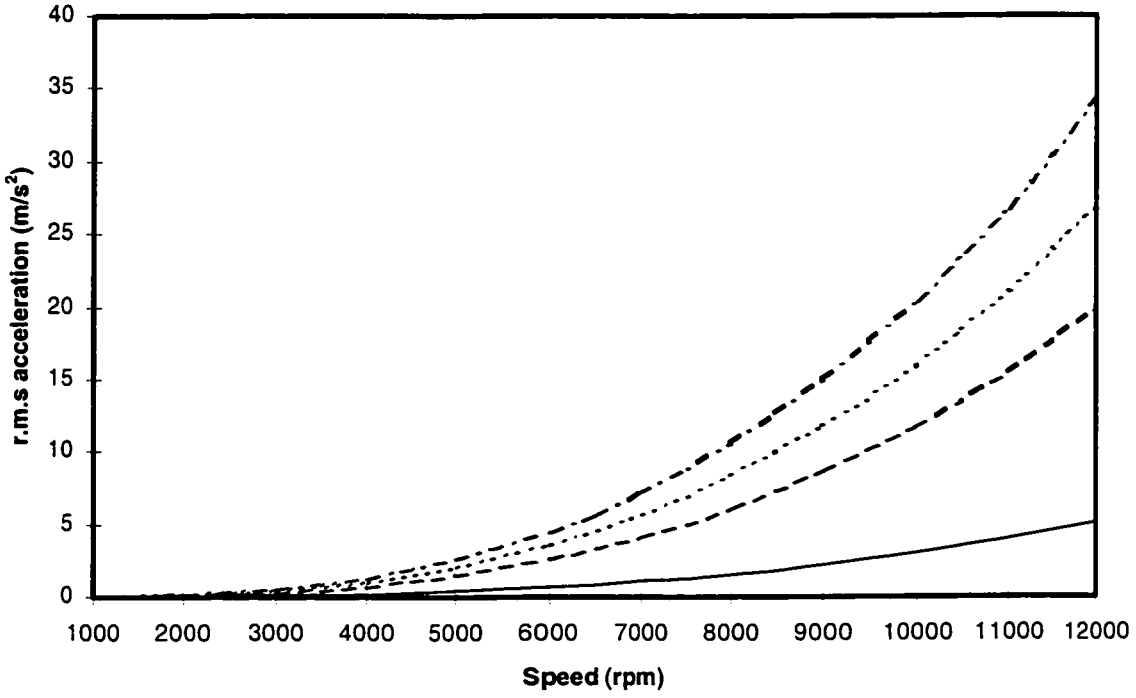

Figure 4.12.b: rms acceleration response of the hand mass under different mass-unbalance and angular speeds (K_{h1}= 10*10^5 +20% N/m).

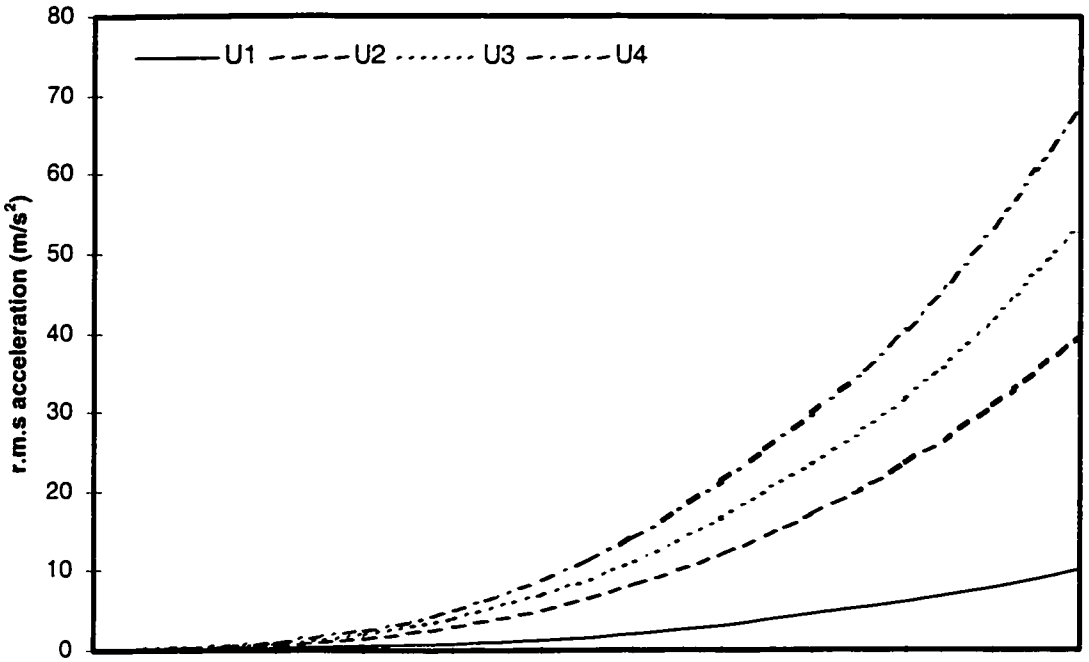

Figure 4.13.a: rms acceleration response of the tool body mass under different mass-unbalance and angular speeds ($K_{h1} = 10*10^5$ -10% N/m).

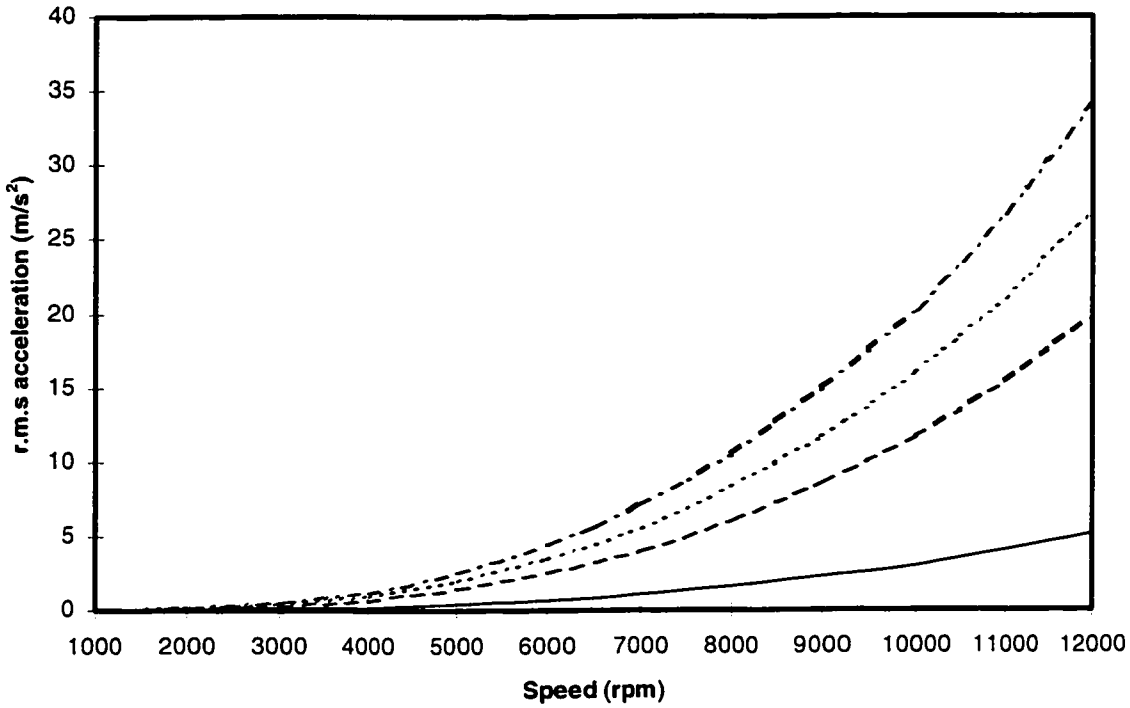

Figure 4.13.b: rms acceleration response of the hand mass under different mass-unbalance and angular speeds ($K_{h1} = 10*10^5$ -10% N/m).

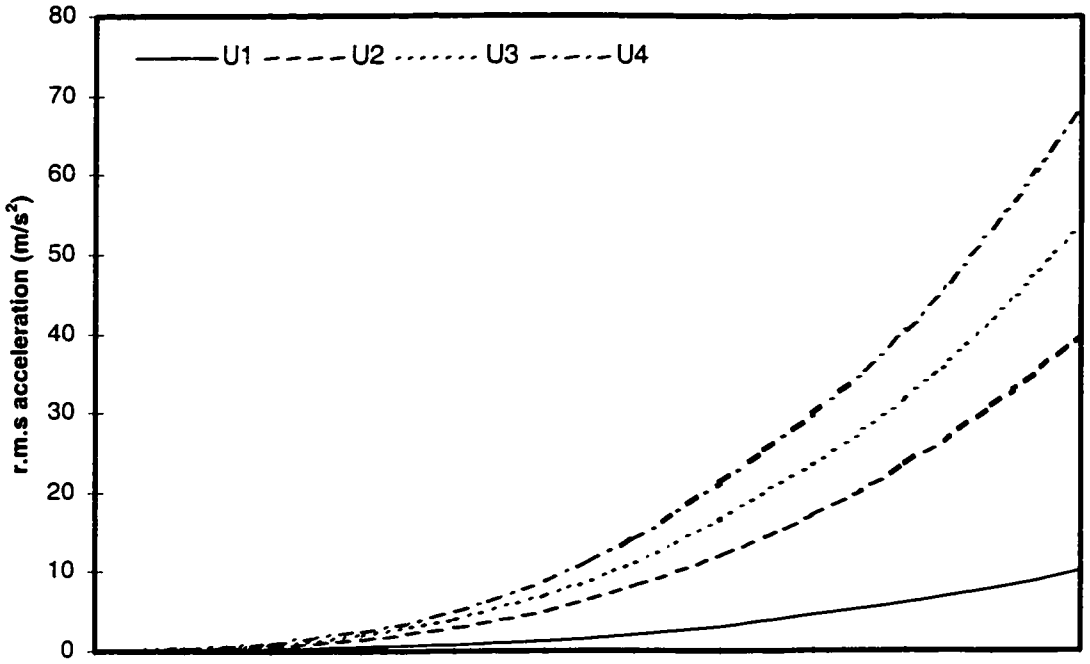

Figure 4.14.a: rms acceleration response of the tool body mass under different mass-unbalance and angular speeds (K_{h1} = 10*10^5 -20% N/m).

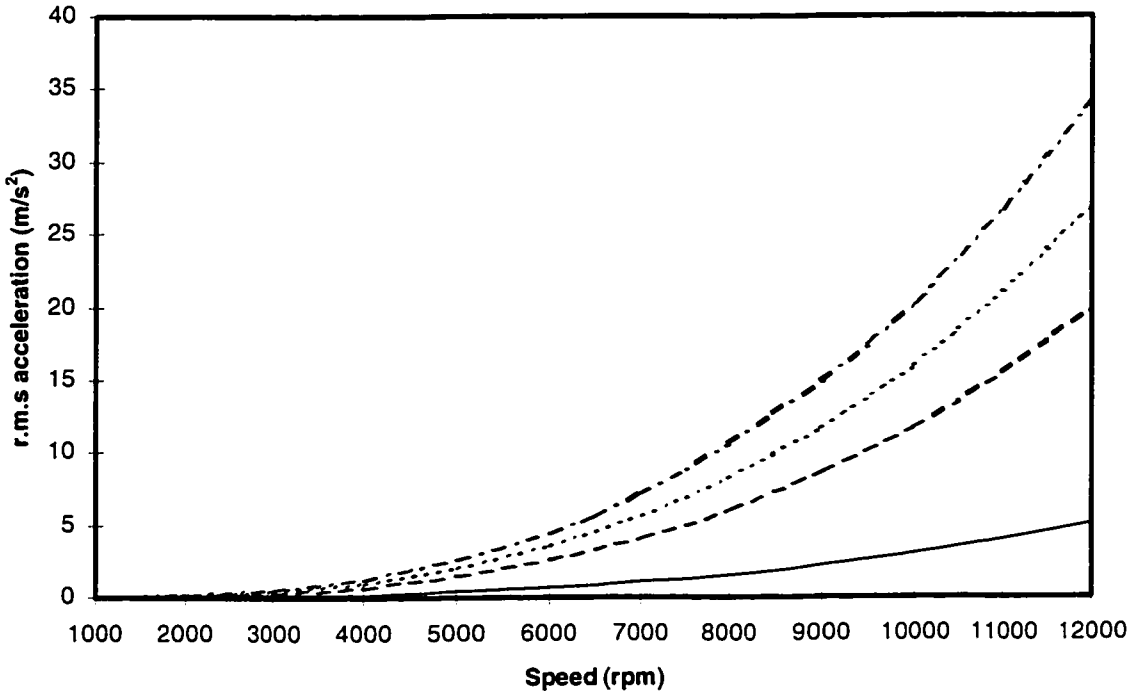

Figure 4.14.b: rms acceleration response of the hand mass under different mass-unbalance and angular speeds (K_{h1} = 10*10^5 -20% N/m).

4.6 Summary

The results suggest that the addition of damping through either protective gloves or handle grips could help reduce the magnitude of HTV, although the reductions would be relatively small. The addition of damping within the bearings would not yield significant effect on the HTV. From the measured data presented in chapter 3, it is evident that use of an auto-balancer could considerably attenuate the mass-unbalance induced hand-transmitted vibration. It is thus desirable to operate hand-held grinders with an auto-balancer unit.

Chapter 5

Conclusions and Recommendations for Future Research

5.1 Major Highlights of the Study

This thesis presents the analysis of hand-transmitted vibration of a hand-held grinder and its assessment in relation to the health risks as functions of the mass unbalance. Moreover, it focuses on the selected design parameters, such as of bearings damping and damping parameters of the visco-elastic hand-handle interface. The major focus of the dissertation research includes dynamic response characterization of the coupled hand-arm and grinder system through analytical and experimental means. In view of the complex nature of the hand-arm system, no attempts are made to incorporate the influence of numerous intrinsic and extrinsic parameters, and to explore the validity of the system model.

The primary objective of this dissertation research was to enhance an understanding of the vibration behavior of a hand-held grinder through laboratory measurements of the coupled hand-held system, and through development and analysis of a simple analytical model. Owing to many complexities associated with analytical characterization of a hand-held grinder, the proposed model represents a preliminary attempt and a considerably simple model.

The major highlights of this investigation are summarized as follows:

1. A coupled human hand-arm and the grinder system was characterized by a eight-DOF model to describe its motion along the y and z-axes in a basicentric coordinate system of the human hand and arm. Parameters of

the proposed model were identified from the reported data on various components. The model is developed specifically to study the contribution due to mass unbalance of the grinding wheel and variations in the damping parameters of the bearings and the hand-handle interface.

2. Laboratory tests were designed and performed to establish the vibration characteristics of the grinder and human hand-arm system for different values of the feed force and mass unbalance using two human subjects. The tool was instrumented to measure the acceleration due to vibration transmitted to the subjects' hand along all the three axes. The measured data were analyzed to derive the vibration transmitted to the hand, along all three translational axes.

3. The measured data were further analyzed to determine the influence of feed force, mass unbalance and the presence of an automatic balancer.

4. A methodology to assess the occupational health and safety risks due to the hand-transmitted vibration is applied and discussed. The dose response relation is employed to determine the number of years of exposure prior to risk of acquiring the VWF.

5. A parametric study is undertaken to study the influence of bearing damping, mass unbalance, and hand model parameters on the magnitude of HTV.

5.2 Conclusions

The following major conclusions are drawn from the analytical and experimental studies performed in this dissertation research:

- The operation of a hand-held grinder causes predominant hand-transmitted vibration in frequency range corresponding to its angular speed of 100-125 Hz along all the three translational irrespective of the magnitude of the feed force and the mass unbalance. In the present study, predominance of hand-transmitted vibration was observed in the 125 Hz band, which corresponded to the operating speed of 7500 rpm.

- The influence of feed force on a freely rotating grinding wheel vibration was observed to be insignificant under the laboratory conditions considered in this study. This could be attributed to uncompensated feed force employed in the study and lack of cutting forces.

- The measured data revealed that the hand-held grinder transmits most significant vibration along the x and y-axes, while the magnitude of HTV along the z-axis was the lowest.

- The magnitudes of hand-transmitted vibration increased significantly with increase in the mass unbalance.

- The eight-hour energy equivalent of the HTV increased nearly 13 folds when a mass-unbalance of 510 gm-mm was introduced.

- The continued exposure to such vibrations induced by 510 gm-mm unbalance at a rotating speed of approximately 7500 rpm could yield VWF symptoms in 10% of the workers in approximately 2.8 years.
- Addition of an auto-balancer to the grinder reduces the magnitudes of transmitted vibration most significantly.
- The presence of the auto-balancer reduces the eight-hour energy equivalent value to nearly 2 m/s^2 under a mass unbalance of 510 gm-mm as compared to 10.7 m/s^2 obtained without the balancer.
- The model results showed the magnitudes of hand-transmitted vibration increase monotonically with increase in the angular speed.
- The magnitude response of hand-transmitted vibration increased significantly with increase in the mass-unbalance.
- An increase in bearing damping resulted in insignificant effect on the magnitude of the tool-body acceleration, which was attributed to considerably higher frequency of the shaft-disc assembly.
- An increase in the hand-handle interface damping that could be realized through the use of anti-vibration gloves or the handle grips would yield some reductions in the magnitudes of hand-transmitted vibration.
- The operation of a hand-held grinder is frequently subject to mass-unbalance excitation arising from the residual unbalance and non-uniform wear and distribution of the cutting forces. The vibration induced by such

excitations could be most effectively attenuated by the use of an auto-balancer.

5.3 Recommendations for Future Work

This dissertation research represents preliminary attempts in characterizing the influence of an automatic balancing unit on the nature of hand-transmitted vibration and in developing an analytical model of the coupled hand-tool system. The study of the coupled hand-grinder system involves many complexities associated with: the biological and biodynamic properties of the hand-arm system; flexibility of the shaft, disc and the body structure; nonlinear properties of the bearings; and the conditions due to many intrinsic and extrinsic variables. The subject dissertation research thus leaves many more challenges that need to be addressed. Some of these are summarized below:

- The present study utilized a limited experiment design involving uncompensated feed forces, only one angular speed and two human subjects. Owing to the severe nature of the hand-transmitted vibration and excellent performance of the auto-balancer, it would be extremely desirable to investigate the experimental performance more thoroughly. It is suggested that the experiment design should involve the following:
  - A larger number of test subjects.
  - Measurements under controlled handgrip and hand-feed forces to study the influence of contact conditions.
  - A measurement at both, right and left, handles.

- Postural variations to consider representative postures.
- Longer magnitudes of mass-unbalance to simulate non-uniformly distributed high magnitude cutting force.

- The development of a reliable analytical model would be highly desirable to study various vibration attenuation mechanisms. The model development would require significant further efforts in the following aspects:
  - A reliable human hand-arm model would need to be developed on the basis of measured biodynamic responses, which could be applied to the tool model.
  - The shaft-rotor system must be referred to incorporate the disc spindle flexibility.
  - A thorough characterization of the bearings would be necessary to define its nonlinear characteristics along all the three-axes.
  - Further efforts would also be desirable to develop and integrate the model of an auto-balancer incorporating freely oscillating balls within a guide way. Such model would allow for the design of optimal auto-balancer.

References

1. Aatola S., Transmission of Vibration to the Wrist and Compression of Frequency Response and Comparison of Frequency Estimators, Journal of Sound and Vibration, 131(3), 497-507, 1989.

2. Abrams C.F Jr, and Suggs C.W, Chain Saw Vibration, Isolation and Transmission through the Human Arm, Transactions of the ASAE, 423-425, 1969.

3. Abrams C.F., A Study of the Transmission of High Frequency Vibration in the Human Arm. Masters Thesis. North Carolina University, Raleigh, 1968.

4. Adolfsson J., A Study of Stability in Autobalancing Systems using Multiple Correction Masses, Department of Mechanics, Royal Institute of Technology, Stockholm, Sweden, 1997.

5. Agafonov Y.V., Automatic Balancer for Hand-Operated Grinding Machines, Vest. Mashinostroenyia, 9, 36-38, 1976.

6. ANSI-S3.34, Guide for the Measurement and Evaluation of Human Exposure to Vibration Transmitted to the Hand, American National Standards Institute, New York, NY, 1986.

7. Bendal, A.W., Hand-Arm Vibration in Great Britain, Proceedings of the Fifth International Conference on Low Frequency Noise and Vibration, Multi-Science Publishing Co., Oxford, 13-20, 1987.

8. Bhat R. B., Vibration Problems in Rotating Machinery, Course notes, Department of Mechanical Engineering, Concordia University, Montreal, Canada, 2001.

9. Bitsch J., Donati P., Poirot R, Roure L., Elaboration of a standard procedure for the measurement of vibration emitted by percussive tools: application to breakers. Scand J. Work Environ Health, 347-350, 1986.

10. Brammer A.J., Exposure of the Hand to Vibration in Industry, NRCC Document No. 22844, NRCC, Ottawa, Canada, 1984.

11. Brammer A.J., Some Problems Associated with the Formulation of Human Response to Vibration, In: W.Taylor, ed. The Vibration Syndrome, Academic Press, London, 1974.

12. Burström L., Measurement of the impedance of the hand and arm International Archives of Occupation and Environ Health 62; 431-439, 1990.

13. Burström L., The influence of biodynamic factors on the mechanical impedance of the hand and arm. Int Arch Occup Environ Health; 69:437-446, 1997.

14. Chang, Chili-Hong, Wang, Mao-Jiun J., Lin, Shu-Chiang, Evaluating the Effects of Wearing Gloves and Wrist Support on Hand-Arm Response while Operating an in-line Pneumatic Screwdriver. Int. J. of Industrial Ergonomics, 24: 473-481, 1999.

15. Cherian T., Control of Hand Transmitted Vibration through Development and Analysis of a Human Hand-Arm-Isolator Model, M.A.Sc. Thesis Concordia University, 1994.

16. Christ E., Anti-Vibration Gloves, Performance Tests, Die Berufsgenossenschaft, 1982.

17. Clarke J.B., and Dalby W., Noise Vibration Control, 16, 146-149, 1985.

18. Cottingham C.E., Effects of the use of Air Hammer on the Hands of Indiana Oolitic-stone cutters, Bulletin of U.S. Bureau of Labour Statistics 236, series 19, 125-133, 1918.

19. Den Hartog J.P., Mechanical Vibration, McGraw Hill Book Company Inc.; fourth edition, 1956.

20. Emanuelsson S., Introducing Automatic Balancing as Means to Reduce Imbalance Induced Vibrations in Electrical and Air-Powered Hand-Held Angle Grinders (Power Tools), SKF Auto-Balancing, Gothenburg, Sweden.

21. Färkkilä M., Grip force in Vibration Disease, Scandinavian Journal of Work Environment and Health, 5, 159-166.

22. Fritz M., Journal of Biomechanics 21, 1165-1171. An improved biomechanical model for simulating the strain of the hand-arm system under vibration stress, 1991.

23. Gargiulo E.P. JR., Machine Design 107-110. A Simple Way to Estimate Bearing Stiffness, 1980.

24. Gemne G., and W. Taylor, Journal of Low Frequency Noise and Vibration, Special Volume: 1-12. Foreword: hand-arm vibration and the central autonomic nervous system, 1983.

25. Goel, V.K., and Rim K., Role of Gloves in Reducing Vibration: Analysis for Pneumatic Chipping Hammer, American Industrial Hygenic Association Journal, 48(1), 9-14, 1987.

26. Goodwin M. J., Dynamics of Rotor-Bearing Systems, London, UK, 1989.

27. Griffin M.J., Evaluating the Effectiveness of Gloves in Reducing Hazards Hand-Transmitted Vibration. Occupational and Environment Medicine (55): 340-348, 1998.

28. Griffin M.J., Handbook of Human Vibration, Academic Press limited, London, 1996.

29. Griffin M.J., Handbook of Human vibration, London: Academic press, 1990.

30. Griffin M.J., Macfarlane C.R. and Norman, C.D., The Transmission of Vibration to the Hand and the Influence of Gloves, In: Vibration Effects on the Hand and Arm Industry, Brammer, A. J. and Taylor, W. eds, John Wiley & Sons, New York, 103-116, 1982.

31. Gurram R., A Study of Vibration Response Characteristics of the Human Hand Arm System, Ph.D dissertation, Concordia University, 1993.

32. Gurram R., Rakheja S., and Brammer A.J., Driving-point Mechanical Impedance of the Human Hand-Arm System: Synthesis and Model Development, Journal of Sound and Vibration, 180, 437-458, 1995.

33. Gurram R., Rakheja S., and Gouw G.J., Vibration Transmission Characteristics of the Hand-Arm and Gloves, International Journal of Industrial Ergonomics, 13, 217-234, 1994.

34. Hamilton A., A Study of Spastic in the Hand of Stonecutters: An effect of the Air Hammer on the Hands of Stonecutters, Industrial Accidents and Hygiene Series, Bulletin 236, No.19, U.S.D.O.L, Bureau of Labor Statistics, 53-66, 1918.

35. Hartung E., Dupis H., and Scheffer M., Acute Effects of Vibration Depending on Different Coupling Forces of the Hand, International Conference of Hand-Arm vibration, 437-449, 1992.

36. Hesse M., Die antwort des hand-arm-systems auf stochastiche erregung und ihre anwendung in schwingungsschutz [dissertation]. Dortmund, Germany, Universittät Dortmund, 1989.

37. Hewitt S., Assessing the Performance of Anti-vibration Gloves -a Possible Alternative to ISO 10819, 1996. Ann. Occup. Hyg., 42:245-252, 1998.

38. Ikeda K., Ishizuka H., Sawada A., Urushiyama K., Vibration acceleration magnitudes of hand-held tools tools and workpieces. Ind Health; 36:197-208, 1998.

39. INRS, Cahierde Notes Documentaries, ND409-110-83, 47-52, 1983.

40. ISO 5349. Guidelines for Measurement and Assessment of Human Exposure to Hand-Transmitted Vibration, 1986.

41. ISO 5349-2, Mechanical Vibration – Measurement and Evaluation of Human Exposure to Hand-Transmitted Vibration- Part 2: Practical Guidance for Measurement in the Workplace, 2001.

42. ISO 8662-2, Hand-held Portable Power Tools -Measurement of Vibrations at the Handle - Part 2: Chipping Hammers and Riveting Hammers, International Standards Organization, Geneva, Switzerland, 1992.

43. ISO 8662-4. Hand-held Portable Power Tools – Measurement of Vibrations at Handle – Part 4, Grinders, 1994.

44. ISO Hand-arm vibration- Method for the Measurement and Evaluation of the Vibration Transmissibility of Gloves, International Standards Organization ISO/108/4/3 N65, 1992.

45. ISO-10068, Mechanical vibration and shock-free, mechanical impedance of the human Hand-arm system at the driving point, 1998.

46. ISO-5349, Mechanical vibration—guidelines for the measurement and the assessment of human exposure to hand-transmitted vibration. International Standard Organization, Geneva, Switzerland, 1986.

47. ISO-8727, Mechanical vibration and shock-human exposure-biodynamic coordinate systems. International Standard Organization, 1997.

48. Nilsagard J.,Richmond H., SKF Spherical Roller Bearing Division, Gothenburg, Sweden, 1993.

49. Kramer E., Dynamics of Rotors and Foundations, Springer-Verlag, Berlin, Germany, 1993.

50. Leake J.P., Health Hazards from the use of the Air Hammer in Cutting Indianna Limestone, Industrial, Accidents and Hygiene series, Bulletin 236, U.S.D.O.L, Bureau of Labor Statistics, 100-113, 1918.

51. Lindell H., Vibration Reduction on the Hand-Held Grinders by Automatic Balancing, Central European Journal of Public Health, 4, 43-45, 1996.

52. Loriga G., Pneumatic tools: Occupation and Health, Ball. Inspect. Lorboro, 2, 35-37, 1911.

53. Lundström R. and Burström L., Mechanical Impedance of the Human Hand-Arm System, Int. Journal of Industrial Ergonomics, 3, 235-242, 1989.

54. Lundström R., Centralized European hand-arm vibration data base, URL: http://umetech.niwl.se/vibration/hav/, 1998

55. M. Daikoku and F. Ishikawa, Proceedings of Fifth International Conference on Hand-ArmVibration. Kanzawa, Japan. Mechanical impedance and vibration model of hand-arm system, 1990.

56. Macfarlane C.R., Anti-Vibrational Gloves and the Dynamic Response of the Human Hand-Arm, United Kingdom Informal Group Meeting on Human Response to Vibration. Univ. College, Swansea, 1980.

57. Macfarlane C.R., The Vibrational Response of Gloves and the Human Hand and Arm, United Kingdom Informal Group Meeting on Human Response to Vibration, Royal Aircraft establishment, Farnborough, 1979.

58. Meirovitch L., Methods of Analytical Dynamics, McGraw Hill Book Company, New York, 1970.

59. Meltzer G., Proceedings of the International Symposium on Man under Vibration Suffering and Protection, Udine, Italy, 210-221. A vibration model for the human hand-arm system, 1979.

60. Miwa T., Design of Vibration Isolators for Hand-Held Vibrating Tools, Third International Symposium of Hand-Arm Vibration, Ottawa, 4, 1981.

61. Miwa T., Vibration – Isolation systems for Hand-Held Vibrating Tools, In Brammer AJ. and Taylor W, eds., Vibration Effects on the Hand and Arm in Industry, New York, Wiley, 303-310, 1982.

62. Miwa T.: Reduction of Grinder Vibration by Balancing. Ind. Hlth, 22, 59-74, 1984.

63. Miwa, T., Yonekawa, Y., Nara A., Kanada, K., and Baba, K., Vibration Isolation Gloves for Portable Vibrating Tools part 4: Vibration Isolation Gloves, Industrial Health (Japan), 17, 141-152, 1979.

64. Nelson C.M., Vibration measurements on percussive pneumatic tools using ring-mounted and tool-mounted accelerometers and laser Doppler velocimeter: a comparison of methods. UK Group Meeting on Human Response to Vibration, 1986 S 1997.

65. Nerm R.M., Vibration Enhancement of Blood Arterial Wall Macromolecule Transport. Proceedings of the International Hand-Arm Vibration Conference, 37-41, 1977.

66. NIOSH, Criteria for a Recommend Standard. Occupational Exposure to Hand-Arm Vibration. National Institute for Occupational Safety and Health. 89-106, 1989.

67. Pelmear P. L., Wasserman D. E., Hand-Arm Vibration-a Comprehensive Guide for Occupational Health Professionals. Beverly Farms, MA: OEM Press, 1998.

68. Pinto I., Stacchint N., Bovenzi M., Paddan G.S., and Griffin M.J., Protection Effectiveness of Anti-vibration Gloves: Field Evaluation and Laboratory Performance Assessment. Proc. of 9th International Conference on Hand-Arm Vibration, Nancy France: Section 15 (2), 2001.

69. Politschuk A.P., and Oblivin N.V., Methods of Reducing the Efforts of Noise and Vibration on Power Saw Operators, Proceedings of International occupational Hand-Arm Vibration Conference, Cincinnati, Ohio, U.S.A, 230-232, 1977.

70. Pyykkő I., Färkkilä M., Toivanen, J., Korhonen O., and Hyvarinen J., Transmission of Vibration in the Hand-Arm System with Special Reference to Change in Compression Force and Acceleration, Scandinavian Journal of Work, Environment and Health, 2, 87-95, 1976.

71. Radwin R.G., Armstrong T.J., Van Bergeijk E., Hand-arm vibration and work-related disorders of the upper limb. In: Pelmear P.L., Wasserman D.E., editors. Hand-arm vibration. Beverly Farms, MA: OEM Press, 122-152, 1998.

72. Radwin R.G., Robert G., Armstrong, Thomas J., and Vanbergeijk, Ernst., Vibration Exposure for Selected Power Hand Tools used in Automobile Assembly, American Industrial Hygiene Association Journal, 51(9): 510-518, 1990.

73. Radwin R.G., Robert G., Armstrong, Thomas J., Assessment of Hand Vibration Exposure on an Assembly line, American Industrial Hygiene Association Journal, 46(4): 211-219, 1985.

74. Rajalingham C., Bhat R.B., Rakheja S., and Automatic Balancing of Flexible Vertical Rotors using a Guided Ball, International Journal of Mechanical Sciences, 9, 825-534, 1998.

75. Rakheja S., and Rajalingham C., Whirl Suppression in Hand-Held Power Tool Rotors using Guided Rolling Balancers, Journal of Sound and Vibration, (217) 3, 453-466, 1998.

76. Rakheja S., Dong R.G., McDowell T., Welcome D.. Wu J., and Schopper A.W., Evaluations of a Transfer Function Method for Predicting Vibration Isolation Performance of Gloves, National Institute for Occupational Safety and Health, Engineering & Control Technology branch, Morgan town, USA, 2002a.

77. Rakheja S., Dong R.G., Smutz W.P., Schopper A., Welcome D., Wu J.Z., Effectiveness of a new method (TEAT) to assess vibration transmissibility of gloves, International Journal of Industrial Ergonomics 30, 33–48, 2001.

78. Rakheja S., R.G. Dong, A. Schopper, D. Welcome, Estimation of tool-specific isolation performance of anti-vibration gloves. International Journal of Industrial Ergonomics 30, 71–87, 2002b.

79. Rakheja S., Wu J. Z., A Comparison of biodynamic models of the Human Hand-Arm System for applications to Hand-Held Power Tools, Journal of Sound and Vibration, 249(1), 55-82 2002c.

80. Rens G., Dubrulle P., and Malchaire J., Efficiency of Conventional Gloves against Vibration, Ann. Occp. Hyg., Vol 31, No.2, 249-254, 1987.

81. Reynolds D. D., and Soedel W., Journal of Sound and Vibration 21, 339-353. Dynamic response of the hand-arm system to a sinusoidal input, 1972.

82. Reynolds D.D., and Angevine E.N., Hand Arm Vibration, part II: Vibration Transmission Characteristics of the Hand and Arm, Journal of sound and vibration, 51(2), 255-265, 1977.

83. Reynolds D.D., and Wilson F.L., Mechanical Tests Stand for Measuring the Vibration of Chain Saw Handles During Cutting Operations, Vibration Effects on the Hand and Arm in Industry edited by A. J Brammer W., and Taylor., 1982.

84. Reynolds D.D., Hand-arm vibration: A review of three year's research, proceedings of the 3rd International Hand-Arm Vibration Conference, Ohio, USA, 99-129, 1977.

85. Reynolds, D.D. and Falkenberg, R.J., A Study of the Hand Vibration on Chipping and Grinding Operators, part II: Four-degree-of-freedom Lumped Parameter Model of the Vibration Response of the Human Hand, Journal of Sound and Vibration, 95, 499-514, 1984.

86. Rodriguez J., Fredericks TK., Vibration transmission characteristics of subjects exposed to uniaxial vibrations at the fingers. In: Lee GCH, editor. Advances in occupational ergonomics and safety. Amsterdam: IOS Press; 327-331, 1999.

87. Rossi G.L., Tomasini E.P., Proposal of a new measurement technique for hand-arm vibration analysis. Proceedings of the SPIE; Vol 2358; First International Conference on Vibration Measurements by Laser Techniques: Advance and Applications; 48-59, 1994.

88. Rothstein T., Report of the Physical Findings in eight Stonecutters from the Limestone Region of Indiana, Industrial Accidents and Hygiene Series, Bulletin 236, U.S.D.O.L, Bureau of Labour Statistics, 67-96, 1918.

89. Starck J., Characteristics of Vibration, Handgrip force, and Hearing loss in Vibration Syndrome. Alkuperaistutkimukset, Department of Mathematics, Physics and Chemistry, University of Kupio, Finland, 1984.

90. Starck J., Pekkarinen J. and Chun Chang L., Transmission of Vibration from Tool Handle to Wrist and to Head; the Kurumr Medical journal, 37, s1-s11, 1990.

91. Suggs C.W., Abrams C.F. Jr., and Cundiff J.S., Attenuation of High Frequency Vibration in Chain Saws, Journal of Sound and Vibration, 2(6), 1968.

92. Suggs C.W., and Abrams C.F. Jr, Vibration Isolation of Power Tools, Proceedings of the 27th Annual Meeting of the Human Factors Society, 1983.

93. Suggs C.W., and Hanks J.M., Resilient Hand grips, In A.J. Brammer and W. Taylor eds., Vibration Effects on the Hand and Arm in Industry, New York, Wiley, 333-337, 1982.

94. Suggs C.W., and Mishoe J.W., Hand-arm vibration: vibrational responses of the human hand. Journal of Sound and Vibration, 53 (Pt II), 545-558, 1977.

95. Suggs C.W., Hanks J.M., and Roberson G.T., Vibration of Power Tool Handles, In Brammer A. J. and Taylor W, eds., Vibration Effects on the Hand Arm in Industry, New York, Wiley, 245-251, 1982.

96. Suggs, C.W., and Mishoe J.W., Hand-arm vibration: Implications drawn from lumped parameter models, Proceedings of the 3rd International Hand-Arm Vibration Conference, Ohio, USA, 136-141, 1977.

97. Tamura H., and Tsuda Y., Bulletin of the JSME 28, 1240-1246. On the Static Running Accuracy of Ball Bearings, 1985.

98. Taylor W., and Pealmear P.L., Vibration White Finger in Industry, A Report Comprising edited versions of papers submitted to the Department of Health and Social Security, 1973.

99. Therale E. L.: Automatic Dynamic Balancing. Machine Design, 11, 103-106, 1950.

100. Tiwari M., Gupta K., and Prakash O., Dynamic Response of an Unbalanced Rotor Supported on Ball Bearings, Journal of Sound and Vibration, 238(5), 757-779, 2000.

101. Tondl A., Some Problems in Rotor Dynamics, Chapman and Hall, London, 1956.

102. Tondl A., Some problems in Rotor Dynamics, House Czechoslovakian Academy of Sciences, Prague, 1965.

103. Wasserman D., Badger D., Doyle T.E., and Marsolis L., Journal of American Society of Safety Engineers, Industrial Vibration-an overview, 19, 38-43, 1974.

104. Wasserman D., Reynolds D. and Thomas D., Vibration syndrome in chipping and grinding workers, Journal of Occ. Med., Vol 26, no. 10, 773-776, 1994.

105. Wood L. A., Suggs C.W. and Abrams C. F., Journal of Sound and Vibration 57, 157-169. Hand-arm vibration. Part III: A distributed parameter dynamic model of the human hand-arm system, 1978.

Appendix A

Terminology

Acroparesthia	Numbness, tingling and other abnormal sensations of one or more of the extremities.
Anatomic	Similar to the bodily structure.
Artery	Tubes conveying blood from the heart.
Blanching	Finger look white and pale.
Carpal tunnel syndrome	Phenomena which results in sensory loss over the median nerve distribution in the fingers.
Cysts	Abnormal sac containing gas, fluid or semisolid material
Dexterity	Skill in handling the things.
Epidemiology	The study of the prevalence and spread of disease in community.
Episodic	Sporadic; occurring irregularly; incidental.
Ischemic	Local anemia (a condition due to the insufficient oxygenation of the blood) due to mechanical obstruction to the blood supply
Insomnia	Condition leading to sleeplessness.
Necrosis	Death of piece of bone or tissue.
Numbness	Deprived of feeling or power of motion.
Percussive	Forcible striking of one body against another.
Phalanges	Bone between two joints of the fingers.
Spasm	Sudden involuntary muscular contraction.
Tingling	Slight pricking or stinging sensation.

Traumatic	causing trauma.
Ulna	Bone of the forearm on the side opposite to the thumb.
Vascular	Containing vessels for conveying blood.

Appendix B

Mass, Stiffness and Damping

Matrix of 4 Degree-of-freedom Hand-Grinder Model

B.1 Mass Matrix

$$\begin{bmatrix} m_T & 0 & 0 & 0 \\ 0 & I_d & 0 & 0 \\ 0 & 0 & m_b & 0 \\ 0 & 0 & 0 & m_h \end{bmatrix}$$

B.2 Damping Matrix

$$\begin{bmatrix} 2c_{b1}+2c_{b2} & 2lc_{b1}+2c_{b2}(l+d) & -2c_{b1}-2c_{b2} & 0 \\ 2lc_{b1}+2c_{b2}(l+d) & 2l^2c_{b1}+2c_{b2}(l+d)^2 & -2lc_{b1}-2c_{b2}(l+d) & 0 \\ -2c_{b1}-2c_{b2} & -2lc_{b1}-2c_{b2}(l+d) & 2c_{b1}+2c_{b2}+c_{h1} & -c_{h1} \\ 0 & 0 & -c_{h1} & c_{h1}+c_{h2} \end{bmatrix}$$

B.3 Stiffness Matrix

$$\begin{bmatrix} 2k_{b1}+2k_{b2} & 2lk_{b1}+2k_{b2}(l+d) & -2k_{b1}-2k_{b2} & 0 \\ 2lk_{b1}+2k_{b2}(l+d) & 2l^2k_{b1}+2k_{b2}(l+d)^2 & -2lk_{b1}-2k_{b2}(l+d) & 0 \\ -2k_{b1}-2k_{b2} & -2lk_{b1}-2k_{b2}(l+d) & 2k_{b1}+2k_{b2}+k_{h1} & -k_{h1} \\ 0 & 0 & -k_{h1} & k_{h1}+k_{h2} \end{bmatrix}$$

Appendix C

Modal Representation in the State-Space Form

$$M = \begin{bmatrix} m_T & 0 & 0 & 0 \\ 0 & I_d & 0 & 0 \\ 0 & 0 & m_b & 0 \\ 0 & 0 & 0 & m_h \end{bmatrix} \begin{Bmatrix} \ddot{z}_d \\ \ddot{\alpha} \\ \ddot{z}_3 \\ \ddot{z}_4 \end{Bmatrix}$$

$$C = \begin{bmatrix} 2c_{b1} + 2c_{b2} & 2lc_{b1} + 2c_{b2}(l+d) & -2c_{b1} - 2c_{b2} & 0 \\ 2lc_{b1} + 2c_{b2}(l+d) & 2l^2c_{b1} + 2c_{b2}(l+d)^2 & -2lc_{b1} - 2c_{b2}(l+d) & 0 \\ -2c_{b1} - 2c_{b2} & -2lc_{b1} - 2c_{b2}(l+d) & 2c_{b1} + 2c_{b2} + c_{h1} & -c_{h1} \\ 0 & 0 & -c_{h1} & c_{h1} + c_{h2} \end{bmatrix}$$

$$K = \begin{bmatrix} 2k_{b1} + 2k_{b2} & 2lk_{b1} + 2k_{b2}(l+d) & -2k_{b1} - 2k_{b2} & 0 \\ 2lk_{b1} + 2k_{b2}(l+d) & 2l^2k_{b1} + 2k_{b2}(l+d)^2 & -2lk_{b1} - 2k_{b2}(l+d) & 0 \\ -2k_{b1} - 2k_{b2} & -2lk_{b1} - 2k_{b2}(l+d) & 2k_{b1} + 2k_{b2} + k_{h1} & -k_{h1} \\ 0 & 0 & -k_{h1} & k_{h1} + k_{h2} \end{bmatrix}$$

Assume $y = \dot{z}_d$

$\dot{y} = \ddot{z}_d$; $\theta = \dot{\alpha}$, and $\dot{\theta} = \ddot{\alpha}$; and

$y_3 = \dot{z}_3$; $\dot{y}_3 = \ddot{z}_3$; $y_4 = \dot{z}_4$; and $\dot{y}_4 = \ddot{z}_4$

$$\begin{Bmatrix} y \\ \theta \\ y_3 \\ y_4 \\ \dot{y} \\ \dot{\theta} \\ \dot{y}_3 \\ \dot{y}_4 \end{Bmatrix} = \begin{Bmatrix} \dot{z}_d \\ \dot{\alpha} \\ \dot{z}_3 \\ \dot{z}_4 \\ \ddot{z}_d \\ \ddot{\alpha} \\ \ddot{z}_3 \\ \ddot{z}_4 \end{Bmatrix} = \begin{bmatrix} A_{4*4} & B_{4*4} \\ -M^{-1}K_{4*4} & -M^{-1}C_{4*4} \end{bmatrix}_G \begin{Bmatrix} z_d \\ \alpha \\ z_3 \\ z_4 \\ \dot{z}_d \\ \dot{\alpha} \\ \dot{z}_3 \\ \dot{z}_4 \end{Bmatrix}$$

where $A = \begin{bmatrix} 0 & 0 & 0 & 0 \\ 0 & 0 & 0 & 0 \\ 0 & 0 & 0 & 0 \\ 0 & 0 & 0 & 0 \end{bmatrix}$

$$B = \begin{bmatrix} 1 & 0 & 0 & 0 \\ 0 & 1 & 0 & 0 \\ 0 & 0 & 1 & 0 \\ 0 & 0 & 0 & 1 \end{bmatrix}$$

$$-M^{-1}K = \begin{bmatrix} -\frac{2*(k_{b1}+k_{b2})}{m_T} & -\frac{2lk_{b1}+2k_{b2}(l+d)}{m_T} & \frac{2*(k_{b1}+k_{b2})}{m_T} & 0 \\ -\frac{2lk_{b1}+2k_{b2}(l+d)}{I_d} & -\frac{2l^2k_{b1}+2k_{b2}(l+d)^2}{I_d} & \frac{2lk_{b1}+2k_{b2}(l+d)}{I_d} & 0 \\ \frac{2*(k_{b1}+k_{b2})}{m_b} & \frac{2lk_{b1}+2k_{b2}(l+d)}{m_b} & -\frac{2k_{b1}+2k_{b2}+k_{h1}}{m_b} & \frac{k_{h1}}{m_b} \\ 0 & 0 & \frac{k_{h1}}{m_h} & -\frac{k_{h1}+k_{h2}}{m_h} \end{bmatrix}$$

$$-M^{-1}C = \begin{bmatrix} -\frac{2*(c_{b1}+c_{b2})}{m_T} & -\frac{2lc_{b1}+2c_{b2}(l+d)}{m_T} & \frac{2*(c_{b1}+c_{b2})}{m_T} & 0 \\ -\frac{2lc_{b1}+2c_{b2}(l+d)}{I_d} & -\frac{2l^2c_{b1}+2c_{b2}(l+d)^2}{I_d} & \frac{2lc_{b1}+2c_{b2}(l+d)}{I_d} & 0 \\ \frac{2*(c_{b1}+c_{b2})}{m_b} & \frac{2lc_{b1}+2c_{b2}(l+d)}{m_b} & -\frac{2c_{b1}+2c_{b2}+c_{h1}}{m_b} & \frac{c_{h1}}{m_b} \\ 0 & 0 & \frac{c_{h1}}{m_h} & -\frac{c_{h1}+c_{h2}}{m_h} \end{bmatrix}$$

$$\begin{Bmatrix} \dot{z}_d \\ \dot{\alpha} \\ \dot{z}_3 \\ \dot{z}_4 \end{Bmatrix} = [G]_{8*8} \begin{Bmatrix} z_d \\ \alpha \\ z_3 \\ z_4 \end{Bmatrix}$$

$$\begin{Bmatrix} \dot{z}_d \\ \dot{\alpha} \\ \dot{z}_3 \\ \dot{z}_4 \end{Bmatrix} = j\omega e^{i\omega t}$$

$$j\omega [I] \begin{Bmatrix} z_d \\ \alpha \\ z_3 \\ z_4 \end{Bmatrix} = [G][I] \begin{Bmatrix} z_d \\ \alpha \\ z_3 \\ z_4 \end{Bmatrix}$$

$$([G] - j\omega [I]) \begin{Bmatrix} z_d \\ \alpha \\ z_3 \\ z_4 \end{Bmatrix} = 0$$